UCLA
UCLA Electronic Theses and Dissertations

Title

The Role of Non-Mutated Signaling Networks and Inflammatory Cytokines in the Initiation and Progression of Prostate Cancer

Permalink

https://escholarship.org/uc/item/38z176qm

Author

Smith, Daniel Alan

Publication Date

2013

Peer reviewed|Thesis/dissertation

eScholarship.org Powered by the California Digital Library
University of California

UNIVERSITY OF CALIFORNIA

Los Angeles

The Role of Non-Mutated Signaling Networks and Inflammatory Cytokines in the Initiation and Progression of Prostate Cancer

A dissertation submitted in partial satisfaction of the requirements for the degree Doctor of Philosophy in Molecular Biology

By

Daniel Alan Smith

2013

© Copyright by

Daniel Alan Smith

2013

ABSTRACT OF THE DISSERTATION

The Role of Cytokines and Signaling Networks in the

Initiation and Progression of Prostate Cancer

By

Daniel Alan Smith

Doctor of Philosophy in Molecular Biology

University of California, Los Angeles, 2013

Professor Owen N. Witte, Chair

Prostate cancer is the most highly diagnosed, non-cutaneous cancer and second leading cause of cancer-related death in the United States. Despite this, the molecular determinants that drive prostate cancer initiation and progression are still poorly understood. Identifying signaling networks that are activated in prostate cancer and how these pathways interact is therefore fundamental to our understanding of prostate cancer. Using a dissociated prostate tissue model, we are able to investigate the role of specific genes in the regeneration and transformation of prostate tissues. This system allows for interrogation of both cell-autonomous genes as well as paracrine factors secreted by the surrounding microenvironment. Further, prostate epithelial tumors can be obtained from defined oncogenic combinations and the pathways and interactions between these oncogenes interrogated through a variety of *ex vivo* techniques.

We used the dissociated prostate tissue system to develop an array of transformation states using defined sets of oncogenes. These tumors were then interrogated using phosphotyrosine enrichment combined with mass spectrometry analysis to identify key signaling nodes activated by specific oncogenic combinations. By defining the signaling networks that are activated by specific oncogenic combinations, we begin to identify common signaling nodes that can be targeted therapeutically.

Whole genome sequencing studies have shown that prostate cancer exhibits a relatively low mutation frequency. We hypothesized that oncogenic transformation could therefore be driven by the over-expression of non-mutated proteins that would then activate specific oncogenic pathways leading to transformation. We interrogated the effects of increased expression of Src kinase and the androgen receptor, and identified that upon heightened co-expression of the non-mutated forms was sufficient to drive prostate transformation. We then interrogated the role of inflammatory cytokines and their ability to drive prostate cancer initiation and progression using interleukin-6 (IL6) and the related oncostatin-M (OSM) cytokines. Increased expression of either IL6 or OSM was sufficient to drive progression of PTEN-initiated lesions, indicating functional synergy. Further, increased expression of these cytokines was associated with an increase in activation of pathways downstream of these inflammatory cytokines. These data indicate that heightened expression of non-mutated genes can promote activation of pathways associated with oncogenesis and are sufficient to drive prostate epithelial transformation.

The dissertation of Daniel Alan Smith is approved.

Michael A. Teitell

Heather R. Christofk

Stephen Smale

Owen N. Witte, Committee Chair

University of California, Los Angeles

2013

DEDICATION

This dissertation is dedicated to my parents, Kathy and Mike Clester and Janet and Alan Smith, and to Jamie Rage, without whom I would have never survived this endeavor.

TABLE OF CONTENTS

LIST OF FIGURES

Chapter 2

Chapter 3

LIST OF TABLES

ACKNOWLEDGMENTS

I would like to thank my mentor, Dr. Owen Witte, for the opportunity to train in his laboratory over the past five years. His guidance and determination have pushed me to excel even beyond my own lofty expectations. I would also like to thank my committee members for their time and dedication to my Graduate work. I have truly benefited from their diverse expertise, experiences and commitment to seeing my work excel.

In addition to his guidance, Dr. Witte has assembled an incredible team of scientists and staff that have been instrumental in my development as a scientist. None of this would have been possible without the constant help of both current and former members of the Witte laboratory. Barbara Anderson, for always helping get everything organized and keeping everything in line. Donghui Cheng has been an invaluable resource and has always been more than patient with my last minute cell sorting and consistent tardiness with getting my samples to her. Yang Zong has been truly indispensible to this work, he has always been willing to discuss at great length any experiment and his knowledge of the field is something we should all strive for. Houjian Cai, who brought be into his work and gave me the opportunity to hone my scientific writing skills. I would also like to thank Justin Drake and Tanya Stoyanova for always being willing to take the time to show me how to do just about any technique imaginable. Deven Lawson, Rita Lukacs, Evan Nair-Gil and Andrew Goldstein for paving the way as Graduate students before me, and always being willing to help me with preparing for my committee meetings and all the other moments of panic with Graduate school. Melissa McCraken has been my unwavering cheerleader for the past six months and without her constant presence, my paper would likely still be wallowing somewhere in the abyss. To everyone else, you have all been a part of this and deserve every bit of my thanks.

I would also like to thank my funding sources that have supported my research and travel to conferences during my Graduate career, including the Tumor Cell Biology training grant (a Ruth L. Kirschstein National Research Service Award), the Molecular Biology Interdepartmental Program travel awards. I would also like to thank those with the Collegium of Teaching Fellows program, you have provided me an opportunity of a lifetime.

Finally, I would like to thank my friends and family. None of this would have been possible without my mom who has pushed me to and beyond my own expectations and without whom, none of this would have been possible. To my dad and stepdad, who have always been there for me and provided amazing guidance and role models to live up to and become. To my stepmom who has always been the coolest stepmom quite possibly ever. My thanks to Jillian Crocetti, you truly are the best friend I have made while at UCLA and have made this experience that much better. To Rob McMahan, I miss you brother and I cannot tell you how glad I am that you are doing so well in Chicago. To Brandon Boone and Matt MARR, for always being there when I needed to relax and live a little. And finally, Jamie Rage, who has been my tether to reality; with all our travels both at home and abroad, all I can say is that I cannot wait to see where we go next.

Chapters 2 and 3 are reproduced with permission from the Proceedings of the National Academy.

Chapter 4 is a version of a manuscript that is in submission.

VITA

2008	B.S. Biochemistry, Conc. in Medicinal Chemistry Arizona State University Tempe, Arizona
2008	Award Recipient Chancellor's Prize University of California, Los Angeles
2009	Teaching Assistant Molecular, Cellular and Developmental Biology University of California, Los Angeles
2009-2011	Award Recipient/Trainee Ruth L. Kirschstein Institutional National Research Service Award Tumor Cell Biology Training Grant University of California, Los Angeles
2010	Teaching Assistant Molecular, Cellular and Developmental Biology University of California, Los Angeles
2012-2013	Award Recipient/Trainee Collegium of University Teaching Fellows (CUTF) University of California, Los Angeles
2013	Lecturer Prostate Cancer: Social and Scientific Implications of an Aging Society CUTF/Microbiology, Immunology and Molecular Genetics University of California, Los Angeles

PUBLICATIONS AND PRESENTATIONS

Simmons CR, Stomel JM, **Smith DA**, Watkins JL, Allen JP, and Chaput JC. A synthetic protein selected for ligand binding affinity mediates ATP hydrolysis. *ACS Chemical Biology* (2009) 4 (8):649-58.

Simmons CR, Magee CL, **Smith DA**, Lauman L, Chaput JC, Allen JP. Three-dimensional structures reveal multiple ADP/ATP binding modes for a synthetic class of artificial proteins. *ACS Biochemistry* (2010) 49 (40):8689-99.

Cai H, **Smith DA,** Memarzadeh S, Lowell CA, Cooper JA, Witte ON. Differential transformation capacity of Src family kinases during initiation of prostate cancer. *Proceedings of the National Academy of Science* (2011) 108 (16):6579-84.

Drake JM, Graham NA, Stoyanova TS, Sedghi A, Goldstein AS, Cai H, **Smith DA**, Zhang H, Komisopoulou E, Huang J, Graeber TG, Witte ON. Oncogene-specific activation of tyrosine kinase networks during prostate cancer progression. *Proceedings of the National Academy of Science* (2012) 109 (5): 1643-1648.

Janzen DM, Rosales MA, Paik DY, Lee DS, **Smith DA**, Witte ON, Iruela-Arispe ML, Memarzadeh S. Signaling through progesterone receptor in the tumor microenvironment is a key regulator of response to hormonal therapy. *Cancer Research* (2013)*In press.*

Smith DA, Kiba A, Zong Y, Witte ON. Interleukin-6 and oncostatin-M synergize with the PI3K/AKT pathway to promote aggressive prostate malignancy in mouse and human tissues. *In preparation for submission.*

Smith DA, Zong Y, Kiba A, Witte ON. (2012) The Role of Interleukin 6 and the Related Oncostatin M in Prostate Cancer. **Oral presentation** at the Molecular Biology Institute Departmental Retreat, Lake Arrowhead Conference Center, CA

Smith DA, Zong Y, Kiba A, Witte ON. (2011) A Novel Role for Oncostatin M in Prostate Tumorigenesis. **Oral presentation** for the Tumor Cell Biology Training Grant Seminar Series, UCLA, Los Angeles, CA.

Smith DA, Zong Y, Kiba A, Witte ON. (2010) A synergistic role for oncostatin-M in the progression of prostate cancer. **Oral presentation** for the Tumor Cell Biology Training Grant Seminar Series, UCLA, Los Angeles, CA.

Smith DA, Zong Y, Kiba A, Witte ON. (2012) A Novel Role for Oncostatin M Ligand in Prostate Tumorigenesis. **Poster presentation** for the AACR Special Conference in Cancer Research: Advances in Prostate Cancer Research, Orlando, FL.

Smith DA, Zong Y, Kiba A, Witte ON. (2011) A Novel Role for Oncostatin M in Prostate Cancer. **Poster presentation** for the Annual Molecular Biology Institute Departmental Retreat, Lake Arrowhead Conference Center, CA.

Smith DA, Zong Y, Kiba A, Witte ON. (2011) A Novel Role for Oncostatin M in Prostate Cancer. **Poster presentation** for the Microbiology, Immunology and Molecular Genetics Departmental Retreat, Los Angeles, CA.

Stoyanova T, Goldstein AS, Zong Y, **Smith DA**, Drake JM, Witte ON. (2011) Pathogenesis of Prostate Cancer. **Poster presentation** for the Annual UCLA ACCESS Affinity Fair, Los Angeles, CA.

Smith DA, Zong Y, Kiba A, Witte ON. (2011) A Novel Role for Oncostatin M Ligand in Prostate Tumorigenesis. **Poster presentation** for the Howard Hughes Medical Institute (HHMI) Annual Science Meeting, Bethesda, MD.

Smith DA, Zong Y, Kiba A, Witte ON. (2010) A Novel Role for Oncostatin M Ligand in Prostate Tumorigenesis. **Poster presentation** for the Molecular Biology Institute Departmental Retreat, Lake Arrowhead Conference Center, CA.

CHAPTER 1

Introduction

Genetic Mutation as the Driver of Tumorigenesis

At the most fundamental level, cancer consists of a series of pathological changes to the genome that manifest as unregulated cellular growth and replication (1). These genetic aberrations are generally characterized as either gain of function in oncogenes or as loss of function of tumor suppressors. Gain of function mutations often confer new functions or inhibit normal regulatory mechanisms, leading to hyper-activation of associated pathways as is commonly observed with activating mutations in the *ras* family of oncogenes (2). Conversely, loss of function mutations in tumor suppressors inhibit the function of proteins usually involved in restraining cellular growth and replication, such as PTEN, or response to genetic damage, such as the P53 and INK4A/ARF genes (3–5). Both gain or loss of function mutations can arise from a variety of mechanisms, including point mutations at critical residues within the protein, insertions or deletions that disrupt the normal gene structure, as well as variations in gene copy number that lead to aberrant expression (1).

Early studies of common mutations identified several core genes with common mutational "hot spots" that are consistently observed either within a single cancer type or throughout multiple cancers. One of the earliest examples of this phenomenon was in the *ras* gene family, where one of residues 12, 13 or 61 was mutated in nearly all tumor samples that exhibited activating *ras* mutations (2). Other examples include the V617F mutation in the JAK2 kinase that has been linked to hematological malignancies such as polycythemia vera and the V600E mutation in the BRAF gene

that is commonly associated with melanoma and colon cancers, among others (6, 7). Identification and characterization of these constitutively activated proteins have provided a platform for the interrogation of targeted therapies using small molecule pharmaceutical inhibitors. While not a single point mutation, the fusion of the Ableson (Abl) tyrosine kinase gene on chromosome 9 with the *Bcr* gene on chromosome 22 results in a protein that lacks the key regulatory domains and exhibits constitutive activity (8, 9). Imatinib, a small molecule inhibitor targeting this kinase, remains one of the most successful targeted therapies and has set the stage for a variety of successive generations of cancer therapeutics (10). Inhibition of the BRAF mutant in melanoma has shown promising results in clinical trials, while inhibitors targeting the MEK pathway have shown increasingly positive results in tumors harboring mutations in the RAS/RAF/MAPK pathway, among others (11, 12). Recent efforts targeting the JAK2 kinase in subsets of myeloproliferative disorders that harbor the V617F mutation discussed previously have recently been moved into clinical trials and are showing promising results (13). In addition to providing targets for small molecule inhibitors, these mutations can also serve as biomarkers that can be used to stratify patients in an effort to maximize clinical efficacy. Recent clinical trials utilizing the EGFR inhibitor gefitinib as a front-line therapy in screened patients that are positive for the EGFR mutation have shown dramatic increases in clinical response (14). This indicates that when combined with increasing use of histological and high-throughput analyses of tumor biopsies, these highly targeted drugs can provide tailored therapeutics through the use of patient stratification criteria (15).

The commonality of these single point mutations throughout a diverse range of cancers has lead to recent efforts to use massively parallel sequencing techniques at both the genome- and transcriptome-wide levels to interrogate large numbers of cancer specimens. These studies have lead to a more detailed understanding of the mutational frequency of previously identified mutations, as

well as prospective identification of novel mutations (16). This has lead to considerable advances in our understanding of the genetic mutations present in breast, colon, lung and pancreatic cancers, among others (17–21). Within the prostate field, recent analyses have identified previously unidentified mutations such as those in the SPOP genes. Interestingly, mutations in this gene were mutually exclusive of the common ETS-family re-arrangements and further our understanding of divergent origins for prostate cancer (22). These techniques can also be applied to revealing potential molecular drivers of rare cancer sub-types of prostate cancer, such as neuroendocrine prostate cancer. A recent study by Rubin and colleagues identified that neuroendocrine cancers were enriched for co-activation of the MYCN and aurora kinase A proteins, providing novel treatment strategies for this aggressive disease (23).

With the many successes of these sequencing techniques, this has potentially lead to an over-emphasis on identifying single point mutations as the functional units of tumorigenesis. Recent sequencing efforts of prostate cancer specimens indicate that prostate cancer exhibits consistently lower mutational frequencies than those observed in other cancers (24, 25). The most common genetic abnormalities observed in prostate cancer remain variations in gene copy number and chromosome translocations, which often lead to aberrant expression of genes not normally expressed in the prostate (24, 26, 27). The most common re-arrangement results in a fusion of the TMPRSS2 promoter with members of the ETS-family of transcription factors, which are normally restricted to the hematopoietic lineage (28). Upon fusion with the androgen-regulated TMPRSS2 promoter, is incorrectly expressed in prostate cells. The functional consequences of this fusion event in promoting prostate tumorigenesis have been confirmed by our laboratory and others (29). These and other studies indicate that a more complete understanding of the genetic landscape of prostate

cancer will require increased emphasis on how variations in the expression of genes can promote transformation in the absence of canonical single nucleotide mutations.

Prostate Anatomy and Physiology

The prostate is a sexual accessory glandular organ that is part of the male reproductive system. It largely consists of a secretory epithelium with a surrounding supportive mesenchyme and is divided into three primary zones: the peripheral, central and transition zones (30). The secretory epithelium of the prostate is comprised of three functionally distinct populations: basal, luminal and neuroendocrine, each of which perform specialized functions involved in the overall function of the prostate gland (31). The prostate basal cells form a semi-contiguous cellular layer along the basement membrane that separates the stromal and epithelial compartments. The luminal cells are specialized secretory cells that are designed to produce and secrete prostatic proteins into the luminal interior of the prostate. Finally, neuroendocrine cells are interspersed throughout the prostate and secrete neuroendocrine specific proteins whose precise function is still unclear (23).

Early experiments utilizing androgen withdrawal followed by re-administration indicated that there exist cells within the prostate that harbor regenerative potential and could represent an endogenous adult stem cell population (32). Work from our lab and others have shown that cells located within the basal cell population exhibit stem cell characteristics and are capable of multi-lineage differentiation, forming each of these distinct epithelial cell populations in prostate regeneration assays (33, 34). We have shown that these stem-like basal cells are efficient targets for transformation and could represent a cell of origin for human prostate cancer despite the ultimately luminal-like phenotype that is commonly observed in prostate cancer patients (34, 35). However, recent studies have shown that both basal and luminal cells are susceptible to transformation by loss

of the tumor suppressor PTEN when in the endogenous prostate niche (36). This indicates that either cell population may potentially function as a tumor cell of origin and is likely to be dependent upon the genetic context.

The Genetics of Prostate Cancer

Prostate cancer remains the most commonly diagnosed, non-cutaneous cancer and second leading cause of cancer-related mortality for men in the United States (37). The overwhelming majority of prostate cancer patients develop adenocarcinoma, an invasive neoplastic growth primarily characterized by the loss of the basal cell layer and overgrowth of the luminal cell population (38). Studies indicate that the prostate malignancy evolves through a series of stages, starting with benign hyperplasia followed by development of benign prostatic intraepithelial neoplasia, and finally, invasive adenocarcinoma (39). In advanced stages, these lesions disseminate throughout the body and establish metastases that primarily localize to the bone and local draining lymph nodes, though the mechanisms that dictate this specificity are still unknown (40). Despite the prevalence of prostate cancer, the mechanisms that drive prostate cancer initiation and progression are still poorly understood.

Various murine models of prostate cancer have been developed to address this issue (41). Models utilizing PTEN loss of function have proven particularly effective in recapitulating events observed in the human disease. Heterozygous PTEN loss of function is reported in at least 30% of primary cancers, with greater than 50% of metastasis exhibiting bi-allelic loss of function (42, 43). Loss of PTEN leads to activation of the PI3K/AKT pathway, of which the oncogenic activity has been shown in both autochthonous and tissue recombination model systems (33, 44). Autochthonous models of Pten loss exhibit varying degrees of aggressive pathology, with most displaying

hyperplasia and PIN at 2 months, invasive carcinoma at 4-6 months, and even rare metastases later in life (3, 45). The highly reproducible kinetics observed in PTEN loss of function models provide a foundation for interrogating factors that promote prostate cancer progression. These models have been used to investigate the roles of cell senescence proteins p53 and $p27^{Kip1}$ as well as other oncogenes commonly associated with transformation, such as KRAS (46, 47). The mechanisms that drive tumorigenesis following loss of PTEN remain poorly understood and are an active field of investigation.

Genetically modified mouse models of human disease remain indispensable tools for cancer research. Increasing availability of tissue, and even cell population specific promoters, has vastly improved the precision with which we can genetically alter cells *in situ*, thereby greatly expanding our ability to interrogate functional mechanisms that drive oncogenic phenotypes. However, the time and cost to generate new models can be prohibitively expensive, limiting their use when interrogating newly identified mutations. Further, differences between mouse and human physiology can also limit their use as drug discovery models. Therefore, our lab sought to develop a model system in which we would be able to readily interrogate the role of potential oncogenes in the development of prostate cancer that would also be readily adaptable to utilizing benign human primary tissue.

The Prostate Tissue Recombination System

Pioneering work by Cunha and colleagues, utilizing largely intact prostate epithelial and mesenchymal layers, built the foundations for interrogating prostate tissue development and interrogating the interactions between these two cell populations (48). Work in our laboratory has focused on the development and utilization of a dissociated prostate tissue regeneration assay to

interrogate oncogenic networks that are capable of initiating prostate tumorigenesis. This assay uses prostate tissue from donor mice, which is dissociated to single cells, recombined with inductive urogenital sinus mesenchymal (UGSM) cells, and engrafted under the kidney capsule (49). This model system allows for regeneration of prostate epithelial tissues and interrogation of either cell autonomous and paracrine factors that affect both regeneration and transformation. In starting with benign prostate epithelium, we are able interrogate the contributions of defined oncogenic stimuli to a transformation phenotype. Recent efforts in our lab have adapted this system to utilize benign human epithelium harvested from radical prostatectomy samples, allowing for interrogation of human tissues using defined oncogenic combinations (34). Using this system, we have begun to elucidate how different oncogenes cooperate to transform both human and mouse prostate epithelial tissues.

Interrogation of Complex Oncogenic Systems

Using the prostate tissue regeneration system, we have been able to recapitulate several stages of the prostate tumorigenesis system. Benign PIN lesions can be obtained by expression of a constitutively active AKT mutant, while progression to invasive and poorly differentiated phenotypes are observed with co-expression of AKT with ERG, AR, or activated KRAS, respectively (29, 50, 51). The reproducible kinetics and histological outcomes of this model system provide the foundation for further study into the mechanisms that drive tumorigenesis under these conditions.

Modulation of protein activity within a cell often occurs through post-transcriptional modifications, commonly through phosphorylation of key serine/threonine or tyrosine residues. These phosphorylated residues can modify the protein conformation, alter the enzymatic activity, and produce binding sites for protein-protein interactions, among other functions (52). The study of the

phosphoproteome allows for the interrogation of pathways that are activated during various cellular processes including mitosis and signal transduction (53, 54). These techniques have been used to interrogate pathways activated in non-small cell lung cancer, confirming previous findings concerning EGFR and c-Met while providing previously unidentified targets such as PDGFRα and DDR1 (55). Immunoaffinity techniques can also be used to enrich for phosphorylation of specific residues (56). Despite the prevalence of tyrosine kinases in contributing to human cancer, tyrosine phosphorylation is estimated to represent less than 1% of the phosphoproteome (57). To interrogate tyrosine phosphorylation, we utilized antibody affinity purification techniques designed to enrich for phosphorylated tyrosine residues from tumor lysates coupled with sensitive mass spectrometry analysis (51). Using this system, we were able to map tyrosine phosphorylation networks from tumors harboring defined oncogenic stimuli. By comparing the phosphoproteomic networks across different oncogenic origins, we can identify common signaling nodes that can be targeted therapeutically.

Tumorigenesis from Non-Mutated Proteins

Recent whole and targeted genome studies indicate that prostate cancer shows relatively few mutations in comparison to many other cancers. Despite the paucity of mutations, recent studies have identified that several pathways commonly associated with transformation are activated or deregulated in some fashion (24). This observation has led our lab to study how genes can function as oncogenes in their wild-type state through modulation of their expression levels.

The androgen receptor is a central pathway in the development and homeostasis of the prostate. At the onset of puberty, increased testosterone production from the testes activates the androgen receptor, spurring development of the male sexual organs. The dependence of the prostatic function

on continued androgen receptor signaling has been shown through the dramatic physiological changes following castration (32). Chemical castration remains one of the most effective treatments for advanced stage prostate cancer, though the vast majority of patients exhibit relapse and develop castration resistant prostate cancer (58). Resistance mechanisms that support castration resistant growth include amplification or mutation of the androgen receptor gene, intra-tumoral synthesis of androgens, or activation of the androgen receptor by alternative signaling pathways, among others (59). Gene amplification of the androgen receptor locus has been identified by several groups, though it appears to be a late event in prostate cancer development as is most commonly associated with metastasis (24). This increase in androgen receptor activity is widely thought to be responsible for the failure of current therapeutic regimes designed to inhibit the androgen receptor pathway (60).

Activation of the members of the SRC family of kinases has been shown in castration resistant prostate cancer as well as other tumors (61). We identified that while increased expression of either AR or SRC alone did not exhibit a robust transformation phenotype, combined over-expression of both AR and SRC was sufficient to transform prostate epithelium. This indicates that while genetically normal, increased expression of these proteins was sufficient to activate an oncogenic network and promote transformation and could explain in part the lack of mutations identified in prostate cancer.

This work led us to interrogate how members of the Src family of kinases could be involved in other transformation systems in the prostate. We had previously identified that increased expression of FGF10 in the stroma promotes tumorigenesis in the prostate epithelium (62). Studies have indicated that FGF10 activates SFK members, offering a potential mechanism of action (63). We found that loss of Src inhibited transformation by FGF10, indicating that this represents a crucial signaling node downstream of the FGF10 receptor (64). Further, we investigated whether other members of

the SFK family could also be involved in prostate tumorigenesis. We found that loss of Fyn and Lyn kinases inhibited transformation by FGF10, but not to the same degree as loss of Src. This same hierarchy was observed using constitutively active mutants of Src, Fyn and Lyn where Src exhibited the strongest oncogenic activity, followed by Fyn and then Lyn. This study indicates that non-mutated SFK family members can mediate oncogenic activity in the prostate, and that different family members can also exhibit functional redundancy in mediating transformation.

Chronic Inflammation in Cancer

Chronic inflammation is proposed as both an etiological and progression factor in many cancers including the colon, lung, liver and prostate (65, 66). Inflammation is observed in nearly all forms of cancer and may represent a central enabling characteristic of tumorigenesis at several stages from initiation, progression and metastasis (65, 67–69). Recent studies have begun elucidating the various factors involved in mediating this chronic inflammatory environment and the potential roles they play in promoting tumorigenesis. Chemokines such as CCL2 have been implicated in mediating metastatic spread of both colon and lung cancers through interactions with the endothelial and infiltrating myeloid cells (70–72). Infiltrating macrophages can increase expression of vascular endothelial growth factor (VEGF), increasing tumor angiogenesis and promoting tumor metastasis (73). Chronic inflammation is thought to increase reactive oxygen species in the local microenvironment and result in heightened levels of oxidative DNA damage (74). This continuous stream of DNA damage has been associated with the development of a sensescence-associated inflammatory state in surrounding benign cells and can lead to further increases in inflammatory cytokine production (75).

With respect to the prostate, chronic prostatitis is very prevalent and affects up to 1 in 5 men during their lifetime. Prospective analysis of autopsied male patients identified that over half of the cohort exhibited signs of chronic inflammation (76). In this same study, the authors identified that up to half of the prostates in which cancer was observed also exhibited signs of inflammation. Further, strong presence of tumor-infiltrating lymphocytes in prostate cancer has been linked to shortened time to biochemical recurrence indicated by rising PSA levels (77). Recent studies employing bacterial colonization of the prostate to elicit chronic inflammatory conditions have observed increased oxidative DNA damage (78), epithelial reactive hyperplasia (79) and murine intraepithelial neoplasia (mPIN) lesions (80). In an independent study using this model, loss of the prostate-specific tumor suppressor Nkx 3.1 was observed in regions of inflammation but not in adjacent normal tissue (81). Increased expression of inflammatory cytokines, including members of the interleukin-6 (IL6) family and others, has been observed in these models and could represent a functional mechanism (79, 82). Therefore, we sought to interrogate the role of inflammation in prostate cancer through over-expression of the pro-inflammatory cytokine IL6 and the related cytokine oncostatin-M (OSM). We identified that neither IL6 nor OSM alone were sufficient to promote transformation of prostate epithelium in our model system. In contrast, increased expression of either cytokine combined with loss of the PTEN tumor suppressor exhibited dramatic synergy with benign lesions induced by loss of PTEN progressing to advanced, invasive adenocarcinoma lesions.

References

1. Hanahan D, Weinberg RA (2000) The Hallmarks of Cancer. *Cell* 100:57–70.

2. Bos JL (1989) ras oncogenes in human cancer: a review. *Cancer Res* 49:4682–4689.

3. Wang S et al. (2003) Prostate-specific deletion of the murine Pten tumor suppressor gene leads to metastatic prostate cancer. *Cancer Cell* 4:209–221.

4. Levine AJ (1997) p53, the Cellular Gatekeeper for Growth and Division. *Cell* 88:323–331.

5. Chin L, Pomerantz J, DePinho RA (1998) The INK4a/ARF tumor suppressor: one gene—two products—two pathways. *Trends Biochem Sci* 23:291–296.

6. Michaloglou C, Vredeveld LCW, Mooi WJ, Peeper DS (2008) BRAF(E600) in benign and malignant human tumours. *Oncogene* 27:877–895.

7. Abe M et al. (2009) The polycythemia vera-associated Jak2 V617F mutant induces tumorigenesis in nude mice. *Int Immunopharmacol* 9:870–877.

8. Shtivelman E, Lifshitz B, Gale RP, Canaani E (1985) Fused transcript of abl and bcr genes in chronic myelogenous leukaemia. *Nature* 315:550–554.

9. Daley GQ, Etten RV, Baltimore D (1990) Induction of chronic myelogenous leukemia in mice by the P210bcr/abl gene of the Philadelphia chromosome. *Science* 247:824–830.

10. Druker BJ et al. (1996) Effects of a selective inhibitor of the Abl tyrosine kinase on the growth of Bcr–Abl positive cells. *Nat Med* 2:561–566.

11. Flaherty KT et al. (2010) Inhibition of Mutated, Activated BRAF in Metastatic Melanoma. *N Engl J Med* 363:809–819.

12. John Yuan W, Keith WM, Kenichi N, Sara W (2007) Recent Advances of MEK Inhibitors and Their Clinical Progress. *Curr Top Med Chem* 7:1364–1378.

13. Quintás-Cardama A et al. (2010) Preclinical characterization of the selective JAK1/2 inhibitor INCB018424: therapeutic implications for the treatment of myeloproliferative neoplasms. *Blood* 115:3109–3117.

14. Sequist LV et al. (2008) First-Line Gefitinib in Patients With Advanced Non–Small-Cell Lung Cancer Harboring Somatic EGFR Mutations. *J Clin Oncol* 26:2442–2449.

15. McDermott U, Settleman J (2009) Personalized Cancer Therapy With Selective Kinase Inhibitors: An Emerging Paradigm in Medical Oncology. *J Clin Oncol* 27:5650–5659.

16. Meyerson M, Gabriel S, Getz G (2010) Advances in understanding cancer genomes through second-generation sequencing. *Nat Rev Genet* 11:685–696.

17. Sjöblom T et al. (2006) The Consensus Coding Sequences of Human Breast and Colorectal Cancers. *Science* 314:268–274.

18. Wood LD et al. (2007) The Genomic Landscapes of Human Breast and Colorectal Cancers. *Science* 318:1108–1113.

19. Ding L et al. (2008) Somatic mutations affect key pathways in lung adenocarcinoma. *Nature* 455:1069–1075.

20. Jones S et al. (2008) Core Signaling Pathways in Human Pancreatic Cancers Revealed by Global Genomic Analyses. *Science* 321:1801–1806.

21. Parsons DW et al. (2008) An Integrated Genomic Analysis of Human Glioblastoma Multiforme. *Science* 321:1807–1812.

22. Barbieri CE et al. (2012) Exome sequencing identifies recurrent SPOP, FOXA1 and MED12 mutations in prostate cancer. *Nat Genet* 44:685–689.

23. Beltran H et al. (2011) Molecular Characterization of Neuroendocrine Prostate Cancer and Identification of New Drug Targets. *Cancer Discov* 1:487–495.

24. Taylor BS et al. (2010) Integrative Genomic Profiling of Human Prostate Cancer. *Cancer Cell* 18:11–22.

25. Berger MF et al. (2011) The genomic complexity of primary human prostate cancer. *Nature* 470:214–220.

26. Taylor BS et al. (2008) Functional Copy-Number Alterations in Cancer. *Plos One* 3:e3179.

27. Albertson DG, Collins C, McCormick F, Gray JW (2003) Chromosome aberrations in solid tumors. *Nat Genet* 34:369–376.

28. Tomlins SA et al. (2005) Recurrent Fusion of TMPRSS2 and ETS Transcription Factor Genes in Prostate Cancer. *Science* 310:644–648.

29. Zong Y et al. (2009) ETS family transcription factors collaborate with alternative signaling pathways to induce carcinoma from adult murine prostate cells. *Proc Natl Acad Sci* 106:12465–12470.

30. Lee CH, Akin-Olugbade O, Kirschenbaum A (2011) Overview of Prostate Anatomy, Histology, and Pathology. *Endocrinol Metab Clin North Am* 40:565–575.

31. Lawson DA, Witte ON (2007) Stem cells in prostate cancer initiation and progression. *J Clin Invest* 117:2044–2050.

32. English HF, Santen RJ, Isaacs JT (1987) Response of glandular versus basal rat ventral prostatic epithelial cells to androgen withdrawal and replacement. *Prostate* 11:229–242.

33. Xin L, Lawson DA, Witte ON (2005) The Sca-1 cell surface marker enriches for a prostate-regenerating cell subpopulation that can initiate prostate tumorigenesis. *Proc Natl Acad Sci U S A* 102:6942 –6947.

34. Goldstein AS, Huang J, Guo C, Garraway IP, Witte ON (2010) Identification of a cell of origin for human prostate cancer. *Science* 329:568–571.

35. Lawson DA et al. (2010) Basal epithelial stem cells are efficient targets for prostate cancer initiation. *Proc Natl Acad Sci U S A* 107:2610–2615.

36. Choi N, Zhang B, Zhang L, Ittmann M, Xin L (2012) Adult Murine Prostate Basal and Luminal Cells Are Self-Sustained Lineages that Can Both Serve as Targets for Prostate Cancer Initiation. *Cancer Cell* 21:253–265.

37. Siegel R, Naishadham D, Jemal A (2013) Cancer statistics, 2013. *CA Cancer J Clin* 63:11–30.

38. Grignon DJ (2004) Unusual subtypes of prostate cancer. *Mod Pathol* 17:316–327.

39. Shen MM, Abate-Shen C (2010) Molecular genetics of prostate cancer: new prospects for old challenges. *Genes Dev* 24:1967–2000.

40. Bubendorf L et al. (2000) Metastatic patterns of prostate cancer: An autopsy study of 1,589 patients. *Hum Pathol* 31:578–583.

41. Roy-Burman P, Wu H, Powell WC, Hagenkord J, Cohen MB (2004) Genetically defined mouse models that mimic natural aspects of human prostate cancer development. *Endocr Relat Cancer* 11:225 –254.

42. Cairns P et al. (1997) Frequent Inactivation of PTEN/MMAC1 in Primary Prostate Cancer. *Cancer Res* 57:4997 –5000.

43. Suzuki H et al. (1998) Interfocal Heterogeneity of PTEN/MMAC1 Gene Alterations in Multiple Metastatic Prostate Cancer Tissues. *Cancer Res* 58:204 –209.

44. Majumder PK et al. (2003) Prostate intraepithelial neoplasia induced by prostate restricted Akt activation: The MPAKT model. *Proc Natl Acad Sci* 100:7841 –7846.

45. Ma X et al. (2005) Targeted Biallelic Inactivation of Pten in the Mouse Prostate Leads to Prostate Cancer Accompanied by Increased Epithelial Cell Proliferation but not by Reduced Apoptosis. *Cancer Res* 65:5730 –5739.

46. Chen Z et al. (2005) Crucial role of p53-dependent cellular senescence in suppression of Pten-deficient tumorigenesis. *Nature* 436:725–730.

47. Di Cristofano A, De Acetis M, Koff A, Cordon-Cardo C, P Pandolfi P (2001) Pten and p27KIP1 cooperate in prostate cancer tumor suppression in the mouse. *Nat Genet* 27:222–224.

48. Lw C et al. (1980) Tissue interactions in prostate development: roles of sex steroids. *Prog Clin Biol Res* 75A:177–203.

49. Xin L, Ide H, Kim Y, Dubey P, Witte ON (2003) In vivo regeneration of murine prostate from dissociated cell populations of postnatal epithelia and urogenital sinus mesenchyme. *Proc Natl Acad Sci* 100:11896–11903.

50. Xin L et al. (2006) Progression of prostate cancer by synergy of AKT with genotropic and nongenotropic actions of the androgen receptor. *Proc Natl Acad Sci* 103:7789–7794.

51. Drake JM et al. (2012) Oncogene-specific activation of tyrosine kinase networks during prostate cancer progression. *Proc Natl Acad Sci* 109:1643–1648.

52. Cohen P (2002) The origins of protein phosphorylation. *Nat Cell Biol* 4:E127–E130.

53. Daub H et al. (2008) Kinase-Selective Enrichment Enables Quantitative Phosphoproteomics of the Kinome across the Cell Cycle. *Mol Cell* 31:438–448.

54. Morandell S et al. (2006) Phosphoproteomics strategies for the functional analysis of signal transduction. *PROTEOMICS* 6:4047–4056.

55. Rikova K et al. (2007) Global Survey of Phosphotyrosine Signaling Identifies Oncogenic Kinases in Lung Cancer. *Cell* 131:1190–1203.

56. Rush J et al. (2005) Immunoaffinity profiling of tyrosine phosphorylation in cancer cells. *Nat Biotechnol* 23:94–101.

57. Del Rosario AM, White FM (2010) Quantifying oncogenic phosphotyrosine signaling networks through systems biology. *Curr Opin Genet Dev* 20:23–30.

58. Huggins C, Hodges CV (1941) Studies on Prostatic Cancer. I. The Effect of Castration, of Estrogen and of Androgen Injection on Serum Phosphatases in Metastatic Carcinoma of the Prostate. *Cancer Res* 1:293–297.

59. Yap TA, Zivi A, Omlin A, de Bono JS (2011) The changing therapeutic landscape of castration-resistant prostate cancer. *Nat Rev Clin Oncol* 8:597–610.

60. Chen CD et al. (2004) Molecular determinants of resistance to antiandrogen therapy. *Nat Med* 10:33–39.

61. Tatarov O et al. (2009) Src Family Kinase Activity Is Up-Regulated in Hormone-Refractory Prostate Cancer. *Clin Cancer Res* 15:3540–3549.

62. Memarzadeh S et al. (2007) Enhanced Paracrine FGF10 Expression Promotes Formation of Multifocal Prostate Adenocarcinoma and an Increase in Epithelial Androgen Receptor. *Cancer Cell* 12:572–585.

63. Sandilands E et al. (2007) Src kinase modulates the activation, transport and signalling dynamics of fibroblast growth factor receptors. *EMBO Rep* 8:1162–1169.

64. Cai H et al. (2011) Differential transformation capacity of Src family kinases during the initiation of prostate cancer. *Proc Natl Acad Sci* 108:6579 –6584.

65. Hanahan D, Weinberg RA (2011) Hallmarks of Cancer: The Next Generation. *Cell* 144:646–674.

66. De Marzo AM et al. (2007) Inflammation in prostate carcinogenesis. *Nat Rev Cancer* 7:256–269.

67. Hussain SP, Hofseth LJ, Harris CC (2003) Radical causes of cancer. *Nat Rev Cancer* 3:276–285.

68. Visser KE de, Eichten A, Coussens LM (2006) Paradoxical roles of the immune system during cancer development. *Nat Rev Cancer* 6:24–37.

69. Qian B-Z, Pollard JW (2010) Macrophage Diversity Enhances Tumor Progression and Metastasis. *Cell* 141:39–51.

70. Van Deventer HW, Palmieri DA, Wu QP, McCook EC, Serody JS (2013) Circulating Fibrocytes Prepare the Lung for Cancer Metastasis by Recruiting Ly-6C+ Monocytes Via CCL2. *J Immunol Baltim Md 1950* 190:4861–4867.

71. Zhao L et al. (2013) Recruitment of a myeloid cell subset (CD11b/Gr1 mid) via CCL2/CCR2 promotes the development of colorectal cancer liver metastasis. *Hepatol Baltim Md* 57:829–839.

72. Wolf MJ et al. (2012) Endothelial CCR2 signaling induced by colon carcinoma cells enables extravasation via the JAK2-Stat5 and p38MAPK pathway. *Cancer Cell* 22:91–105.

73. Ruffell B, Affara NI, Coussens LM (2012) Differential macrophage programming in the tumor microenvironment. *Trends Immunol* 33:119–126.

74. Pavlides S et al. (2010) The autophagic tumor stroma model of cancer: Role of oxidative stress and ketone production in fueling tumor cell metabolism. *Cell Cycle Georget Tex* 9:3485–3505.

75. Rodier F et al. (2009) Persistent DNA damage signalling triggers senescence-associated inflammatory cytokine secretion. *Nat Cell Biol* 11:973–979.

76. Delongchamps NB et al. (2008) Evaluation of Prostatitis in Autopsied Prostates—Is Chronic Inflammation More Associated With Benign Prostatic Hyperplasia or Cancer? *J Urol* 179:1736–1740.

77. Kärjä V et al. (2005) Tumour-infiltrating lymphocytes: A prognostic factor of PSA-free survival in patients with local prostate carcinoma treated by radical prostatectomy. *Anticancer Res* 25:4435–4438.

78. Elkahwaji JE, Zhong W, Hopkins WJ, Bushman W (2007) Chronic bacterial infection and inflammation incite reactive hyperplasia in a mouse model of chronic prostatitis. *The Prostate* 67:14–21.

79. Boehm BJ, Colopy SA, Jerde TJ, Loftus CJ, Bushman W (2012) Acute bacterial inflammation of the mouse prostate. *The Prostate* 72:307–317.

80. Elkahwaji JE, Hauke RJ, Brawner CM (2009) Chronic bacterial inflammation induces prostatic intraepithelial neoplasia in mouse prostate. *Br J Cancer* 101:1740–1748.

81. Khalili M et al. (2010) Loss of Nkx3.1 expression in bacterial prostatitis: a potential link between inflammation and neoplasia. *Am J Pathol* 176:2259–2268.

82. Jerde TJ, Bushman W (2009) IL-1 Induces IGF-Dependent Epithelial Proliferation in Prostate Development and Reactive Hyperplasia. *Sci Signal* 2:ra49.

CHAPTER 2

Oncogene-Specific Activation of Tyrosine Kinase Networks During Prostate Cancer Progression

Justin M. Drake[a], Nicholas A. Graham[b,c], Tanya Stoyanova[a], Amir Sedghi[a], Andrew S. Goldstein[c,d,e,k], Houjian Cai[a,l], **Daniel A. Smith[a,f]**, Hong Zhang[g], Evangelia Komisopoulou[b,c,h,i], Jiaoti Huang[d,g,k], Thomas G. Graeber[b,c,h,i], Owen N. Witte[a,c,j,k,*]

[a]Department of Microbiology, Immunology, and Molecular Genetics,

[b]Crump Institute for Molecular Imaging,

[c]Department of Molecular and Medical Pharmacology,

[d]Jonsson Comprehensive Cancer Center,

[e]Department of Urology,

[f]Molecular Biology Institute Interdepartmental Ph.D. Program,

[g]Department of Pathology and Laboratory Medicine,

[h]Institute for Molecular Medicine, [i]California NanoSystems Institute, and

[j]Howard Hughes Medical Institute, David Geffen School of Medicine, UCLA, Los Angeles, CA 90095, USA.

[k]Eli and Edythe Broad Center of Regenerative Medicine and Stem Cell Research, UCLA, Los Angeles, CA 90095, USA.

[l]Current location: Department of Medicine and Hollings Cancer Center, Medical University of South Carolina, Charleston, SC 29425.

Abstract

Dominant mutations or DNA amplification of tyrosine kinases are rare among the oncogenic alterations implicated in prostate cancer. We demonstrate that castration resistant prostate cancer in man exhibits increased tyrosine phosphorylation, raising the question of whether enhanced tyrosine kinase activity is observed in prostate cancer in the absence of specific tyrosine kinase mutation or DNA amplification. We generated a mouse model of prostate cancer progression using commonly perturbed non-tyrosine kinase oncogenes and pathways and detected a significant upregulation of tyrosine phosphorylation at the carcinoma stage. Phosphotyrosine peptide enrichment and quantitative mass spectrometry identified oncogene-specific tyrosine kinase signatures, including activation of EGFR, EPHA2 and JAK2. Kinase:substrate relationship analysis of the phosphopeptides also revealed ABL and SRC tyrosine kinase activation. The observation of elevated tyrosine kinase signaling in advanced prostate cancer and identification of specific tyrosine kinase pathways from genetically-defined tumor models points to new therapeutic approaches using tyrosine kinase inhibitors for advanced prostate cancer.

Introduction

The future of effective cancer treatment is based on the emerging concept of personalized therapy which requires detailed analysis of the oncogenic lesions that drive disease. One prominent oncogenic change seen in many cancers is somatic activating mutations of tyrosine kinases, including BCR-ABL in CML, c-KIT in gastrointestinal stromal tumors (GIST), and EGFR in lung cancer (1-3). The dependency on tyrosine kinase activation in these tumors has led to successful clinical treatment with tyrosine kinase inhibitors (4-6). In prostate cancer, great progress has been made in identifying the genetic determinants of disease progression such as increased expression of androgen receptor (AR) and MYC, *PTEN* deletion, and ETS family gene fusions (7-11). However, recent

large-scale cancer genome studies show that activating somatic mutations or DNA amplification of tyrosine kinase genes are rare in prostate cancer (8). This reveals why administration of tyrosine kinase inhibitors clinically for the treatment of advanced prostate cancer has been less effective and strongly implies that a more complete understanding of the tyrosine kinases that contribute to this disease is warranted (12, 13).

Despite the paucity of activating somatic mutations in tyrosine kinases, recent evidence suggests that tyrosine kinase phosphorylation in prostate cancer contributes to disease progression. In androgen depleted conditions, ACK1, SRC, and HER-2/neu tyrosine kinase activity can restore AR function in prostate cancer cells (14-17). Increased expression of the tyrosine kinase c-SRC and AR can synergistically drive frank carcinoma of the mouse prostate (18). This relationship results in robust activation of SRC tyrosine kinase and MAPK signaling (18). SRC activity was also observed in a subset of castration resistant prostate cancer (CRPC) patients which correlated with lower overall survival and increased metastatic disease (19). This data supports the idea that tyrosine kinase activity may play a prominent role in prostate cancer progression in the absence of activating mutations.

Nearly 50% of tyrosine kinases are thought to contribute to human cancers, yet tyrosine phosphorylation represents less than 1% of the phosphoproteome (20). Sensitive and specific methods capable of enriching tyrosine phosphorylated peptides via antibody binding followed by quantitative mass spectrometry (MS) identification has become useful for the elucidation of tyrosine kinase signaling pathways, nodes, and negative feedback mechanisms in different cancer types (21-23). The ability to sensitively characterize pathway alterations in the presence of activated tyrosine kinases or tyrosine kinase inhibitors can allow for the identification of new potential drug targets (21, 24). We utilize this approach to identify and characterize tyrosine kinase signaling networks in transformed tissues that do not express mutated tyrosine kinases.

Global tyrosine phosphorylation in clinical prostate cancer samples was measured by immunohistochemistry (IHC) and showed a substantial increase in tyrosine phosphorylation in late stage disease. To study this in a controlled manner, we evaluated tyrosine phosphorylation in a mouse model of prostate cancer progression using oncogenes common to prostate tumorigenesis and observed robust tyrosine phosphorylation in the advanced tumor phenotypes. Unbiased phosphotyrosine proteomics was used to investigate the specific tyrosine kinase signaling pathways activated by each of the non-tyrosine kinase oncogenes. Analysis of the tyrosine phosphoproteome of these tumors revealed oncogene-specific tyrosine kinase activation including EGFR, EPHA2, JAK2, ABL, and SRC.

Results

Tyrosine phosphorylation is increased in clinical castration resistant prostate cancer samples. We performed IHC staining of prostate cancer tissue microarrays with the tyrosine phosphorylation specific antibody 4G10 to evaluate phosphotyrosine expression during disease progression. Castration resistant (androgen independent) prostate cancer (CRPC) exhibited a robust increase in phosphotyrosine staining intensity when compared to benign prostate, the precursor lesion high grade prostatic intraepithelial neoplasia (HGPIN), or hormone naïve (androgen-dependent) prostate cancer (HNPC) (Fig. 1A). Analysis of these tissue microarray samples indicated that 44% of CRPC specimens stain for phosphotyrosine at moderate to high levels (staining intensity 2-3), while only 11% of normal, 2% of HGPIN, and 2% of HNPC (Fig. 1B). Further, the average staining intensity of all the CRPC tissue samples was significantly increased by over 2-fold when compared to the other clinical phenotypes (Fig. 1C). This data reveals that tyrosine phosphorylation is present and elevated in CRPC and raises the notion that systemic treatment of patients with this disease may induce this response.

Tyrosine phosphorylation is robust in mouse models of advanced prostate cancer. The observation of increased tyrosine phosphorylation in late stage prostate cancer specimens raises the question of whether tyrosine kinase activity is evident in prostate cancer models that do not express mutated or amplified tyrosine kinases. We recapitulated different stages of prostate cancer ranging from PIN to adenocarcinoma using the prostate in vivo regeneration model system (25, 26). We chose four of the most commonly perturbed oncogenes in prostate cancer, both in androgen dependent and independent states: activated AKT (myristoylated AKT, resembling *PTEN* deletion, ~40-70% of prostate cancers), AR amplification (~20-60% of prostate cancers), ERG rearrangements (~40-70% of prostate cancers), and activated K-RAS (K-RASG12V, resembling RAS/RAF pathway activation, observed in ~40-50% of prostate cancers) (7, 8, 11, 27-30).

We infected total mouse prostate cells with AKT alone or in combination with each respective oncogene using a lentiviral vector delivery system (Fig. 2A) and evaluated the histological phenotype of the resulting tumors after 12 weeks. These tumors displayed histological characteristics of PIN (AKT), well-differentiated and less aggressive cancer (AKT/ERG), or adenocarcinoma (AKT/AR and AKT/K-RASG12V) (Fig. 2B). IHC and western blot analysis confirmed ectopic expression of each oncogene (Fig. S1A-B). IHC staining and western blot analyses displayed a gradient of phosphotyrosine expression in these tumors ranging from low to undetectable levels of tyrosine phosphorylation in the normal and indolent lesions (mouse prostate, AKT, or AKT/ERG) to very high levels in the more advanced tumors (AKT/AR and AKT/K-RASG12V) (Fig. 2B, S2A-B).

Phosphoproteomic profiling identifies oncogene-dependent tyrosine phosphorylation of kinases and phosphatases. We enriched for tyrosine phosphorylated peptides and performed

quantitative label-free MS to identify phosphopeptides that contribute to this increased tyrosine phosphorylation (21, 31). We identified 139 phosphopeptides corresponding to 102 proteins (Table S1). Statistical analysis (ANOVA, 0.2 cutoff) revealed differential phosphorylation of 116 phosphopeptides corresponding to 87 proteins across all of the tumor phenotypes. Unsupervised hierarchical clustering analysis identified unique and overlapping patterns of tyrosine phosphorylated peptides for each tumor type, with an increased abundance of tyrosine phosphorylation events observed in the more advanced tumors (AKT/AR and AKT/K-RASG12V) (Fig. 3A, S3). These data demonstrate oncogene-specific signatures of phosphotyrosine activation across the spectrum of prostate cancer progression.

From the MS data, the activation sites of several tyrosine kinases and protein phosphatases were identified in the specific tumor types (Table 1, Fig. S3, S4) (32). Consistent with these findings, western blotting confirmed high levels of a second EGFR phosphorylation site (Y^{1068}) and PTPN11 (SHP-2) Y^{584} in AKT/ERG tumors (Fig. 3B). Activation of the JAK/STAT pathway was also revealed in AKT/AR tumors as high levels of phosphorylation of STAT3 Y^{705} were observed. Western blotting confirmed activation of the upstream kinase JAK2$^{Y1007/08}$ and STAT3 Y^{705} in this tumor type (Fig. 3B). We additionally identified an increase in phosphorylation of PTK2B/PYK2/FAK2 Y^{579} and Y^{849} in AKT/K-RASG12V tumors and western blot confirmed the phosphorylation of the activation site Y^{402} of PTK2B (Fig. 3B). Together, this data demonstrates that each combination of prostate cancer oncogenes generates distinct patterns of tyrosine kinase and phosphatase activity.

Bioinformatic inference of tyrosine kinase activity reveals enrichment of dasatinib targets in AKT/AR tumors. In addition to direct observation of phosphorylated tyrosine kinases and

phosphatases by MS, we sought to use the phosphotyrosine peptide data to infer kinase activities specific to each tumor type. We predicted the activated kinases directly upstream for each observed phosphorylation site using known relationships from PhosphoSite (32), kinase motifs from PhosphoMotif Finder (33) and Phosida (34), and predictions from NetworKin (35). We then performed an enrichment analysis of kinase-associated phosphorylation targets (see Methods) to determine which kinase activities were predicted to be highly active in each tumor type.

Using this unbiased bioinformatic approach, we identified a statistically significant enrichment of the EGFR kinase substrate (D|E)pY in AKT/ERG but not in AKT/AR or AKT/K-RASG12V tumors (Fig. S5, Table S2). Notably, this bioinformatic prediction was in direct agreement with our phosphoproteomic and western blot data (Fig. 3B). Inference of kinase activity in AKT/K-RASG12V tumors further revealed an enrichment of ERK1/2 and MEK1/2 substrates, consistent with direct activation of MAPK signaling by the K-RASG12V oncogene (Fig. 4B, S4, Table S2) (36).

Evaluating kinase activity from AKT/AR phosphopeptides revealed statistically significant enrichment of two motifs associated with ABL and SRC kinases (EXIpYXXP and (I|V|L|S)XpYXX(L|I), respectively) (37). Because these kinases are both targets of the tyrosine kinase inhibitor, Dasatinib, we combined these motifs into a "Dasatinib target" group and found enrichment of predicted ABL and SRC substrates in AKT/AR tumors (Fig. 4A, Table S2). AKT/K-RASG12V and AKT/ERG tumors demonstrated modest and no enrichment of these motifs, respectively. Western blotting and IHC validated this bioinformatic prediction, as both SRC Y^{416} and ABL Y^{245} were highly phosphorylated only in the AKT/AR tumor type while SRC Y^{416} but not ABL Y^{245} were phosphorylated in AKT/ERG and AKT/K-RASG12V tumors (Fig. 4B, C). This result demonstrates that substrate-based bioinformatic approaches for inferring kinase activity can reveal

oncogene-specific tyrosine kinase activation not originally identified directly by phospho-MS.

Assembly of oncogene-specific tyrosine kinase signaling networks from phosphoproteomic data and public databases. We next sought to combine our phosphopeptide and bioinformatics data with information from public databases of protein-protein interactions (Human Protein Reference Database (HPRD)) and post-translational modifications (Phosphosite) to manually construct tyrosine kinase signaling networks for each oncogene combination. In AKT/ERG tumors, identification of the EGFR substrate Y^{771} of phospholipase C, gamma 1 (PLCG1) and EGFR interacting proteins catenin, delta 1 (p120 catenin, CTNND1), PTPN11, and PTPRA suggest strong association and activation of the EGFR tyrosine kinase pathway (Fig. 5). In AKT/AR tumors, detection of elevated SRC and ABL activity prompted us to investigate other substrates and binding partners of these kinases within our phosphoproteomic data. The identification of SRC and ABL substrates Y^{705} of STAT3, Y^{14} of caveolin-1 (CAV-1) and $Y^{1007/1008}$ of JAK2 with binding partners vinculin (VCL) Y^{822}, paxillin (PXN) Y^{118}, CTNND1 Y^{96}, and PTPN11 Y^{62} suggest that, along with JAK2, these kinases act in concert towards the development of AKT/AR tumors (Fig. 5). The identification of the activation site of EPHA2 Y^{595} and downstream effectors ERK1 Y^{204} and ERK2 Y^{184} reveals strong MAPK activation in AKT/K-RASG12V tumors (Fig. 5). Further, the identification of VCL Y^{822} and PXN Y^{118} in AKT/AR and AKT/K-RASG12V tumors suggests that regulation of focal adhesions may be important for motility and survival in these tumors. The phosphorylation of PXN at Y^{118} by focal adhesion kinase (FAK) increases cell motility and survival which are characteristic features of cells that have undergone an epithelial-to-mesenchymal transition (EMT) (38). The possibility of an EMT phenotype would be consistent with previous tumor phenotypes where SRC activation was observed (18). The manual curation of phosphotyrosine networks suggest novel associations of tyrosine kinase signaling with defined oncogenic insults in

prostate cancer.

Discussion

Many studies have linked the aberrant activation of tyrosine kinases by somatic mutation or DNA amplification to a wide array of cancers (39, 40). We demonstrate oncogene-specific signatures of global phosphotyrosine activity without ectopic expression of mutant tyrosine kinases in a mouse model of prostate cancer progression. This activation of tyrosine kinase signaling suggests the presence of alternative mechanisms regulating tyrosine kinase activity not related to activating mutations (18, 21, 22). These include but are not limited to loss of negative feedback mechanisms (e.g. increased or decreased phosphatase activity), transcriptional upregulation of kinases, or increased stabilization of tyrosine kinases through decreased protein degradation (22, 41, 42). Our data suggests that some of these mechanisms may control tyrosine kinase signaling in our mouse model of prostate cancer.

Tyrosine phosphorylation of the protein tyrosine phosphatase PTPN11 may contribute to the phosphotyrosine signatures observed in our tumors. Activity of this phosphatase is often associated with increased signaling activity (43, 44). This phosphatase was highly phosphorylated on Y^{62} and Y^{584} in AKT/AR and AKT/ERG tumors, respectively. In EGFR expressing fibroblasts, epidermal growth factor (EGF) stimulation resulted in Y^{584} phosphorylation of PTPN11 leading to RAS/ERK pathway activation (45). This supports our findings that Y^{584} of PTPN11 is highly phosphorylated in AKT/ERG tumors and suggests receptor tyrosine kinase pathway-mediated activation of PTPN11. PTPN11 inhibition leads to decreased xenograft growth of lung and prostate tumors and reduced activity of numerous tyrosine kinases, including SRC (46). PTPN11 $Y^{62/63}$ activation results in tyrosine dephosphorylation of the inactive site of SRC Y^{530} by regulation of the Csk regulator

PAG/Cbp, indicating that SRC activity in AKT/AR tumors may be dependent on PTPN11 activation (43, 46).

Transcriptional upregulation of tyrosine kinases may also enhance tyrosine kinase activity as suggested by the phosphorylation of EPHA2 at Y^{595} in the AKT/K-RASG12V tumors. EPHA2 was shown to be a transcriptional target of the RAS-MAPK pathway and ligand stimulated EPHA2 negatively regulates RAS activity (47). Constitutive activation of RAS through mutation bypasses the negative regulation of EPHA2 and results in increased MAPK activation, which is in direct agreement with our phosphoproteomic data. This may reveal why high expression levels of EPHA2 protein are observed in breast and prostate cancer and supports further clinical investigation of the connection between RAS mutation and EPHA2 status in these diseases (48, 49).

Tyrosine kinase activation offers therapeutic opportunities following the emerging successes of tyrosine kinase inhibitor therapies (5, 50). Our observation of SRC activity supports previous work that this kinase synergizes with other genes, including AR, to contribute to prostate adenocarcinoma (18, 51). SRC has also been shown to interact with the intracellular region of HER2 supporting the notion that Src may be an important node for targeted therapy in advanced prostate cancer (17, 52). In support of this data, the SRC and ABL tyrosine kinase inhibitor Dasatinib in combination with docetaxel is currently in phase III clinical trials for advanced prostate cancer and has shown modest phase I/II trial results in overall patient survival (53). Due to the heterogeneity of prostate cancer, this modest effect may be a result of the general administration of Dasatinib without stratification of patients based on SRC and ABL activity.

Strong activation of the EGFR pathway was observed in AKT/ERG-expressing mouse prostate

tumors. Roughly half of all prostate cancer patients display the *TMPRSS2-ERG* translocation, a gene re-arrangement fusing the androgen regulated promoter of *TMPRSS2* with the ETS transcription factor *ERG*, which is considered to be a marker for prostate cancer progression from PIN to adenocarcinoma (54). The product of the *TMPRSS2-ERG* translocation was shown to interact with the enzyme poly (ADP-ribose) polymerase 1 (PARP1) and inhibition of this enzyme abrogates growth of prostate cancer xenografts that ectopically express Erg (55). PARP1 inhibition represents the first specific treatment option for patients with *TMPRSS2-ERG* translocations. Our data suggests that EGFR activity level is another candidate target in patients with *TMPRSS2-ERG* translocations. This is in agreement with recent reports of $SPINK1^{+}/ETS^{-}$ prostate cancers where SPINK1-mediated growth occurs via EGFR signaling, demonstrating alternative pathways to activate EGFR (56). It will be important to further evaluate the relationship between EGFR activity and ERG clinically.

Our data suggests the molecular stratification of patients to target prostate cancer with tyrosine kinase inhibitors even in tumors without obvious tyrosine kinase mutations. Future work will extend this approach to prostate cancer patients to match tyrosine kinase inhibitor therapies with signaling activation patterns for targeted treatment of this disease.

Materials and Methods

Lentiviral vector construction, Prostate regeneration and prostate epithelial viral infections, Western Blot and Immunohistochemistry, and Clinical Prostate Tissue Microarrays can be found in Supplementary Materials.

Quantitative analysis of phosphotyrosine peptides by mass spectrometry

300-500 mg of frozen tumor mass was homogenized and sonicated in urea lysis buffer (20 mM

HEPES pH 8.0, 9 M urea, 2.5 mM sodium pyrophosphate, 1.0 mM beta-glycerophosphate, 1% N-octyl glycoside, 2 mM sodium orthovanadate). 35 mg of total protein was used for phosphotyrosine peptide immunoprecipitation as previously described (21, 57, 58). Additional details can be found in the Supplementary Materials.

Prediction of Kinase-Substrate Relationships

For each phospho-peptide, we predicted the potential upstream kinases using three types of data: i) NetworKIN 2.0 kinase-substrate relationships (http://networkin.info/version_2_0/search.php), ii) PhosphoSite kinase-substrate dataset (http://www.phosphosite.org/), and iii) consensus kinase motifs culled from the Human Protein Reference Database's PhosphoMotif Finder (http://www.hprd.org/PhosphoMotif_finder) and Phosida (http://www.phosida.de/).

Enrichment Analysis of Kinase activity

Phospho-tyrosine peptides were ranked by the signal-to-noise ratio observed for a given perturbation (e.g. AKT/AR tumors compared to AKT alone). Having annotated the phospho-peptides with their predicted upstream kinases, we calculated a Kolmogorov-Smirnov statistic against the expected distribution for each upstream kinase. The statistical significance of enrichment was then determined by permutation analysis. This approach is analogous to the Normalized Enrichment Score of Gene Set Enrichment Analysis (59). The enrichment scores for all putative upstream kinases are shown in Table S2. Additional details can be found in the Supplementary Materials.

Acknowledgments

We thank members of the Witte lab for helpful comments and discussion on the manuscript. We thank the Tissue Procurement Core Laboratory at University of California, Los Angeles (UCLA) for assistance on tissue processing and H&E staining. JMD is supported by the Department of Defense

Prostate Cancer Research Program (PC101928). JMD, NAG, and DAS are supported by the UCLA Tumor Biology Program (US Department of Health and Human Services, Ruth L. Kirschstein Institutional National Research Service Award no. T32 CA009056). TS is supported by the California Institute for Regenerative Medicine Training Grant (TG2-01169). ASG is supported by a Career Development Award from the SPORE in prostate cancer (PI: Robert Reiter). JH is supported by UCLA SPORE in Prostate Cancer (PI: Robert Reiter), Department of Defense Prostate Cancer Research Program (PC101008), CalTech-UCLA Joint Center for Translational Medicine Program, and National Cancer Institute (1R01CA158627-01; PI: Leonard Marks). TGG is partially supported by the CalTech-UCLA Joint Center for Translational Medicine. JH and ONW are supported by a Prostate Cancer Foundation Challenge Award (PI: Owen Witte). ONW is an Investigator of the Howard Hughes Medical Institute.

Figure Legends

Figure 1. Robust phosphotyrosine expression is observed in castration resistant prostate cancer (CRPC) specimens. (A) A representative image of immunohistochemical staining using the phosphotyrosine specific antibody, 4G10, of prostate specimens ranging from normal to CRPC. Tissue spots from patients with CRPC show high levels of phosphotyrosine expression in the epithelial compartment. (B) Increased tyrosine phosphorylation is observed in CRPC, with nearly 50% of the patients displaying high intensity staining (2-3) when compared to normal, HGPIN, or HNPC tissues. (C) The average staining intensity of all of the tissues clearly show a significant increase of tyrosine phosphorylation in CRPC patients. HGPIN: high grade prostatic intraepithelial neoplasia, HNPC: hormone naïve prostate cancer, HRPC: hormone refractory prostate cancer. *** <0.001, 1way ANOVA. Scale bar=200 μm.

Figure 2. Phosphotyrosine expression is increased during prostate cancer progression. (A) Lentiviral vector diagram displaying the organization of oncogene and fluorescent marker expression used in these tumors. (B) Gross and histological morphology of each tumor type after 12 week engraftment in SCID mice using the prostate regeneration protocol. Fluorescence corresponds to expression of a particular oncogene. IHC staining of progressive mouse tumor phenotypes reveals an increasing gradient of phosphotyrosine expression with more aggressive tumors expressing higher levels than indolent tumors. TI=transillumination, H&E=hematoxylin and eosin, pY=phosphotyrosine. Scale bars=50 μm.

Figure 3. Unique phosphotyrosine signatures are observed in a mouse model of prostate cancer progression. (A) Heatmap representing unique clusters of tyrosine phosphorylation for each mouse tumor phenotype. Each row corresponds to a unique phosphopeptide. Red=hyperphosphorylation, green=hypophosphorylation for each phospho-peptide. (B) Specific tyrosine kinases are observed in an oncogene-specific fashion. Signal-to-noise ratio (SNR) (relative to AKT) was calculated for each phosphorylation event and plotted. Positive SNR confirms elevation of that particular phosphorylation event. Western blotting validates indicated oncogene-specific phosphorylation results.

Figure 4. Bioinformatic analysis reveals enrichment of dasatinib tyrosine kinase targets in AKT/AR tumors. A. Enrichment analysis of tyrosine phosphosite motifs reveals enrichment of phospho-substrates of the tyrosine kinases ABL and SRC, targets of the tyrosine kinase inhibitor dasatinib, in AKT/AR tumors. No significant enrichment of these phosphopeptides were observed in either AKT/ERG or AKT/K-RASG12V tumors. Enrichment scores for all kinase motifs are

shown in Table S2. (B) Western blot and IHC (C) staining for the activated kinases ABL, SRC, or ERK1/2 reveals tumor-specific activation of these kinases. Scale bars = 50 μm.

Figure 5. Curation of phosphoproteomic profiling and bioinformatics delineates distinct tyrosine kinase signaling pathways in an oncogene-specific manner. Selected substrate and interaction pathways from each tyrosine kinase were generated from a combination of our phosphoproteomics data set and the HPRD and Phosphosite databases. An elevated phosphorylation event identified by MS is indicated by a phosphorylation residue depicted above the protein and color-coded. Solid arrow: protein is a direct substrate of the upstream kinase at that site. Dashed arrow: protein interacts directly with the upstream kinase/protein. Dotted arrow: protein is found within the pathway of the upstream kinase/protein.

Figure 1

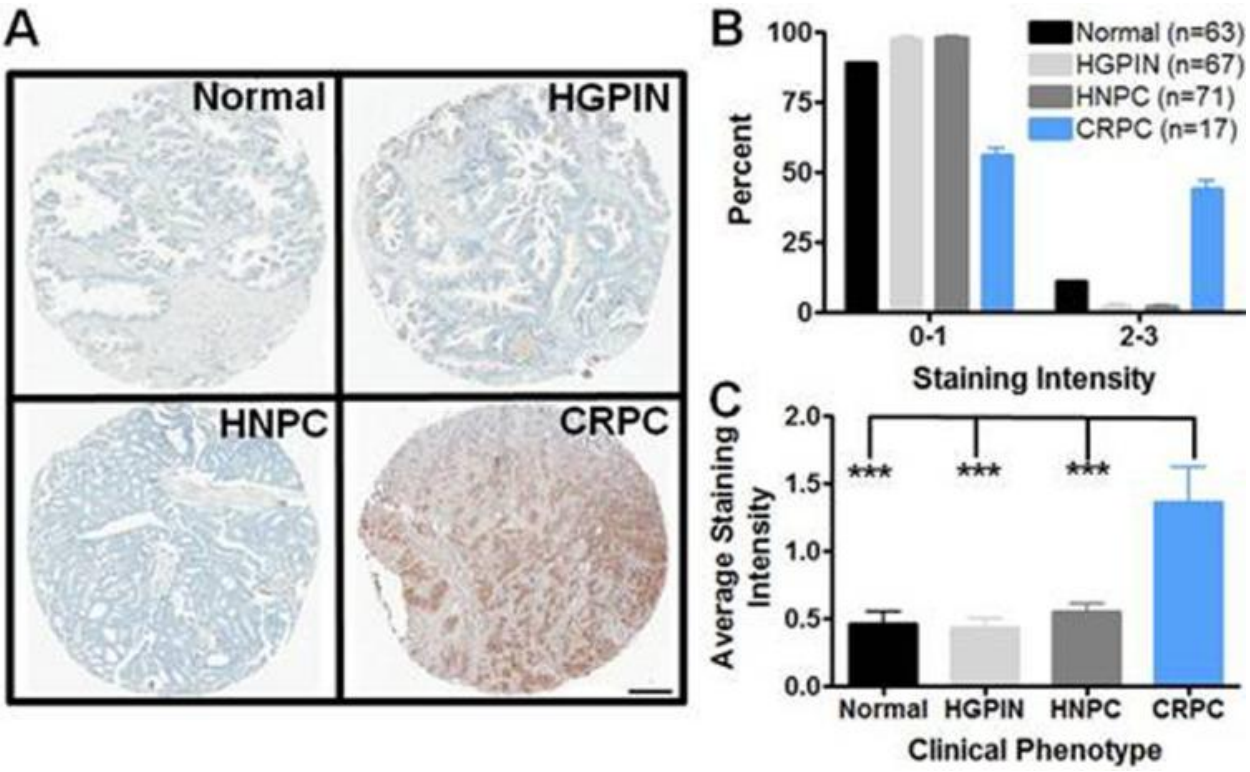
A
Normal
HGPIN
HNPC
CRPC
B
Normal (n=63)
HGPIN (n=67)
HNPC (n=71)
CRPC (n=17)
Percent
100
75
50
25
0
0-1
2-3
Staining Intensity
C
Average Staining Intensity
2.0
1.5
1.0
0.5
0.0
***
***
***
Normal
HGPIN
HNPC
CRPC
Clinical Phenotype

Figure 2

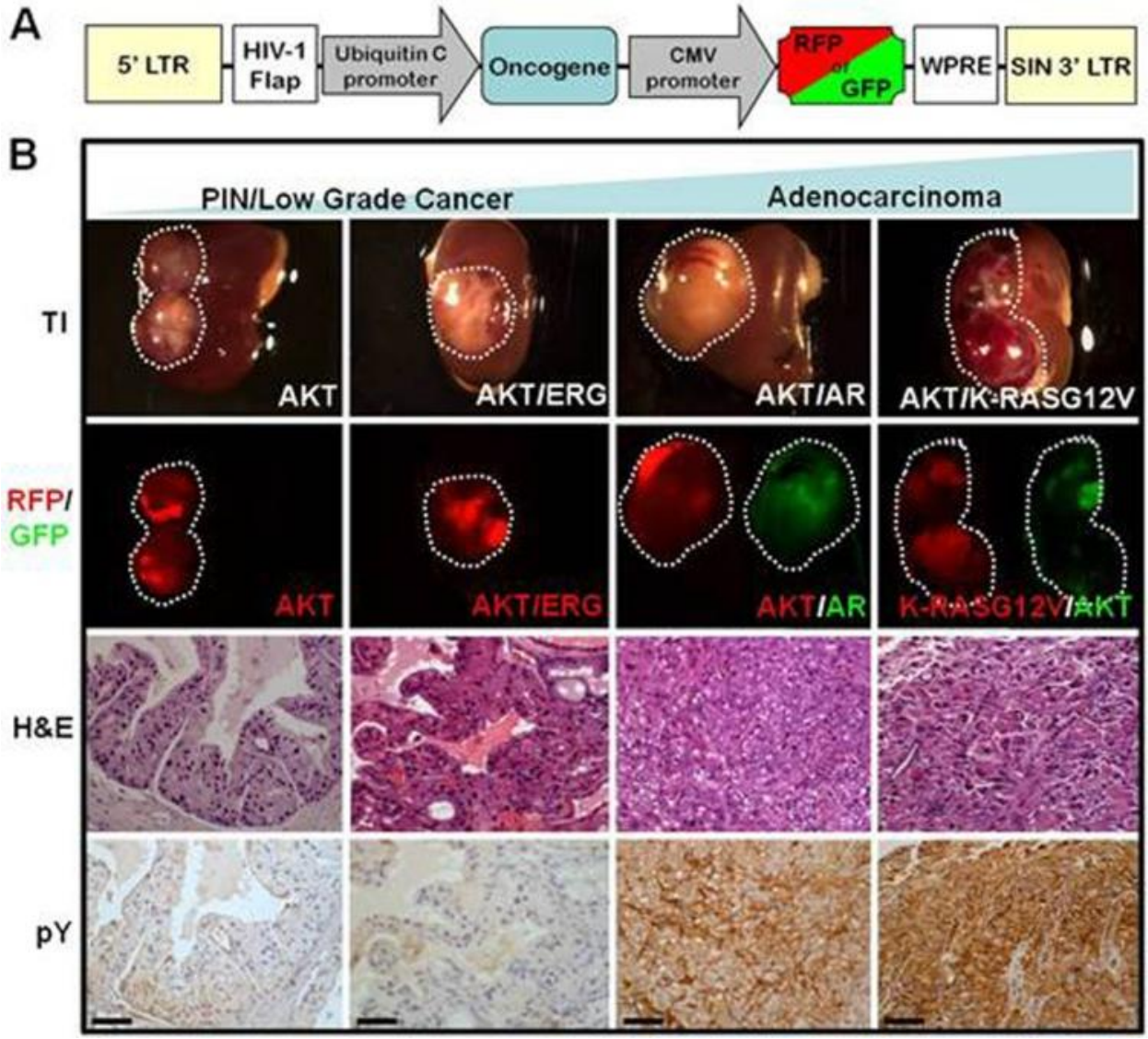
A
5' LTR
HIV-1 Flap
Ubiquitin C promoter
Oncogene
CMV promoter
RFP or GFP
WPRE
SIN 3' LTR
B
PIN/Low Grade Cancer
Adenocarcinoma
TI
RFP/ GFP
H&E
pY
AKT
AKT/ERG
AKT/AR
AKT/K-RASG12V

Figure 3

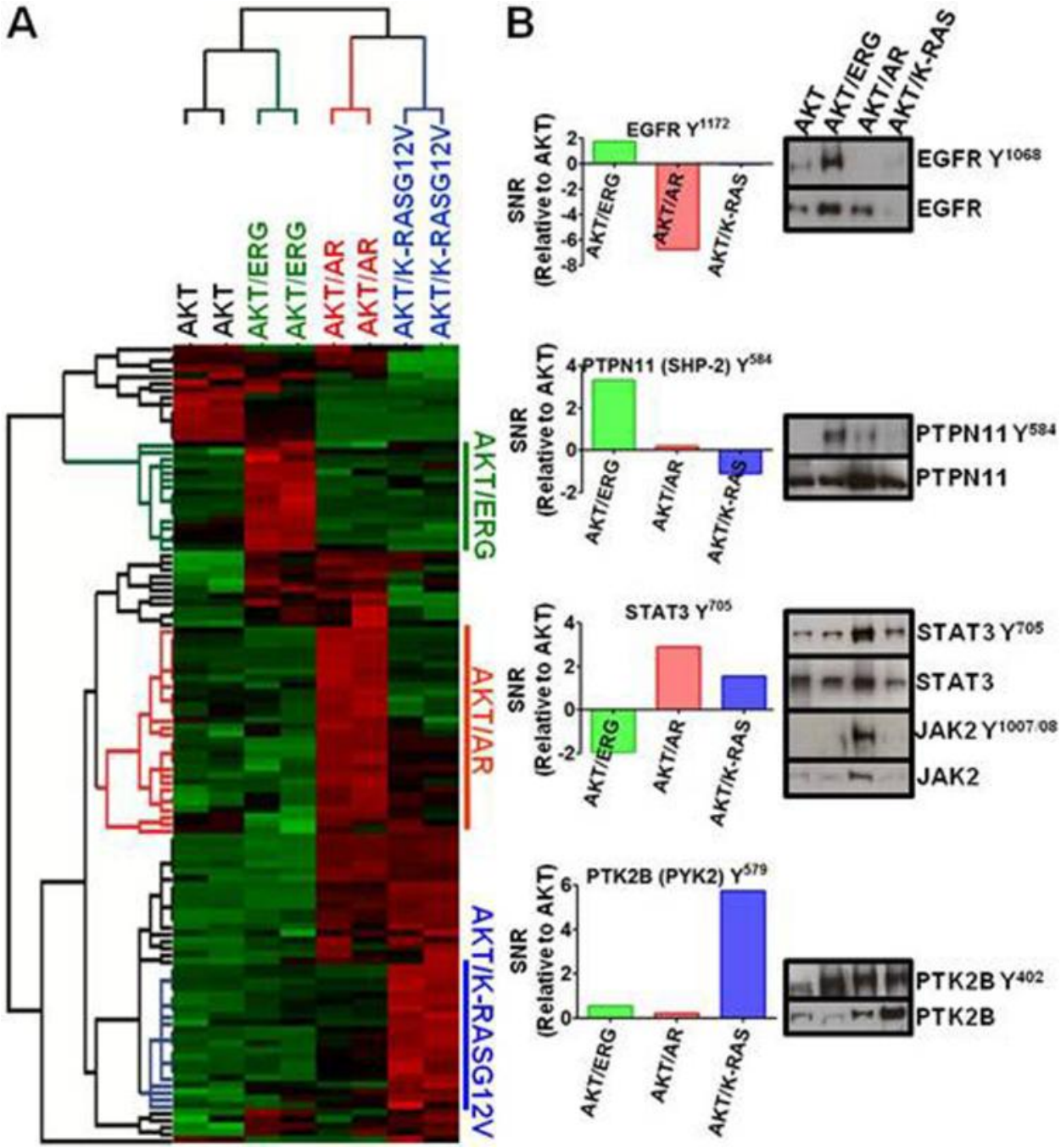
A
AKT
AKT
AKT/ERG
AKT/ERG
AKT/AR
AKT/AR
AKT/K-RASG12V
AKT/K-RASG12V
AKT/ERG
AKT/AR
AKT/K-RASG12V
B
AKT
AKT/ERG
AKT/AR
AKT/K-RAS
EGFR Y1172
SNR (Relative to AKT)
EGFR Y1068
EGFR
PTPN11 (SHP-2) Y584
PTPN11 Y584
PTPN11
STAT3 Y705
STAT3 Y705
STAT3
JAK2 Y1007/08
JAK2
PTK2B (PYK2) Y579
PTK2B Y402
PTK2B

Figure 4

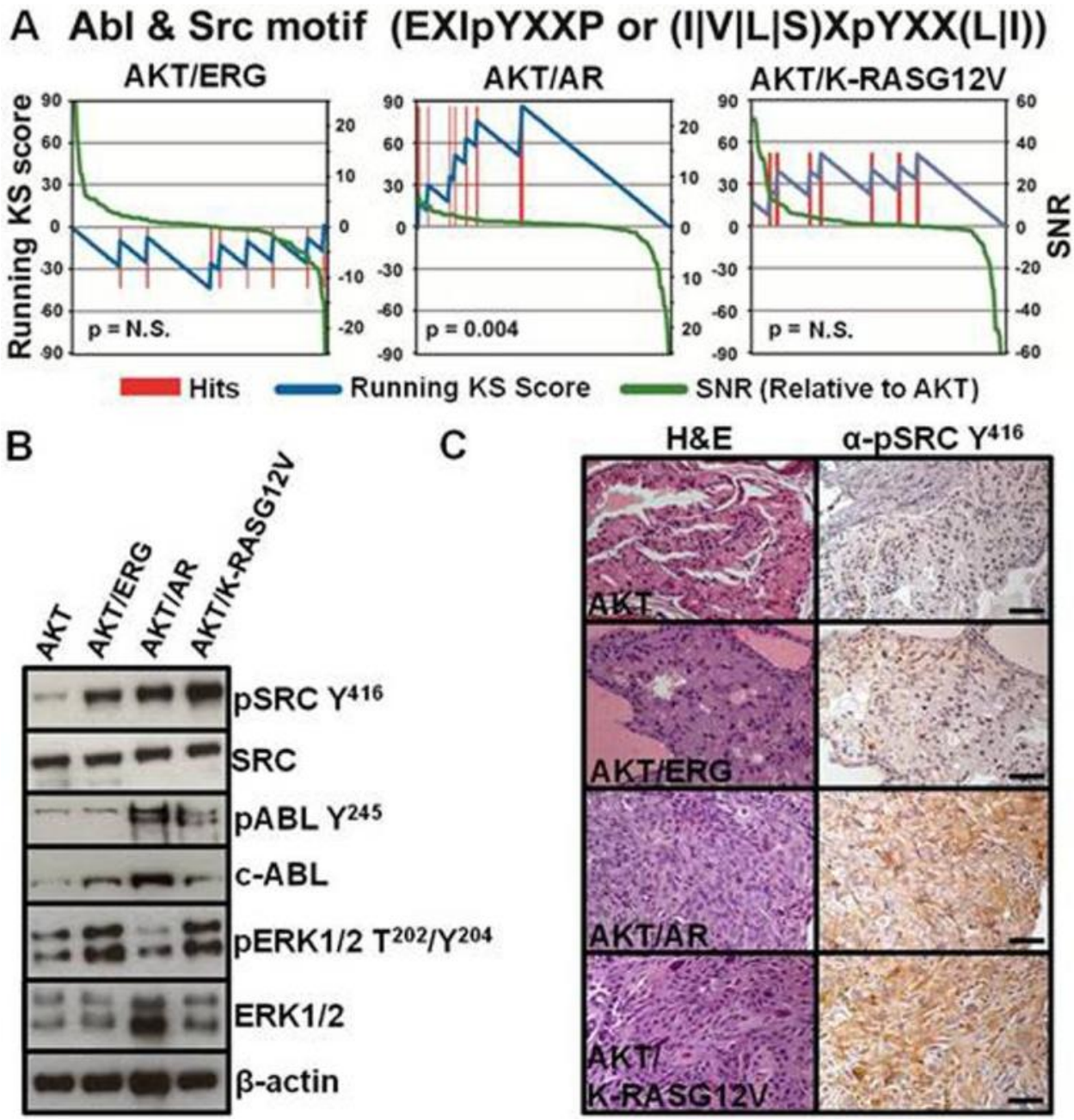
A Abl & Src motif (EXIpYXXP or (I|V|L|S)XpYXX(L|I))
AKT/ERG
AKT/AR
AKT/K-RASG12V
Running KS score
SNR
p = N.S.
p = 0.004
p = N.S.
Hits
Running KS Score
SNR (Relative to AKT)
B
AKT
AKT/ERG
AKT/AR
AKT/K-RASG12V
pSRC Y416
SRC
pABL Y245
c-ABL
pERK1/2 T202/Y204
ERK1/2
β-actin
C
H&E
α-pSRC Y416
AKT
AKT/ERG
AKT/AR
AKT/
K-RASG12V

Figure 5

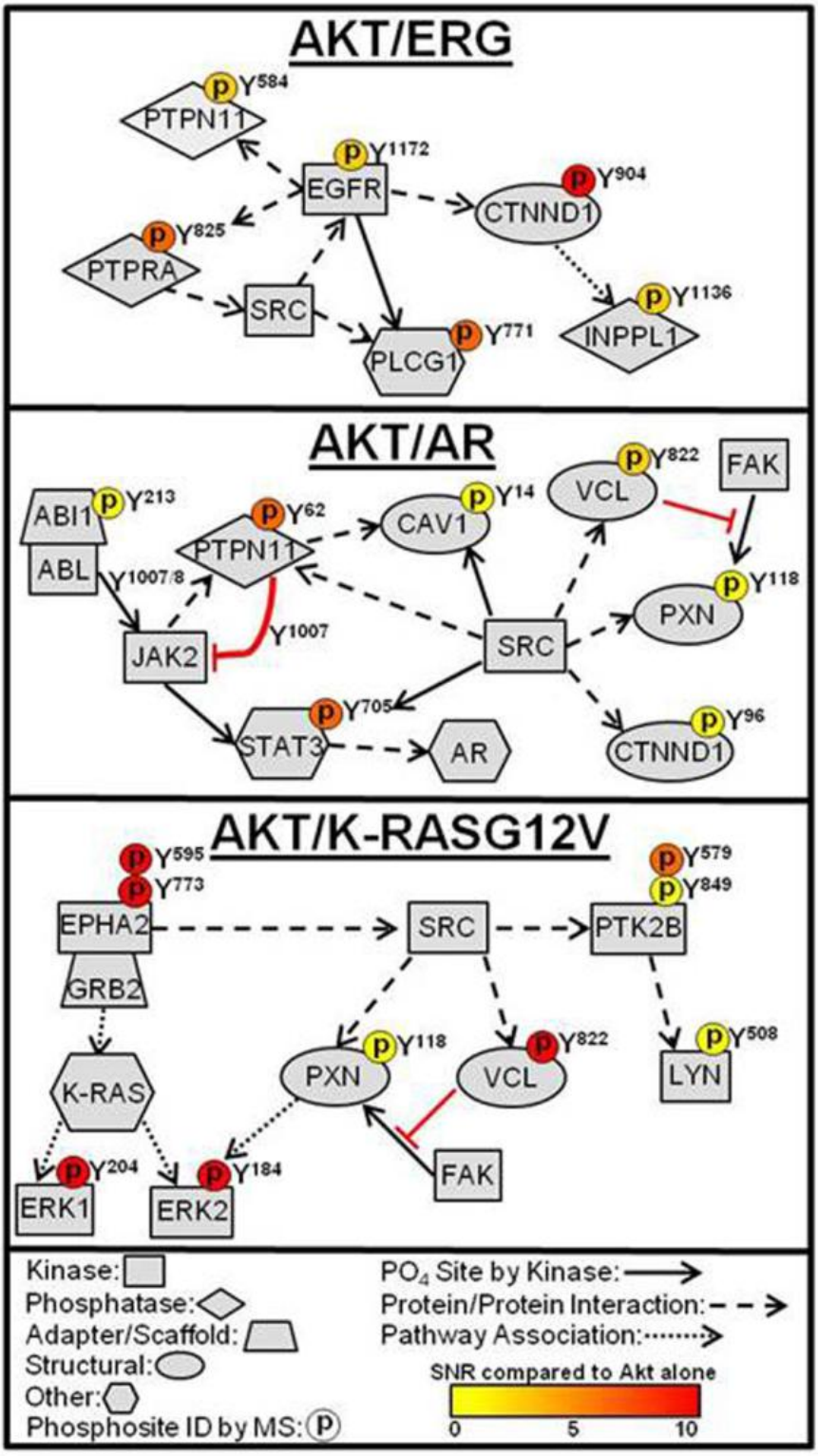
AKT/ERG
PTPN11
Y584
EGFR
Y1172
CTNND1
Y904
PTPRA
Y825
SRC
PLCG1
Y771
INPPL1
Y1136
AKT/AR
ABI1
Y213
ABL
Y1007/8
PTPN11
Y62
CAV1
Y14
VCL
Y822
FAK
PXN
Y118
JAK2
Y1007
SRC
STAT3
Y705
AR
CTNND1
Y96
AKT/K-RASG12V
Y595
Y773
EPHA2
GRB2
SRC
Y579
Y849
PTK2B
K-RAS
PXN
Y118
VCL
Y822
LYN
Y508
FAK
ERK1
Y204
ERK2
Y184
Kinase:
Phosphatase:
Adapter/Scaffold:
Structural:
Other:
Phosphosite ID by MS:
PO4 Site by Kinase:
Protein/Protein Interaction:
Pathway Association:
SNR compared to Akt alone
0
5
10

Table 1

Table 1. Oncogene-Specific Phospho-Activation of Tyrosine Kinases and Phosphatases*

Oncogene Combination	Tyrosine Kinase (Phosphoresidue)	Tyrosine Phosphatase (Phosphoresidue)	Functional Significance#
AKT/ERG	EGFR (Y^{1172})	PTPN11 (Y^{584}) PTPRA (Y^{825})	Enzymatic activation
		INPPL1 (Y^{1136})	Unknown
AKT/AR	JAK2 ($Y^{1007/1008}$)‡	PTPN11 (Y^{62})	Enzymatic activation
AKT/ K-RASG12V	EPHA2 (Y^{595})		Enzymatic activation
	LYN (Y^{508})		Enzymatic Inhibition
	PTK2B (Y^{579}) PTK2B (Y^{849}) EPHA2 (Y^{773})		Unknown
AKT/ERG AKT/AR AKT/ K-RASG12V	FER (Y^{402})		Alters cell motility

*All measured phosphorylation events are relative to AKT-only lesions.
#Source: Phosphosite (phosphosite.org)
‡ JAK2 was not identified by MS, but inferred based on high STAT3 Y^{705} phosphorylation observed in AKT-AR tumors

Supplemental Materials and Methods

Clinical Prostate Tissue Microarrays

The prostate TMA was constructed as previously described (1). Briefly, 75 prostatectomy specimens from patients never treated with hormonal therapy were reviewed and areas of normal prostate, HGPIN and HNPC were marked for sampling. Tumors ranged from Gleason patterns 2 to 5. Two to three cores per samples, measuring 0.6 mm in diameter, were obtained from selected regions in each donor paraffin block and transferred to a recipient paraffin block and the resulting block contained a total of 200 cores. A section was obtained from the TMA for H&E staining as quality control and unstained sections were used for immunohistochemical staining.

Another TMA was constructed from transurethral resection tissue blocks from 20 patients who failed hormonal therapy (CRPC) and developed urinary obstruction. Similarly, 2 cores were taken from each donor block and transferred to a recipient block. A section was obtained from the TMA for H&E staining as quality control and unstained sections were used for immunohistochemical staining.

Lentiviral vector construction

Construction of the plasmids carrying the oncogenes myristoylated AKT (mAKT), AR, AKT-ERG are described previously (2-4). The plasmid 12544 carrying K-RASG12V DNA was purchased from Addgene (Cambridge, MA) (5). The open reading frame of K-RASG12V was amplified by PCR using the following primers: forward primer, 5'-CATCATACTAGTGCCACCatgactgaatataaacttgtggtagttg-3'; and reverse primer, 5'-CATCATGTTACCttacataattacacactttgtctttgacttc-3'. The PCR product was digested with SpeI and HpaI enzyme, while the lentiviral vector FUCRW-Cre was digested with the same enzyme which

released the Cre gene and generated the lentiviral backbone with SpeI and HpaI cohesive ends. The K-RASG12V fragment was ligated into the lentiviral backbone and is designated as FU-K-RASG12V-CRW.

Prostate regeneration and prostate epithelial viral infections

The regeneration process, lentivirus preparation, titering, and infection of dissociated prostate cells were performed as described previously under University of California, Los Angeles, safety regulations for lentivirus usage (6). Housing, maintenance, and all surgical and experimental procedures were undertaken in compliance with the regulations of the division of Laboratory Animal Medicine of the University of California, Los Angeles. Prostate regeneration adapted from previous reports (7). Dissociated prostate cell suspension was prepared from 6- to 10-week-old Bl6 mice. The dissociated cells were infected with lentivirus to generate the following tumors: FU-mAKT-CRW (MOI ~60) for mAKT' tumors, FU-mAKT-IRES-ERG-CRW (MOI ~50) for mAKT/ERG tumors, FU-mAKT-CRW (MOI ~40) and FU-AR-CGW (MOI ~40) for mAKT/AR tumors, and FU-mAKT-CGW (MOI ~40) and FU-K-RASG12V-CRW (MOI ~40) for mAKT/K-RASG12V tumors. Infected cells (2×10^5) were mixed with urogenital sinus mesenchyme (UGSM) (2×10^5). Grafts were implanted under the kidney capsule in SCID mice the following morning and allowed to regenerate for 12 weeks.

Western Blot and Immunohistochemistry

Tumors were either flash frozen (western analysis) or fixed in 10% buffered formalin overnight, embedded in paraffin, and sectioned at 4 μm (IHC analysis). For westerns, equal protein amounts of urea lysates were used from tissues prepared as described in 'Quantitative analysis of phosphotyrosine peptides by mass spectrometry'. Antibodies were diluted as follows: AKT (1:1000,

Santa Cruz), pAKT S^{473} (1:2000, Cell Signaling), ERG (1:500, Epitomics), AR (1:1000, Santa Cruz), K-RAS (1:250, Calbiochem), 4G10 (1:2500, Millipore), pEGFR Y^{1068} (1:1000, Cell Signaling), EGFR (1:1000, Cell Signaling), pPTPN11 Y^{584} (1:1000, Cell Signaling), PTPN11 (1:1000 Cell Signaling), pSTAT3 Y^{705} (1:2000, Cell Signaling), STAT3 (1:1000, Cell Signaling), pJAK2 $Y^{1007/1008}$ (1:500, Cell Signaling), JAK2 (1:1000, Cell Signaling), pERK1/2 $^{T202/Y204}$ (1:2000, Cell Signaling), ERK1/2 (1:1000, Cell Signaling), pPTK2B Y^{402} (1:1000, Cell Signaling), PTK2B (1:1000, Cell Signaling), pSRC Y^{416} (1:1000, Cell Signaling), SRC (1:5000, Cell Signaling), c-ABL (1:5000, Witte Lab) (8), and pABL Y^{245} (1:500, Cell Signaling). ECL substrate (Millipore) was used for detection and development on GE/Amersham film. For IHC, sections were stained with hematoxylin and eosin for representative histology. Tissue sections were heated at 65ºC for 1 hour to melt the paraffin followed by rehydration. Antigen retrieval was performed using citric acid buffer and visualization was performed using EnVision^{+} system (Dako). The same primary antibodies from western blots were used, unless explicitly stated, and diluted as follows: 4G10 (1:1000), pSRC Y^{416} (1:50), pSTAT3 Y^{705} (1:200), AKT (1:300, Cell Signaling), AR (1:200), and ERG (1:50). All primary antibodies recognizing tyrosine phosphorylated motifs were diluted in commercial antibody diluent (Cell Signaling).

Quantitative analysis of phosphotyrosine peptides by mass spectrometry

The hybridoma was purchased from The Developmental Studies Hybridoma Bank, The University of Iowa and purified antibody was then chemically conjugated to Protein G beads using dimethyl pimelimidate (DMP) as described (CSH Protocols; doi:10.1101/pdb.prot4303). Phosphotyrosine peptide immunoprecipitation was performed with pan-specific anti-phosphotyrosine antibodies (clone 4G10,) using 35 mg of total protein isolated from 300-500 mg frozen tumor mass as previously described (9, 10). Phosphorylated peptides were analyzed by liquid chromatography tandem mass spectrometry (LC-MS/MS) using an Eksigent autosampler coupled with Nano2DLC

pump (Eksigent, Dublin, CA) and LTQ-Orbitrap (Thermo Fisher Scientific, Waltham, MA). The samples were loaded onto an analytical column (10 cm x 75 μm i.d.) packed with 5 μm Integrafit Proteopep2 300 Å C18 (New Objective, Woburn, MA). Peptides were eluted into the mass spectrometer using a HPLC gradient of 5% to 40% Buffer B in 45 min followed by a quick gradient of 40% to 90% Buffer B in 10 min, where Buffer A contains 0.1% formic acid in water and Buffer B contains 0.1% formic acid in acetonitrile. All HPLC solvents were Ultima Gold quality (Fisher Scientific). Mass spectra were collected in positive ion mode using the Orbitrap for parent mass determination and the LTQ for data dependent MS/MS acquisition of the top 5 most abundant peptides. Each sample was analyzed twice (replicate runs) and in each run one-half of the sample was injected. MS/MS fragmentation spectra were searched using SEQUEST (Version v.27, rev. 12, Thermo Fisher Scientific) against a database containing the combined human-mouse IPI protein database (downloaded December 2006 from ftp.ebi.ac.uk). Search parameters included carbamidomethyl cysteine (*C) as a static modification. Dynamic modifications included phosphorylated tyrosine, serine, or threonine (pY, pS, pT, respectively) and oxidized methionine (*M). Results derived from database searching were filtered using the following criteria: Xcorr >1.0(+1), 1.5(+2), 2(+3); peptide probability score <0.001; dCn >0.1; and mass accuracy <25 ppm (parts per million) with Bioworks version 3.2 (Thermo Electron Corp.). We estimated the false-positive rate of sequence assignments at 0.5% on the basis of a composite target-reversed decoy database search strategy (11). AScore was used to more accurately localize the phosphate on the peptide (12). Peptide peaks sequenced in experimental tumors and control lines but not others were located in the remaining samples by aligning the chromatogram elution profiles using a dynamic time warping algorithm (9, 10). Relative amounts of the same phosphopeptide across samples run together were determined using custom software to integrate the area under the unfragmented (MS1) monoisotopic peptide peak (10, 13). All peaks corresponding to phosphosites were inspected

manually and any errors in the automated quantitation were corrected. MS2 spectra for all reported phosphopeptides are available under the PRIDE accession numbers 20879-20889 (14).

Data Analysis

The number of unique phosphorylation sites identified in our experiments was determined by collapsing multiple phosphopeptide ions representing the same phosphorylation site. Multiple detections of the same phosphosite includes phosphopeptides of different ion charge state, modification (e.g. oxidized methionine), and missed trypsin cleavage sites. Multiple detections were compared to ensure no disagreement in trend, and the MS ion with the highest intensity across the samples in an experimental batch was kept as representative for subsequent data analysis. The phosphosite residue numbers listed correspond to the International Protein Index (IPI) accession number in the mouse genome, and any phospho-peptides that did not map to the mouse genome were removed. For clustering, we removed any peptides which had an ANOVA score less than 0.2. Hierarchical clustering was performed using the Cluster program with the Pearson correlation and pairwise complete linkage analysis (15). Java TreeView was used to visualize clustering results (16). Quantitative data for each phosphopeptide can be found in Table S1.

Enrichment Analysis of Kinase activity

Permutation analysis was performed by randomly shuffling the peptide ranked list, followed by calculation of the Kolmogorov-Smirnov statistic for this permutation. After 1,000 permutations, the fraction of randomly ranked lists resulting in a Kolmogorov-Smirnov statistic greater than or equal to the observed value was defined as the permutation-based frequency of random occurrence (i.e. the permutation-based p-value). To normalize for the different number of predictions for each upstream kinase, we calculated the Normalized Kolmogorov-Smirnov score by dividing the

observed enrichment score by the mean of the absolute value of all permutation enrichment scores.

Supplemental Figure Legends

Supplemental Figure 1. Confirmation of oncogene expression in mouse tumors. (A) Immunohistochemical staining for AKT, androgen receptor (AR), and ERG show expression of these proteins in the respective tumors investigated. ERG staining can also localize to endogenous endothelial cells as shown in AKT/AR and AKT/K-RASG12V tumors. (B) Western blot analysis confirms the expression of each oncogene after lentiviral transduction and tumor formation. Arrows: myristoylated AKT expression is shown at the higher molecular weight. ERG expression from the lentiviral vector. ERG expression at the lower molecular weight is from other cells within the tissue (e.g. endothelial cells). Scale bars = 50 μm.

Supplemental Figure 2. Analysis of tyrosine phosphorylation in mouse prostate and tumors. (A) IHC analysis reveals little tyrosine phosphorylation in normal mouse prostate, similar to what is observed in indolent prostate cancer. (B) Western blot analysis using the phosphotyrosine-specific antibody 4G10 reveals increased levels of phosphorylation in the more aggressive tumors. Scale bars = 50 μm, inset = 100 μm.

Supplemental Figure 3. Global quantitative phosphoprofiling of prostate cancer progression reveals phosphorylation events with distinct oncogene-specific profiles. The phosphoprofiling heatmap of Figure 4A with the protein and residue identities of the phosphorylation events listed: Gene symbol, phosphosite residue number, Entrez gene product name, phosphopeptide (charge state of mass spectrometry ion).

Supplemental Figure 4. Identification of activated tyrosine kinases in non-tyrosine kinase driven prostate tumors. (A-L) Relative abundance of phosphopeptide levels of tyrosine kinases, substrates, and phosphatases during progression of prostate cancer. Signal-to-noise ratio (SNR) (relative to AKT) was calculated for each phosphopeptide and plotted. Data from the full phosphoprofiling data set depicted in Figure 4A. (M) Immunohistochemical staining for tyrosine phosphorylated STAT3 (pSTAT3 Y^{705}) reveals tumor-specific activation of this particular phosphorylation event. Scale bars = 50 μm.

Supplemental Figure 5. Enrichment of EGFR target substrates in AKT/ERG tumors. A statistical analysis of tyrosine phosphorylated motifs reveals an enrichment of phosphopeptides of the tyrosine kinase EGFR in AKT/ERG tumors. No significant enrichment of these phosphopeptides were observed in either AKT/AR or AKT/K-RASG12V tumors. Enrichment scores for all kinase motifs are shown in Table S2.

Supplemental Figure 1

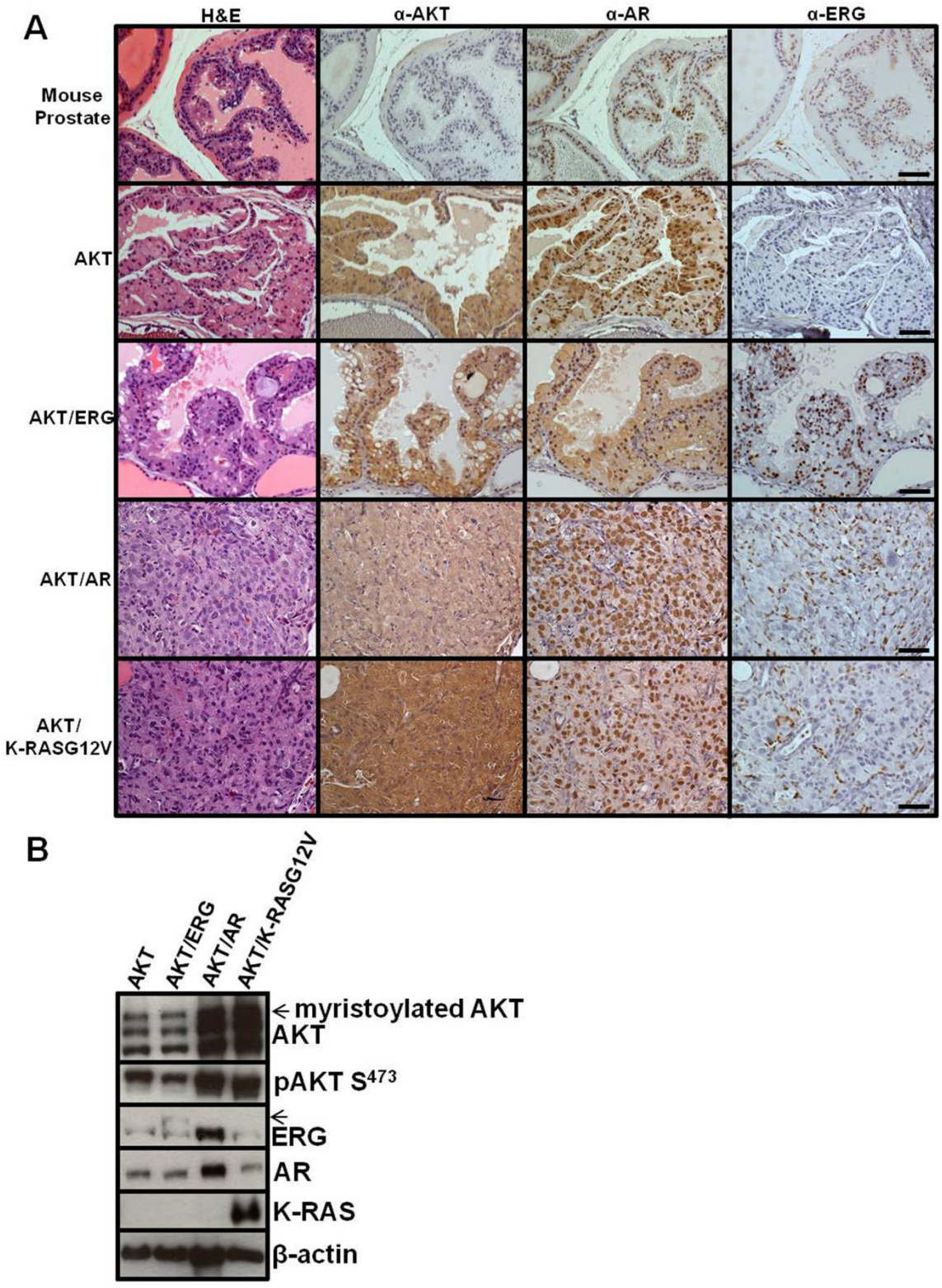

Supplemental Figure 2

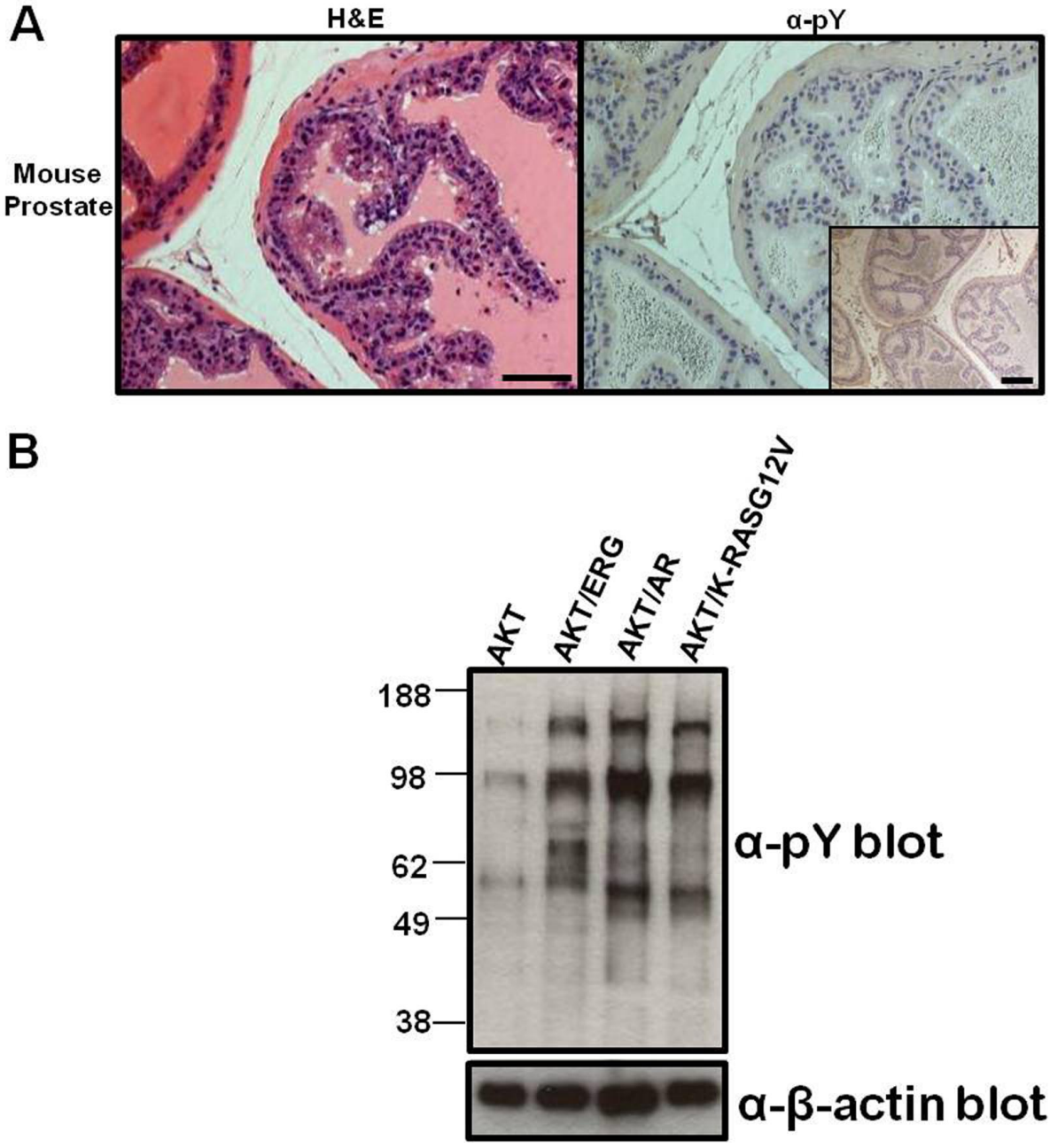

Supplemental Figure 3

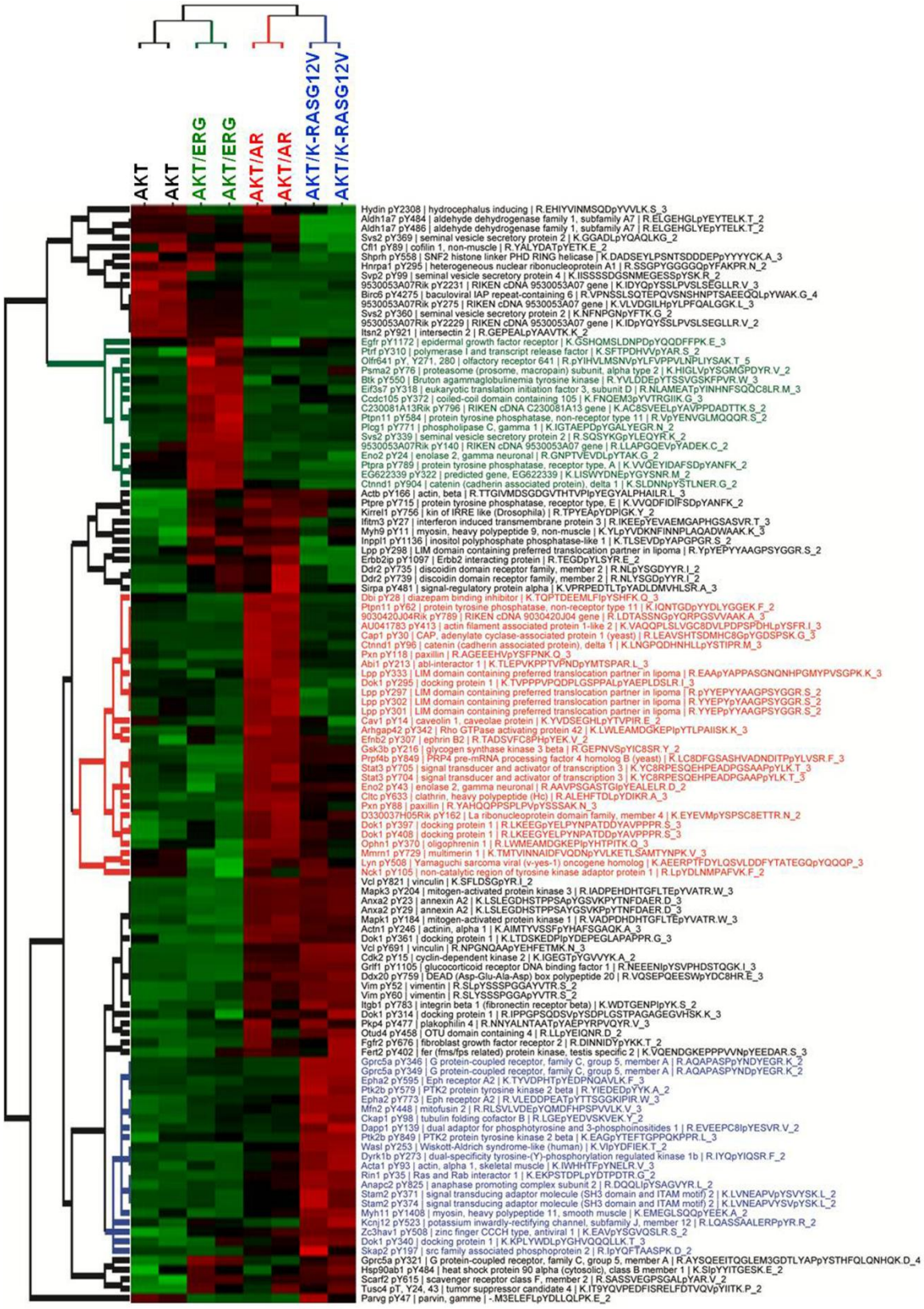

Supplemental Figure 4

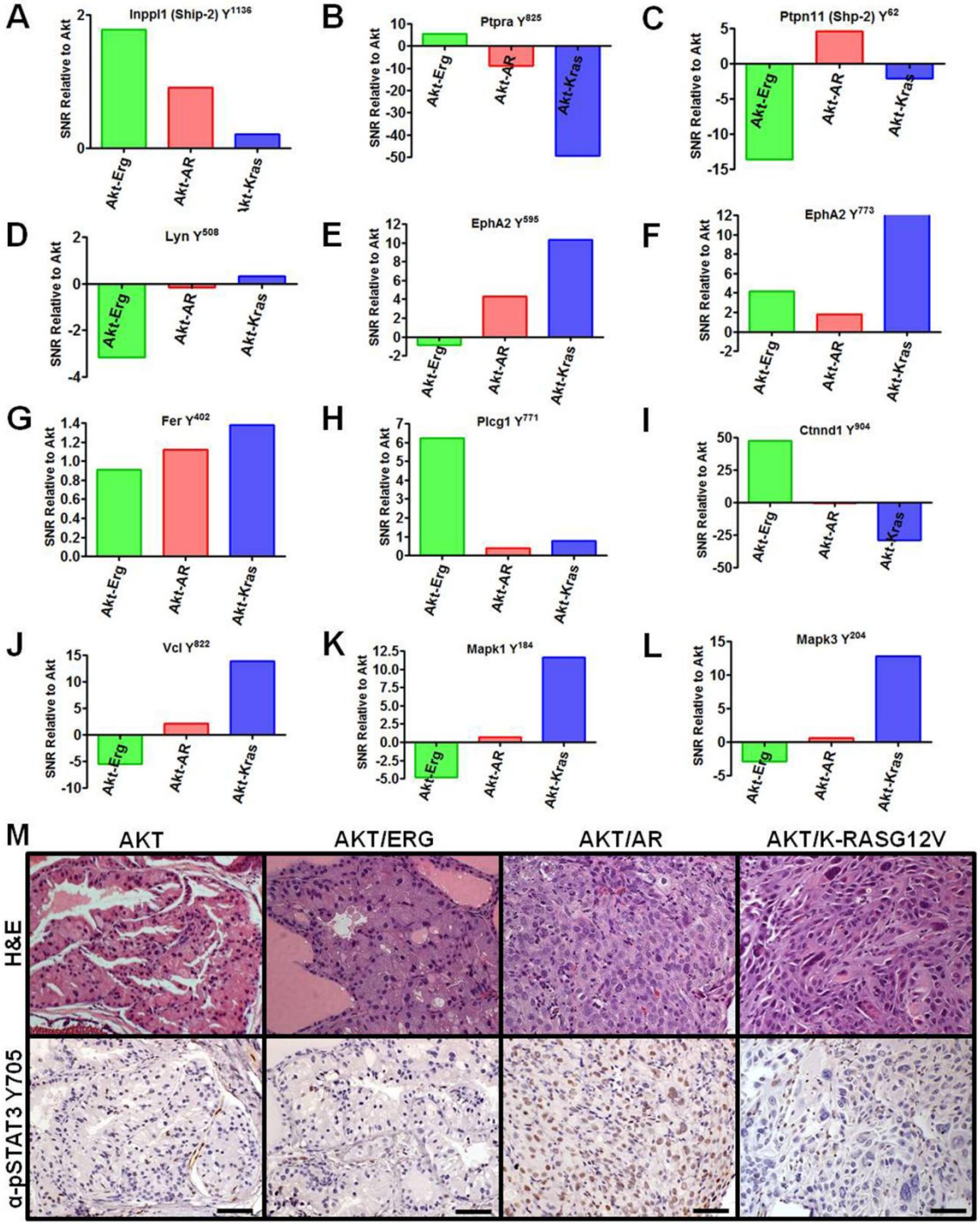

Supplemental Figure 5

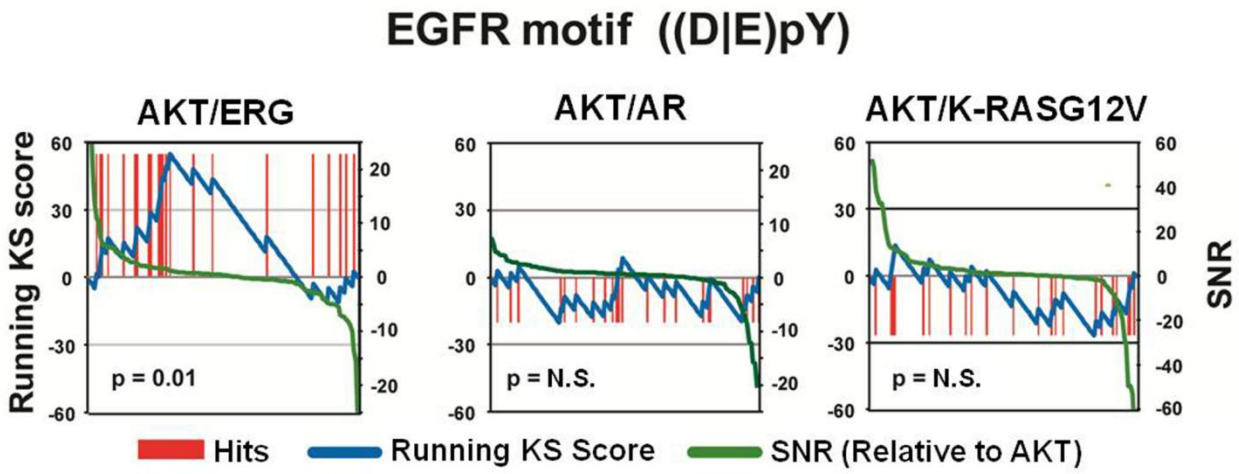

References

1. Nakahara M*, et al.* (1998) A novel gain-of-function mutation of c-kit gene in gastrointestinal stromal tumors. *Gastroenterology* 115(5):1090-1095.

2. Ben-Neriah Y, Daley GQ, Mes-Masson AM, Witte ON, & Baltimore D (1986) The chronic myelogenous leukemia-specific P210 protein is the product of the bcr/abl hybrid gene. *Science* 233(4760):212-214.

3. Dienstmann R, Martinez P, & Felip E (2011) Personalizing therapy with targeted agents in non-small cell lung cancer. *Oncotarget* 2(3):165-177.

4. Kim KS*, et al.* (2005) Predictors of the response to gefitinib in refractory non-small cell lung cancer. *Clin Cancer Res* 11(6):2244-2251.

5. Druker BJ*, et al.* (2001) Activity of a specific inhibitor of the BCR-ABL tyrosine kinase in the blast crisis of chronic myeloid leukemia and acute lymphoblastic leukemia with the Philadelphia chromosome. *N Engl J Med* 344(14):1038-1042.

6. Heinrich MC*, et al.* (2003) Kinase mutations and imatinib response in patients with metastatic gastrointestinal stromal tumor. *J Clin Oncol* 21(23):4342-4349.

7. Tomlins SA*, et al.* (2005) Recurrent fusion of TMPRSS2 and ETS transcription factor genes in prostate cancer. *Science* 310(5748):644-648.

8. Taylor BS*, et al.* (2010) Integrative genomic profiling of human prostate cancer. *Cancer Cell* 18(1):11-22.

9. Visakorpi T*, et al.* (1995) In vivo amplification of the androgen receptor gene and progression of human prostate cancer. *Nat Genet* 9(4):401-406.

10. Jenkins RB, Qian J, Lieber MM, & Bostwick DG (1997) Detection of c-myc oncogene amplification and chromosomal anomalies in metastatic prostatic carcinoma by fluorescence in situ hybridization. *Cancer Res* 57(3):524-531.

11. Yoshimoto M*, et al.* (2006) Interphase FISH analysis of PTEN in histologic sections shows genomic deletions in 68% of primary prostate cancer and 23% of high-grade prostatic intra-epithelial neoplasias. *Cancer Genet Cytogenet* 169(2):128-137.

12. Pezaro C*, et al.* (2009) An open-label, single-arm phase two trial of gefitinib in patients with advanced or metastatic castration-resistant prostate cancer. *Am J Clin Oncol* 32(4):338-341.

13. Curigliano G*, et al.* (2007) Absence of epidermal growth factor receptor gene mutations in patients with hormone refractory prostate cancer not responding to gefitinib. *Prostate* 67(6):603-604.

14. Guo Z*, et al.* (2006) Regulation of androgen receptor activity by tyrosine phosphorylation. *Cancer Cell* 10(4):309-319.

15. Mahajan NP*, et al.* (2007) Activated Cdc42-associated kinase Ack1 promotes prostate cancer progression via androgen receptor tyrosine phosphorylation. *Proc Natl Acad Sci U S A* 104(20):8438-8443.

16. Liu Y*, et al.* (2010) Dasatinib inhibits site-specific tyrosine phosphorylation of androgen receptor by Ack1 and Src kinases. *Oncogene* 29(22):3208-3216.

17. Craft N, Shostak Y, Carey M, & Sawyers CL (1999) A mechanism for hormone-independent prostate cancer through modulation of androgen receptor signaling by the HER-2/neu tyrosine kinase. *Nat Med* 5(3):280-285.

18. Cai H, Babic I, Wei X, Huang J, & Witte ON (2010) Invasive prostate carcinoma driven by c-Src and androgen receptor synergy. *Cancer Res*.

19. Tatarov O*, et al.* (2009) SRC family kinase activity is up-regulated in hormone-refractory prostate cancer. *Clin Cancer Res* 15(10):3540-3549.

20. Del Rosario AM & White FM (2010) Quantifying oncogenic phosphotyrosine signaling networks through systems biology. *Curr Opin Genet Dev* 20(1):23-30.

21. Rubbi L*, et al.* (2011) Global phosphoproteomics reveals crosstalk between Bcr-Abl and negative feedback mechanisms controlling Src signaling. *Sci Signal* 4(166):ra18.

22. Sun T*, et al.* (2011) Activation of multiple proto-oncogenic tyrosine kinases in breast cancer via loss of the PTPN12 phosphatase. *Cell* 144(5):703-718.

23. Rikova K*, et al.* (2007) Global survey of phosphotyrosine signaling identifies oncogenic kinases in lung cancer. *Cell* 131(6):1190-1203.

24. Li J*, et al.* (2010) A chemical and phosphoproteomic characterization of dasatinib action in lung cancer. *Nat Chem Biol* 6(4):291-299.

25. Lawson DA*, et al.* (2010) Basal epithelial stem cells are efficient targets for prostate cancer initiation. *Proc Natl Acad Sci U S A* 107(6):2610-2615.

26. Goldstein AS, Huang J, Guo C, Garraway IP, & Witte ON (2010) Identification of a cell of origin for human prostate cancer. *Science* 329(5991):568-571.

27. Bismar TA*, et al.* (2011) PTEN genomic deletion is an early event associated with ERG gene rearrangements in prostate cancer. *BJU Int* 107(3):477-485.

28. Linja MJ*, et al.* (2001) Amplification and overexpression of androgen receptor gene in hormone-refractory prostate cancer. *Cancer Res* 61(9):3550-3555.

29. Clark J*, et al.* (2007) Diversity of TMPRSS2-ERG fusion transcripts in the human prostate. *Oncogene* 26(18):2667-2673.

30. Brenner JC & Chinnaiyan AM (2009) Translocations in epithelial cancers. *Biochim Biophys Acta* 1796(2):201-215.

31. Rush J*, et al.* (2005) Immunoaffinity profiling of tyrosine phosphorylation in cancer cells. *Nat Biotechnol* 23(1):94-101.

32. Hornbeck PV, Chabra I, Kornhauser JM, Skrzypek E, & Zhang B (2004) PhosphoSite: A bioinformatics resource dedicated to physiological protein phosphorylation. *Proteomics* 4(6):1551-1561.

33. Amanchy R*, et al.* (2007) A curated compendium of phosphorylation motifs. *Nat Biotechnol* 25(3):285-286.

34. Gnad F, Gunawardena J, & Mann M (2011) PHOSIDA 2011: the posttranslational modification database. *Nucleic Acids Res* 39(Database issue):D253-260.

35. Linding R*, et al.* (2008) NetworKIN: a resource for exploring cellular phosphorylation networks. *Nucleic Acids Res* 36(Database issue):D695-699.

36. Schubbert S, Shannon K, & Bollag G (2007) Hyperactive Ras in developmental disorders and cancer. *Nat Rev Cancer* 7(4):295-308.

37. Keshava Prasad TS*, et al.* (2009) Human Protein Reference Database--2009 update. *Nucleic Acids Res* 37(Database issue):D767-772.

38. Subauste MC*, et al.* (2004) Vinculin modulation of paxillin-FAK interactions regulates ERK to control survival and motility. *J Cell Biol* 165(3):371-381.

39. Kan Z*, et al.* (2010) Diverse somatic mutation patterns and pathway alterations in human cancers. *Nature* 466(7308):869-873.

40. Olivier M & Taniere P (2011) Somatic mutations in cancer prognosis and prediction: lessons from TP53 and EGFR genes. *Curr Opin Oncol* 23(1):88-92.

41. Bao J, Gur G, & Yarden Y (2003) Src promotes destruction of c-Cbl: implications for oncogenic synergy between Src and growth factor receptors. *Proc Natl Acad Sci U S A* 100(5):2438-2443.

42. Pasquale EB (2010) Eph receptors and ephrins in cancer: bidirectional signalling and beyond. *Nat Rev Cancer* 10(3):165-180.

43. Zhang SQ*, et al.* (2004) Shp2 regulates SRC family kinase activity and Ras/Erk activation by controlling Csk recruitment. *Mol Cell* 13(3):341-355.

44. Cunnick JM*, et al.* (2002) Regulation of the mitogen-activated protein kinase signaling pathway by SHP2. *J Biol Chem* 277(11):9498-9504.

45. Mitra S, Beach C, Feng GS, & Plattner R (2008) SHP-2 is a novel target of Abl kinases during cell proliferation. *J Cell Sci* 121(Pt 20):3335-3346.

46. Ren Y*, et al.* (2010) Critical role of Shp2 in tumor growth involving regulation of c-Myc. *Genes Cancer* 1(10):994-1007.

47. Macrae M*, et al.* (2005) A conditional feedback loop regulates Ras activity through EphA2. *Cancer Cell* 8(2):111-118.

48. Walker-Daniels J*, et al.* (1999) Overexpression of the EphA2 tyrosine kinase in prostate cancer. *Prostate* 41(4):275-280.

49. Zelinski DP, Zantek ND, Stewart JC, Irizarry AR, & Kinch MS (2001) EphA2 overexpression causes tumorigenesis of mammary epithelial cells. *Cancer Res* 61(5):2301-2306.

50. Verweij J*, et al.* (2004) Progression-free survival in gastrointestinal stromal tumours with high-dose imatinib: randomised trial. *Lancet* 364(9440):1127-1134.

51. Cai H*, et al.* (2011) Differential transformation capacity of Src family kinases during the initiation of prostate cancer. *Proc Natl Acad Sci U S A* 108(16):6579-6584.

52. Ishizawar RC, Miyake T, & Parsons SJ (2007) c-Src modulates ErbB2 and ErbB3 heterocomplex formation and function. *Oncogene* 26(24):3503-3510.

53. Araujo JC*, et al.* (2011) Dasatinib combined with docetaxel for castration-resistant prostate cancer: Results from a phase 1-2 study. *Cancer*.

54. Carver BS*, et al.* (2009) Aberrant ERG expression cooperates with loss of PTEN to promote cancer progression in the prostate. *Nat Genet* 41(5):619-624.

55. Brenner JC*, et al.* (2011) Mechanistic rationale for inhibition of poly(ADP-ribose) polymerase in ETS gene fusion-positive prostate cancer. *Cancer Cell* 19(5):664-678.

56. Ateeq B*, et al.* (2011) Therapeutic targeting of SPINK1-positive prostate cancer. *Sci Transl Med* 3(72):72ra17.

57. Skaggs BJ*, et al.* (2006) Phosphorylation of the ATP-binding loop directs oncogenicity of drug-resistant BCR-ABL mutants. *Proc Natl Acad Sci U S A* 103(51):19466-19471.

58. Zimman A*, et al.* (2010) Activation of aortic endothelial cells by oxidized phospholipids: a phosphoproteomic analysis. *J Proteome Res* 9(6):2812-2824.

59. Subramanian A*, et al.* (2005) Gene set enrichment analysis: a knowledge-based approach for interpreting genome-wide expression profiles. *Proc Natl Acad Sci U S A* 102(43):15545-15550.

Supplementary References

1. Huang J*, et al.* (2005) Differential expression of interleukin-8 and its receptors in the neuroendocrine and non-neuroendocrine compartments of prostate cancer. *Am J Pathol* 166(6):1807-1815.

2. Xin L, Lawson DA, & Witte ON (2005) The Sca-1 cell surface marker enriches for a prostate-regenerating cell subpopulation that can initiate prostate tumorigenesis. *Proc Natl Acad Sci U S A* 102(19):6942-6947.

3. Zong Y*, et al.* (2009) ETS family transcription factors collaborate with alternative signaling pathways to induce carcinoma from adult murine prostate cells. *Proc Natl Acad Sci U S A* 106(30):12465-12470.

4. Xin L*, et al.* (2006) Progression of prostate cancer by synergy of AKT with genotropic and nongenotropic actions of the androgen receptor. *Proc Natl Acad Sci U S A* 103(20):7789-7794.

5. Khosravi-Far R*, et al.* (1996) Oncogenic Ras activation of Raf/mitogen-activated protein kinase-independent pathways is sufficient to cause tumorigenic transformation. *Mol Cell Biol* 16(7):3923-3933.

6. Xin L, Ide H, Kim Y, Dubey P, & Witte ON (2003) In vivo regeneration of murine prostate from dissociated cell populations of postnatal epithelia and urogenital sinus mesenchyme. *Proc Natl Acad Sci U S A* 100 Suppl 1:11896-11903.

7. Lukacs RU, Goldstein AS, Lawson DA, Cheng D, & Witte ON (2010) Isolation, cultivation and characterization of adult murine prostate stem cells. *Nat Protoc* 5(4):702-713.

8. Schiff-Maker L*, et al.* (1986) Monoclonal antibodies specific for v-abl- and c-abl-encoded molecules. *J Virol* 57(3):1182-1186.

9. Rubbi L*, et al.* (2011) Global phosphoproteomics reveals crosstalk between Bcr-Abl and negative feedback mechanisms controlling Src signaling. *Sci Signal* 4(166):ra18.

10. Skaggs BJ*, et al.* (2006) Phosphorylation of the ATP-binding loop directs oncogenicity of drug-resistant BCR-ABL mutants. *Proc Natl Acad Sci U S A* 103(51):19466-19471.

11. Elias JE, Haas W, Faherty BK, & Gygi SP (2005) Comparative evaluation of mass spectrometry platforms used in large-scale proteomics investigations. *Nat Methods* 2(9):667-675.

12. Beausoleil SA, Villen J, Gerber SA, Rush J, & Gygi SP (2006) A probability-based approach for high-throughput protein phosphorylation analysis and site localization. *Nat Biotechnol* 24(10):1285-1292.

13. Zimman A*, et al.* (2010) Activation of aortic endothelial cells by oxidized phospholipids: a phosphoproteomic analysis. *J Proteome Res* 9(6):2812-2824.

14. Vizcaino JA*, et al.* (2010) The Proteomics Identifications database: 2010 update. *Nucleic Acids Res* 38(Database issue):D736-742.

15. Eisen MB, Spellman PT, Brown PO, & Botstein D (1998) Cluster analysis and display of genome-wide expression patterns. *Proc Natl Acad Sci U S A* 95(25):14863-14868.

16. Saldanha AJ (2004) Java Treeview--extensible visualization of microarray data. *Bioinformatics* 20(17):3246-3248.

CHAPTER 3

Differential transformation capacity of Src Family Kinases during the initiation of prostate cancer.

Houjian Cai[†], **Daniel A. Smith**[‡], Sanaz Memarzadeh[§,¶], Clifford A. Lowell[‖], Jonathan A. Cooper[**], and Owen N. Witte[*,†,¶]

[*]Howard Hughes Medical Institute, University of California, Los Angeles, Los Angeles, California 90095

[†]Department of Microbiology, Immunology, and Molecular Genetics, University of California, Los Angeles, CA 90095

[‡]Molecular Biology Institute, University of California, Los Angeles, CA 90095

[§]Department of Obstetrics and Gynecology, David Geffen School of Medicine, University of California, Los Angeles, **C**A 90095

[¶]Eli & Edythe Broad Center of Regenerative Medicine and Stem Cell Research, University of California, Los Angeles, CA 90095

[‖]Department of Laboratory Medicine, University of California, San Francisco, CA 94143

[**]Fred Hutchinson Cancer Research Center, Seattle, WA 98109

Abstract

Src family kinases (SFKs) are pleiotropic activators that are responsible for integrating signal transduction for multiple receptors that regulate cellular proliferation, invasion, and metastasis in a variety of human cancers. Independent groups have identified increased expression of individual SFK members during prostate cancer progression, raising the question of whether SFKs display functional equivalence. Here, we show that Src kinase, followed by Fyn kinase and then Lyn kinase, exhibit ranked tumorigenic potential during both paracrine-induced and cell autonomous initiated prostate cancer. This quantitative variation in transformation potential appears to be regulated in part by post-translational palmitoylation. Our data indicates that development of inhibitors against specific SFK members could provide novel targeted therapeutic strategies.

Introduction

Src family kinases (SFKs) are a group of non-receptor tyrosine kinases composed of nine highly homologous members with four conserved protein domains (1). All SFK members have an SH4 domain that mediates membrane association via myristoylation and, depending on the SFK, palmitoylation, as well as SH3 and SH2 domains that mediate inter- and intra-molecular interactions and finally the SH1 kinase domain (1). SFKs represent central convergence points for multiple receptors and cell autonomous signaling pathways that mediate enhanced cellular proliferation, cell migration and metastatic potential in cancer progression (1, 2). Drug resistance and failure to efficiently inhibit SFKs has spurred the development of a new generation of SRC inhibitors that are currently in clinical trials. These drugs represent a prospectively efficacious therapeutic strategy against numerous solid malignancies and second-line treatment of leukemia (3). However, due to the high homology of SFK members and kinase domains conserved in numerous receptor tyrosine kinases, these inhibitors targeting Src kinase and BCR/ABL also inhibit other SFK members and/or

several receptor tyrosine kinases (3). Off-target effects by these drugs can impair normal tissue function, leading to clinically adverse symptoms including diarrhea, rash and cardiac toxicity (4, 5).

Despite structural similarities, individual SFK members have specific cellular functions in normal development. Genetic knockout of Src, Lyn, or Fyn kinases in mice and derivative cells respectively exhibit defects in the development of bone, peripheral B cells, or T cell receptor signaling (6-8). The specificity of individual SFK members may rely on their preferential association with cell surface receptors. For example, c-Src, but not Fyn or Lyn is associated with $\alpha_{IIb}\beta_3$ integrin in blood platelet signal cascades (9). In contrast, Lyn and Fyn, but not Src, are preferentially recruited to the Fc receptor γ chain and mediate platelet glycoprotein VI receptor signal transduction (10). In human glioblastoma cells, cooperation of integrin $\alpha_v\beta_3$ with platelet-derived growth factor receptor is dependent upon Lyn, but not Fyn, to regulate cell migration (11).

Previous studies from our lab have identified that enhanced expression of wild-type Src and androgen receptor (AR) in naive murine prostate cells results in poorly differentiated adenocarcinoma. This indicates that while rarely mutated in human prostate cancer, Src kinase can still fulfill a functional role in prostate cancer initiation and progression (12, 13). This study, in light of the diverse cellular functions exhibited by SFK members, raises the question of whether individual SFKs are functionally equivalent with respect to tumorigenesis.

To investigate potential quantitative variation in transformation of prostate epithelium by SFK members, we utilized an *in vivo* prostate regeneration system that allows investigation of prostate transformation by both paracrine and cell-autonomous oncogenic stimuli (14, 15). Using this system, we investigated the differential functions of individual SFKs in mediating both paracrine FGF10-induced and cell autonomous transformation of prostate epithelium. We demonstrate that individual SFK members are differentially utilized during FGF10-induced prostate cancer. Epithelial deficiency of Src kinase blocks FGF10-induced tumorigenesis and diminishes the heightened

expression of epithelial AR normally associated with paracrine FGF10 signaling, while knockout of Fyn kinase partially inhibits transformation, and loss of Lyn kinase had no effect. We further demonstrate that SFKs have distinct roles in cell autonomous initiation of prostate cancer. Ectopic expression of constitutively activated Src, Fyn and Lyn kinases exhibit differential capacities for transformation of prostate epithelium. Src kinase presented the strongest oncogenic phenotype, followed by Fyn and then Lyn. Palmitoylation plays an essential role in mediating the distinct functions of Src and Fyn kinases with respect to prostate tumorigenesis. Gain of palmitoylation of Src kinase inhibits tumorigenesis induced by constitutively active Src kinase, while loss of palmitoylation of Fyn, but not Lyn, kinase accelerated tumorigenesis. These data collectively demonstrate that SFK members exhibit distinct intracellular functions and differential response to paracrine signals in the initiation of prostate cancer.

Results

Selective loss of SFKs inhibits paracrine FGF10 induced PIN and carcinoma

Aberrant paracrine signaling from the tumor microenvironment can act as a driving factor in tumorigenesis (16). Fibroblast growth factor (FGF)/fibroblast growth factor receptor (FGFR) paracrine signaling is one of many important pathways in the initiation of numerous cancers (17, 18). We have previously shown that chronic exposure to paracrine FGF10 leads to murine prostatic intraepithelial neoplasia (mPIN) and adenocarcinoma (14) with lesions exhibiting enhanced levels of phosphorylated SFK proteins (Fig. 1, A and B). Further, western analysis of primary murine prostate tissue confirmed endogenous expression of SFK members Src, Fyn and Lyn (Fig S1A). This evidence, combined with studies reporting that Src kinase can mediate FGF signaling (2, 19), indicates functional utilization of SFK members in FGF10-induced transformation.

To assess differential utilization of SFK members during paracrine-induced prostate adenocarcinoma, we used mice bearing targeted knockouts of Src, Fyn or Lyn kinase. Prostate epithelium from $Src^{-/-}Fyn^{+/-}$, $Fyn^{+/-}$, $Fyn^{-/-}$, or $Lyn^{-/-}$ knockout mice and wild type (WT) littermates were combined with FGF10- or GFP-transduced urogenital sinus mesenchymal cells (FGF10-UGSM or GFP-UGSM) (Fig. 1A). In a normal prostate regeneration system, UGSM provides an inductive environment for the regeneration of prostate tissue (20). $Src^{-/-}Fyn^{+/-}$ mice were used because $Src^{-/-}Fyn^{-/-}$ mice are embryonic lethal. Similar regenerative capacity and transformative response to FGF10 in WT controls suggests that genetic heterogeneity present in the different backgrounds does not affect these processes (Fig. S2). Further, the histology of regenerated tissue from $Fyn^{+/-}$ with FGF10-UGSM or GFP-UGSM was similar to its WT counterpart (Fig. S2), indicating that Fyn haploinsufficiency does not affect transformation. Regenerated tissues from knockout mice combined with GFP-UGSM displayed normal prostate tubules containing $CK8^+$ luminal cells and $CK5^+$ basal cells and exhibited typical AR expression patterns (Fig. 1C-D; Fig. S3). This suggests that Src, Fyn, and Lyn kinases are individually dispensable for regeneration of prostate glandular tissue.

Regenerated tissue from WT epithelia combined with FGF10-UGSM exhibited well-differentiated prostate adenocarcinoma, characterized by expansion of the $CK8^+$ luminal population with few $CK5^+$ basal cells (Fig.1, C-D). Similar to WT epithelium, tissues regenerated from $Lyn^{-/-}$ epithelium combined with FGF10-UGSM displayed neoplastic growth (Fig. 1, C-D). Tissues from $Fyn^{-/-}$ epithelial cells with FGF10-UGSM primarily exhibited mPIN lesions, characterized by an expansion of the $CK8^+$ luminal population with maintenance of $CK5^+$ cells (Fig. 1, C-D). In striking contrast, regenerated tissues from $Src^{-/-}Fyn^{+/-}$ epithelium combined with FGF10-UGSM presented normal histology, indicated by normal glandular structures with $CK8^+$ luminal and $CK5^+$ basal

epithelial layers (Fig. 1, C-D). Collectively, our results indicate that the oncogenic effects of FGF10 are largely mediated by Src and Fyn kinases in prostatic epithelium.

Selective loss of SFKs leads to a diminution of epithelial AR in response to paracrine FGF10

Our previous study identified that the expression of epithelial AR increases in response to paracrine FGF10 signaling (14). To investigate modulation of AR expression in the context of paracrine FGF10 and selective loss of SFK members, we examined the expression of AR in regenerated tissues from SFK knockout tissue by immunohistochemistry (IHC).

Expression of AR in grafts derived from $Src^{-/-}Fyn^{+/-}$, $Fyn^{-/-}$, or $Lyn^{-/-}$ epithelial cells with control UGSM was similar to grafts derived from WT littermates (Fig. S3). Selective loss of Lyn did not alter the expression pattern of AR and cyclin D1 in FGF10 grafts compared to WT prostate epithelia while expression of AR and cyclin D1 was decreased to a lesser extent in tissues regenerated from $Fyn^{-/-}$ epithelium (Fig. 2). In contrast, the epithelial expression of AR and cyclin D1 was down-regulated in tissues regenerated from $Src^{-/-}Fyn^{+/-}$ epithelium combined with FGF10-UGSM cells compared to WT prostate epithelia. Collectively, the data indicate that loss of Src kinase, and to a certain extent of loss of Fyn but not Lyn kinase, modulate expression of AR and cyclin D1 in response to paracrine FGF10.

Inhibition of Src family kinase signaling by a dominant negative Src kinase mutant attenuates FGF10-induced adenocarcinoma.

To support that Src family kinases mediate FGF10 signaling, we blocked SFK signaling by ectopic expression of Src(Y529F/K298M), an open conformation, kinase dead mutant of Src kinase (21). Dissociated prostate epithelial cells were transduced with either control vector or Src(Y529F/K298M) and combined with FGF10-UGSM cells. Both control and Src(Y529F/K298M) vectors contained an RFP fluorescent reporter driven by a separate CMV

promoter. Tubules infected with control vector exhibited FGF10 induced adenocarcinoma (Fig.3), with transformed tubules presenting increased AR expression. In contrast, tubules infected with dominant negative Src kinase were phenotypically normal and expressed low amounts of AR when compared to neighboring RFP negative tubules (Fig. 3). As the dominant negative Src kinase could inhibit signaling through multiple SFK members, this data does not indicate hierarchical significance. However, it does strongly support a role for SFK signaling mediating transformation and increased epithelial AR expression in response to chronic FGF10 signaling.

Constitutively active SFK members exhibit differential oncogenic potential in primary prostate cells.

Our results indicate that SFK members are not functionally equivalent in the context of paracrine-induced carcinoma, therefore we asked if this pattern was conserved in cell autonomous transformation by SFK members. Independent labs have reported increased expression and activation of wild-type Src, Fyn and Lyn with prostate cancer progression (22-24). We generated lentivirus bearing constitutively active Src (Y529F), Fyn (Y528F) or Lyn (Y508F) kinase with an RFP reporter (Fig. 4A) and confirmed expression by western analysis (Fig. S1B). While rarely observed in human cancers, constitutively active mutants phenocopy the synergy of c-Src and AR in prostate cancer and chronic SFK activation by signal transduction pathways (13).

To assess differential cell autonomous transformation in primary cells, dissociated prostate epithelial cells were transduced with Src(Y529F), Fyn(Y528F) or Lyn(Y508F) kinase and combined with WT UGSM. Src(Y529F) tumors lacked glandular structure and were predominantly $CK8^+$ luminal cells, characteristic of poorly differentiated invasive adenocarcinoma (Fig 4, B). Tubules over-expressing Fyn(Y528F) exhibited mPIN lesions with stratified layers of $CK8^+$ luminal cells (Fig. 4B). In contrast, over-expression of Lyn (Y508F) resulted in phenotypically normal regeneration (Fig. 4B). Collectively, these *in vivo* results clearly demonstrate that cell autonomous

expression of constitutively active SFKs in naïve adult prostate epithelium results in dramatically different phenotypes.

Alteration of palmitoylation sites change oncogenic potential of constitutively active Src and Fyn kinases in prostate cancer

To investigate potential mechanisms for the observed differences in transformation between SFK members, we asked if alteration of the palmitoylation status of SFK members modulates transformation capacity. Segregation of SFK members into lipid rafts by palmitoylation could further enhance preferential interactions with receptors and determine functional specificity (25, 26). To address this, wild-type and constitutively active Src and Fyn kinases were respectively mutated at predicted palmitoylation sites (Fig.5A) (25). We transduced $Src^{-/-}Yes^{-/-}Fyn^{-/-}$ (SYF) fibroblasts with control or palmitoylation mutant Src and Fyn kinases and assessed *in vitro* colony formation in soft agar. Compared to controls, the Src(S3C/S6C) or Src(Y529F/S3C/S6C) palmitoylation mutants exhibited reduced colony formation and attenuated Src activation while Fyn(C3S/C6S) or Fyn(Y528F/C3S/C6S) palmitoylation mutants exhibited dramatically increased colony formation or the size of colony (Fig. S4). In addition, gain of palmitoylation sites in Src(S3C/S6C) or Src(Y529F/S3C/S6C) mutants attenuated expression of phospho-Src kinase (Fig. S4).

We then assessed transformation activity of Src palmitoylation mutants in the prostate regeneration assay. Src (Y529F) grafts displayed solid tumors without glandular structure (Fig. 5B) and exhibited primarily $CK8^+$ but not $CK5^+$ cells, both E-cadherin and vimentin expression, elevated phospho-Src(Y416) and phosphorylated tyrosine levels (Fig. 5C). In contrast, Src(Y529F/S3C/S6C) infected tubules were predominantly normal with a few displaying low-grade hyperplasia. These tubules exhibited normal CK8 and CK5 patterns, expressed E-cadherin but not vimentin with low levels of phospho-Src(Y416) and phospho-tyrosine. Additionally, both Src(Y529F/S3C/S6C) and Src(Y529F) regenerations displayed similar levels of total Src kinase

(Fig.5C). Finally, Src (Y529F) grafts also exhibited increased expression of phospho-ERK and phospho-FAK, but not Cbp and phospho-AR, as compared with Src(Y529F/S3C/S6C) tissue (Fig. S5).

We next examined if loss of predicted palmitoylation sites in Fyn kinase would likewise alter prostate transformation efficiency *in vivo*. In contrast to the mPIN lesions induced by Fyn(Y528F), lesions induced by Fyn(Y529F/C3S/C6S) presented as poorly differentiated invasive carcinoma and resembled transformation by Src(Y529F) (Fig. 5B and C). The transformed tissues exhibited $CK8^+$ but not $CK5^+$ cells, vimentin but not E-cadherin expression, and highly elevated levels of pSrc(Y416) and phospho-tyrosine (Fig. 5C). Fyn expression was assessed using a Src kinase antibody that exhibits cross-reactivity for other SFK members. The total Fyn expression was elevated in Fyn(Y529F/C3S/C6S) transformed tissues when compared to Fyn(Y529F) (Fig. 5C). In addition to changing how Fyn is trafficked within the cell, Fyn palmitoylation mutants could also exhibit higher stability, leading to more efficient expression (27, 28). Additionally, the expression of phospho-FAK was increased in Fyn(Y529F/C3S/C6S) transformed tissue, but not the expression of Cbp, phospho-ERK and phospho-AR (Fig. S5). Finally, expression of Lyn(Y508F) loss of palmitoylation mutants resulted in phenotypically normal regenerations (Fig. S6). Collectively, our studies suggest that palmitoylation modification of the SH4 domain modulates tumorigenic potential of constitutively active Src and Fyn kinases by regulating downstream signaling.

Discussion

Despite separate lines of evidence that indicate Src, Fyn and Lyn kinases are each up-regulated in prostate cancer (22-24), our findings indicate that 1) individual SFK members differentially mediate paracrine FGF10 signal transduction and transformation and 2) exhibit differential capacity for cell autonomous transformation. SFKs have been considered as potential

drug targets in prostate cancer. Dasatinib (Sprycel; Bristol Myers-Squibb), saracatinib (formerly AZD0530; AstraZeneca) and bosutinib (previously SKI-606;Wyeth) represent three inhibitors of Src kinase being used in the clinical trials (3). Dasatinib has high affinity for Src and BCR-ABL, but also targets other SFK members, c-KIT, PDGFR, and ephrin A2. Similarly, saracatinib can effectively inhibit Src and other SFK members with activity against ABL and activated mutant forms of EGFR, while bosutinib is a dual Src/ABL kinase inhibitor that also targets other SFK members without inhibition of KIT or PDGFR (3). While these inhibitors exhibit clinical efficacy, reports have identified toxic effects including centrosomal and mitotic spindle defects to normal cells, reduced tubular secretion of creatinine, and cardiac toxicity (4, 29, 30). Several adverse clinical symptoms such as renal failure, nausea, fatigue, lethargy, anorexia, proteinuria, vomiting and diarrhea are also associated with treatment (3). Although the mechanisms leading to these adverse symptoms are unknown, given the functional differences of SFKs observed in our study, it becomes prudent to investigate whether selective, rather than broad, inhibition of SFKs could represent an effective treatment strategy and potentially reduce adverse effects.

The transformation capacity of SFK members is directly related to their differential localization within plasma membrane microdomains that is determined in part by N-terminal lipid modification (25, 31). With respect to Src kinase, activity is seemingly dependent upon its distribution between plasma membrane microdomains that sequester inhibitory factors and substrate access outside of these domains (26). By enhancing the association of Src kinase with hydrophobic microdomains by artificial palmitoylation, its oncogenic activity is likely inhibited by endogenous regulatory mechanisms (26, 31). In contrast, loss of palmitoylation mutation in Fyn kinase results in gain of function that phenocopies activated Src kinase, likely due to some overlapping substrate specificities (32). This is also reflected in their differential responses to FGF and EGF signaling (33). In addition, modification of the N-terminus of Src Family kinases including palmitoylation and

myristoylation could alter their localization at cell membrane, and subsequently influence protein expression and activity (27, 28). That mutation of palmitoylation sites in Lyn kinase does not increase transformation activity indicates that microdomain localization is not the sole determinant of activity and rather extends to substrate specificity as well. This notion is supported by studies identifying largely non-overlapping signaling mechanisms (11) and trafficking patterns (34) between SFK members Src, Fyn and Lyn. Finally, while our studies provide evidence that palmitoylation modification can modulate cell autonomous transformation activity, it remains to be seen if this plays a role in the human disease.

Our results support previous studies that FGF10-induced prostate adenocarcinoma exhibits elevated AR expression in epithelial cells (14). Over 80% of castration resistant prostate cancer cases express high levels of AR and androgen-responsive genes (35). Our study suggests that specific SFK members are critical in mediating FGF10-induced transformation and the subsequent increase in AR expression, offering an *in vivo* mechanism linking FGF10 signal transduction and AR expression. Supporting a role for SFK members in modulating AR expression, a study by DaSilva et al. (36) identified that stabilization of AR by PTHrP/EGFR signaling is mediated by Src kinase. In our study, epithelial loss of Src kinase presented the greatest inhibitory effect on transformation and up-regulation of AR, indicating the greatest functional significance. Supporting this hypothesis, enhancement of FGF10/FGFR→Src kinase→AR signaling pathway by co-expression of wild type Src kinase and AR in prostate epithelium results in a potent synergistic transformation phenotype (13). Collectively, these results imply that targeting this signaling pathway represents an important route for treating prostate tumorigenesis.

Materials and Methods

Plasmids

Control FUCGW and FGF10-FUCGW vectors were prepared as described (14). The open reading frames of murine Src and Fyn kinases were amplified by PCR from cDNA of mouse spleen or thymus using primer pairs of Src(F)-Gene and Src(R)-Gene, and Fyn(F)-Gene and Fyn(R)-Gene, respectively. The open reading frame of human Lyn kinase was PCR amplified from a plasmid generated as described (37). PCR products were cloned into the Xba1 and EcoR1 sites of the FUCRW lentivector, in which RFP is constitutively expressed by the CMV promoter (Figure 2A). Constitutively active Src kinase was generated by site-directed mutagenesis with the QuikChange kit (Stratagene) using the primer pair Src(Y529F)-F/Src(Y529F)-R encoding for phenylalanine at residue 529. Constitutively active Fyn and Lyn kinase mutants were generated by PCR amplification using primer pairs Fyn(F)-Gene/Fyn(Y529F)-R and Lyn(F)-Gene/Lyn(Y508F)-R with substituted nucleotides encoding phenylalanine at residues 528 and 508, respectively. The tyrosine to phenylalanine mutation in SFK members allows adoption of an open conformation of the catalytic domain, leading to constitutive activation (38). Palmitoylation mutants of Src, Fyn and Lyn kinases were generated by PCR amplification using primer pairs palm-Src-F/Src(R)-Gene or Src(Y529F)-R, palm-Fyn-F/ Fyn(R)-Gene or Fyn(Y528F)-R, palm-lyn-F/Lyn(R)-Gene or Lyn(Y508F)-R. Primer sequences are listed in supplemental table 1 with underlined nucleotides indicating point mutations.

Mice strains, prostate regeneration and prostate epithelial viral infections

Mouse strains used in this study include: 1) $Fyn^{+/-}$, $Fyn^{+/-}Src^{-/-}$ and wild type littermates on a BL6/129S7 mixed genetic background and were maintained in Jonathan Cooper's lab; 2) $Fyn^{-/-}$ and wild type littermates on a BL6/129S7 mixed genetic background and were purchased from Jackson Labs; 3) $Lyn^{-/-}$ and wild type littermates on a BL6 background and were maintained in Clifford Lowell's and Owen Witte's labs.

Regeneration and transduction of prostate epithelium

The regeneration process, lentivirus preparation, titering, and transduction of dissociated prostate cells were performed under University of California, Los Angeles safety regulations for lentivirus usage as described previously (20). Lab animal housing, maintenance, and all surgical and experimental procedures were undertaken in compliance with the regulations of the Division of Laboratory Animal Medicine of the University of California, Los Angeles. Prostate regenerations were prepared as described (20). In brief, dissociated prostate cell suspensions were prepared from 6- to 10-week old male mice. 1-2 x 10^5 dissociated prostate cells were transduced with lentivirus carrying the gene of interest at an MOI of 50. Transduced cells were mixed with 1-2 x 10^5 UGSM cells and suspended in collagen. Grafts were implanted under the kidney capsule in SCID mice and allowed to regenerate for 6-8 weeks.

Immunohistochemistry and Western analysis

Following regeneration, hosts were sacrificed and grafts were recovered via surgical resection of the kidney. Transilluminated and fluorescent images were taken using a dissecting microscope. Grafts were fixed in 10% buffered formalin overnight, embedded in paraffin and sectioned at 4 μm. Sections were stained with hematoxylin and eosin (H&E) for representative histology. Immunohistochemical (IHC) stains were visualized using the EnVision+ system (DAKO USA). Primary antibodies for Src kinase (1:250; Cell Signaling), phospho-Src family (Tyr416) (1:50; Cell Signaling), AR (1:200; Santa Cruz Biotechnology), phospho-AR (Ser213/210; 1:50; Imgenex), Cbp (ab14989; 1:200; Abcam), phospho-FAK (ab4803; 1:150; Abcam), phospho-Erk (#4376; 1:50; Cell signaling) were used. For immunofluorescent analysis, sections were incubated with primary antibodies against vimentin (1:250; Abcam), E-cadherin (1:250; BD Transduction Laboratories), CK5 (Covance, Berkeley, CA; 1:1000), or CK8 (Covance; 1:1000) and visualized by Alexa-594 or Alexa-488 conjugated secondary antibodies (Molecular Probes, Eugene, OR; 1:1000). For

biotinylated secondary antibodies, sections were incubated with FITC-conjugated streptavidin (Molecular Probes; 1:250). Sections were counterstained with DAPI (Vector Laboratories, Burlingame, CA) and analyzed by fluorescent microscopy. Primary antibodies for phospho-Src family (Tyr416) (1:1000; Cell Signaling), Erk2 (1:5000; Santa Cruz Biotechnology) were used in western analysis.

Acknowledgements

We thank Li Xin, Deanna Janzen, Yang Zong, Andrew Goldstein, Tanya Stoyanova, and Justin Drake for technical help and scientific discussions, Esther Jhingan and Moham M. Ansari for maintaining the Src knockout mice colony. We thank the Tissue Procurement Core Laboratory at UCLA for assistance on tissue processing and H&E staining. This work was supported by funds from the U.S. Army Medical Research and Material Command grants W81XWH-08-1-0329 to H.C. and the Prostate Cancer Foundation Challenge Award (O.N.W). J.A.C. is supported by RO1CA41072. C.A.L. is supported by RO1Al65495 and Al68150. SM is supported by PCF Young Investigators Award, BIRCWH grant (NIH/NICHHD 5 K12 HD001400), UCLA Jonsson Comprehensive Cancer Center Foundation Seed Grant, The Eli & Edythe Broad Center of Regenerative Medicine and Stem Cell Research Award and The Scholars in Translational Medicine gift. DAS is supported by the UCLA Tumor Biology Program USHHS Ruth L. Kirschstein Institutional National Research Service Award # T32 CA009056. O.N.W. is an Investigator of the Howard Hughes Medical Institute.

Author Contributions

H.C. and O.N.W. designed research; H.C. and S.M. performed research; H.C., C.A.L., J.A.C., D.A.S., and O.N.W. analyzed data; and H.C., D.A.S., and O.N.W. wrote the paper.

Figure Legends

Figure 1 Selective loss of SFKs differentially inhibit paracrine FGF10 induced PIN and carcinoma

A) Schematic of prostate regeneration assay. Reconstituted prostate tissues are generated from a recombination of prostate epithelial cells with GFP(control)/FGF10-UGSM under subrenal capsule.

B) Paracrine-FGF10 induced multifocal prostate adenocarcinoma shows elevated expression of activated Src kinase. Western and IHC analysis of pSrc(Y416), which cross-reacts with analogous sites in SFK members, in regenerated tissue derived from GFP or FGF10-UGSM. (Scale bar: 100μm)

C-D) Histological analysis of regenerated tissues by H&E and IHC for basal CK5 and luminal CK8. Regenerated tissues were derived from primary prostate cells of wild type, Src-/-Fyn+/-, Fyn-/-, and Lyn-/- combined with GFP-UGSM or FGF10-UGSM. Inserts provide high magnification to highlight cytokeratin expression. (Scale bar: 100μm)

Figure 2 Selective loss of SFKs led to a diminution of epithelial AR in response to paracrine FGF10

IHC analysis of AR and cyclin D1 expression in the regenerated tissue derived from primary prostate cells of wild type, Src-/-Fyn+/-, Fyn-/-, and Lyn-/- combined with FGF10-UGSM. (Scale bar: 100μm)

Figure 3 Over-expression of dominant negative Src kinase mutant inhibits paracrine FGF10-induced prostate adenocarcinoma.

H&E staining, fluorescent microscopy and IHC analysis shows histology, Src(Y529F/K298M)-infected RFP^+ tubules, and expression of Src, AR, and cyclin D1 in regenerated tissues derived from

primary prostate cells transduced with vector or Src(Y529F/K298M) and combined with FGF10-UGSM.

Figure 4 Ectopic expression of constitutive active Src family kinases in primary prostate cells shows hierarchical role of SFKs in the initiation of prostate cancer.

A) Schematic of obtaining prostate epithelial cells, lentiviral infection (with bicistronic vector encoding activated SFKs and the fluorescent marker RFP) and transplantation to induce prostate carcinoma under subrenal capsule. The expression of SFK gene is driven by the ubiquitin promoter, while RFP is driven by the CMV promoter.

B) H&E staining, RFP signal, and IHC staining of CK5 (red)/CK8 (green) and AR in regenerated tissue derived from primary prostate cells infected with mAKT (control), Src(Y529F), Fyn (Y528F), and Lyn(Y508F). Inserts provide high magnification to highlight cytokeratin expression. (Scale bar: 100μm)

Figure 5 Alteration of palmitoylation sites change oncogenic potential of constitutively active Src and Fyn kinases in prostate cancer.

A) Schematic of SFKs mutations at palmitoylation sites. The serine 3 and 6 sites of Src(Y529F), and the cysteine 3 and 6 sites of Fyn(Y528F) were mutated to cysteine and serine, respectively. Src(Y529F/S3C/S6C) gains two palmitoylation sites, and Fyn(Y529F/C3S/C6S) loses two palmitoylation sites.

B) Regenerated prostate grafts were derived from $2x10^5$ of prostate cells infected with Src (Y529F), Src(Y529F/S3C/S6C), Fyn (Y528F) or Fyn (Y528F/C3S/C6S).

C) H&E staining, RFP signal, and IHC staining of CK5(red)/CK8(green), E-cad(red)/Vim(green), Src kinase, phospho-Src (Y416), and phosphotyrosine in regenerated tissues derived from primary prostate cells infected with Src(Y529F), Src(Y529F/S3C/S6C), Fyn(Y528F) and

Fyn(Y528F/C3S/C6S). Inserts provide high magnification to highlight cytokeratin expression. (Scale bar: 100μm)

Figure 1

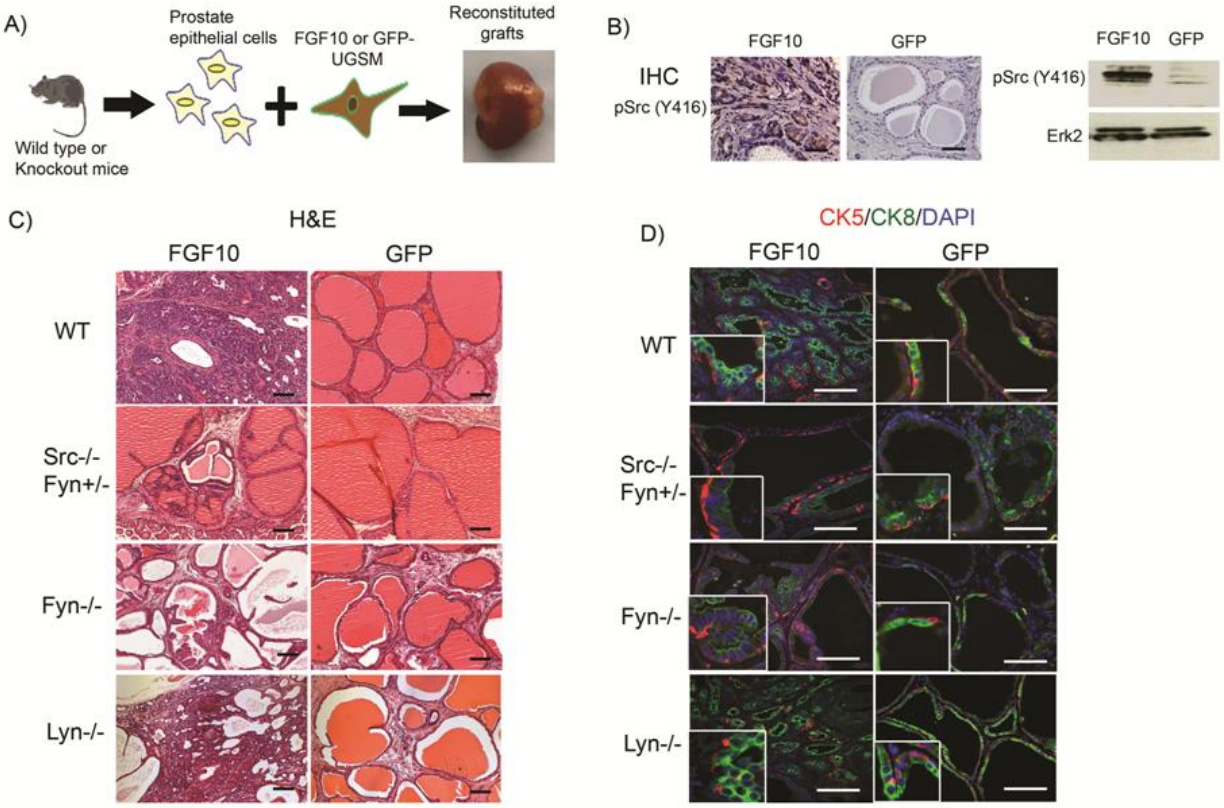
A)
Prostate epithelial cells
FGF10 or GFP-UGSM
Reconstituted grafts
Wild type or Knockout mice
B)
FGF10
GFP
IHC
pSrc (Y416)
FGF10
GFP
pSrc (Y416)
Erk2
C)
H&E
FGF10
GFP
WT
Src-/- Fyn+/-
Fyn-/-
Lyn-/-
D)
CK5/CK8/DAPI
FGF10
GFP
WT
Src-/- Fyn+/-
Fyn-/-
Lyn-/-

Figure 2

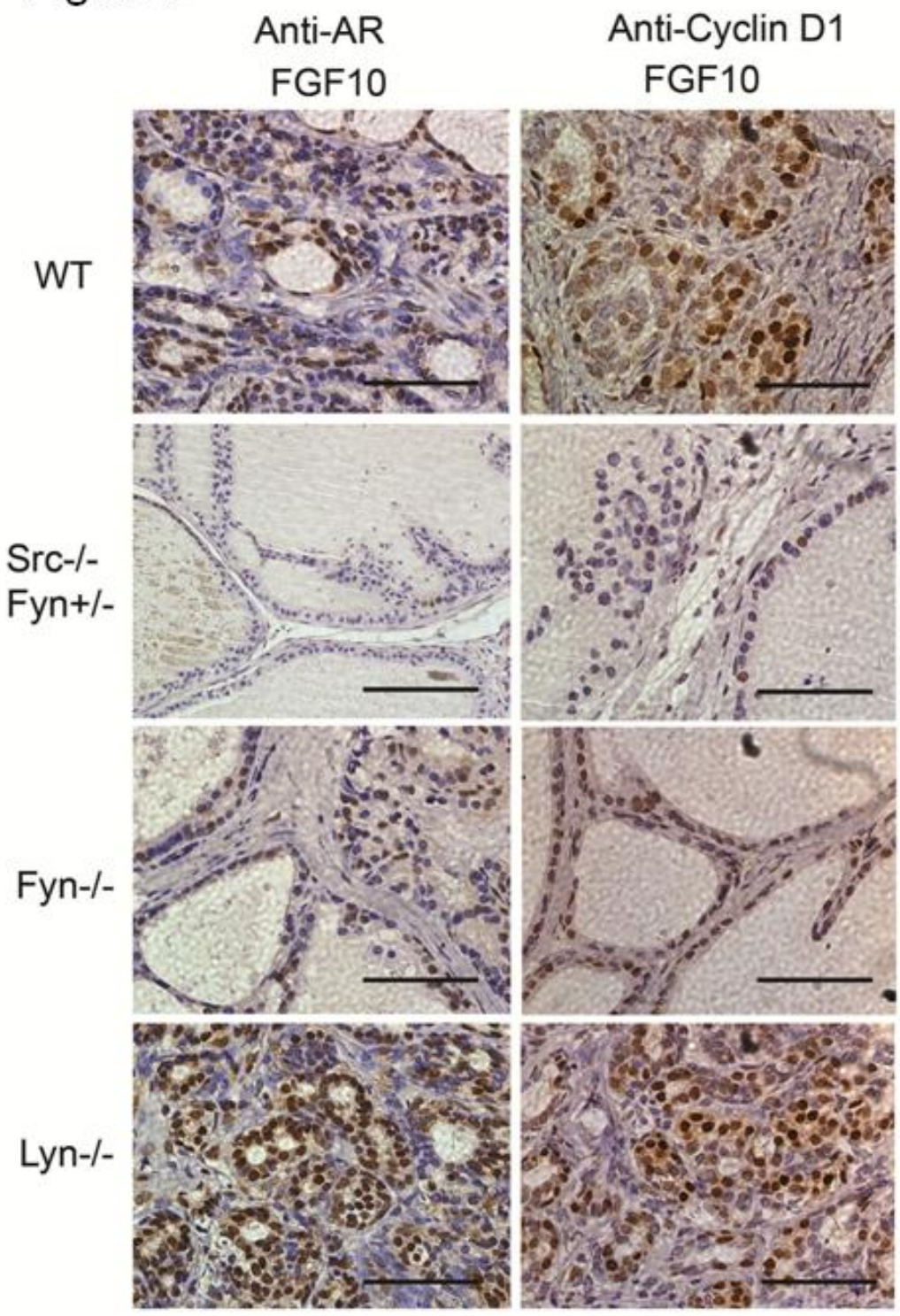

Figure 3

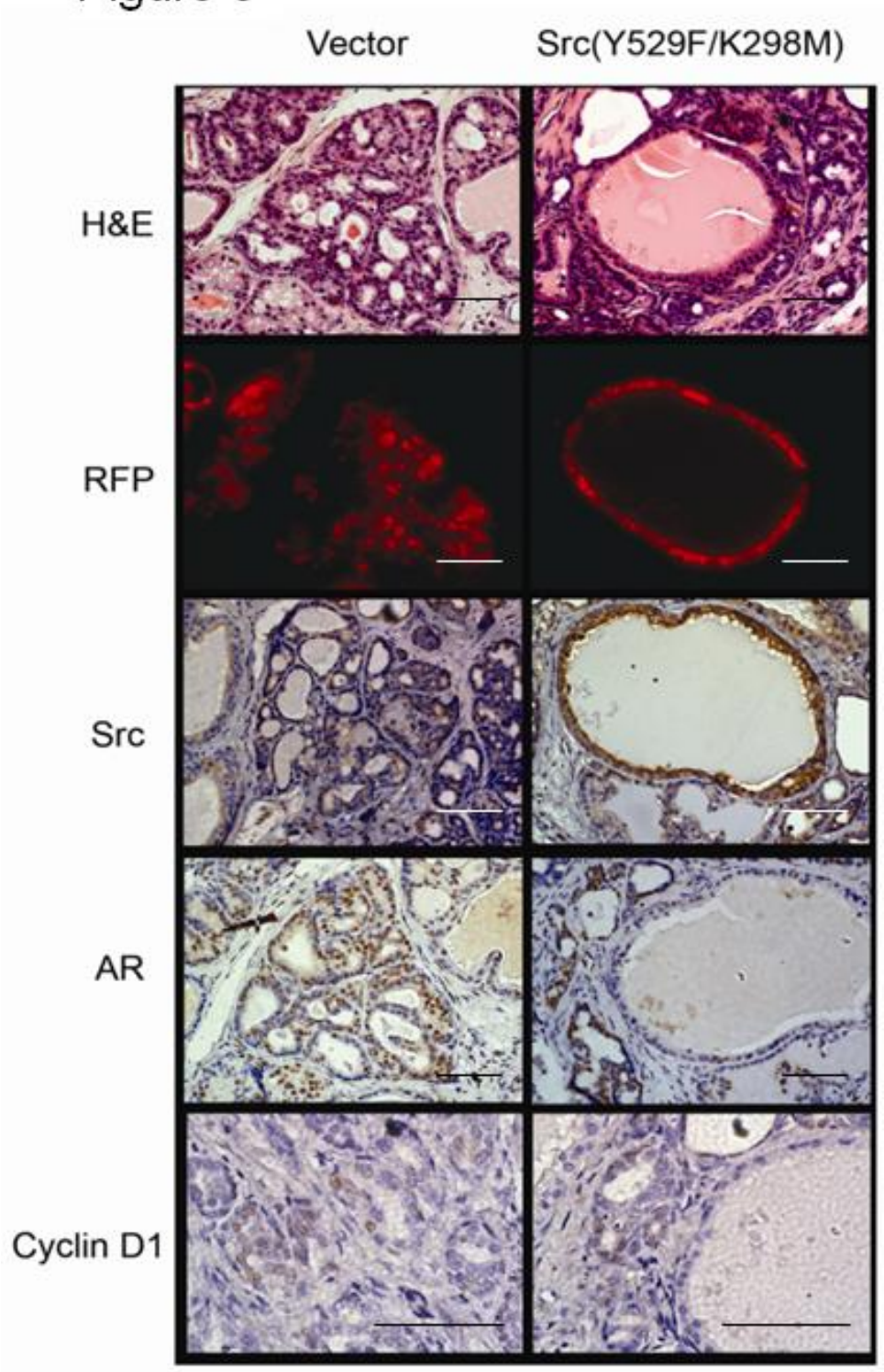

Figure 4

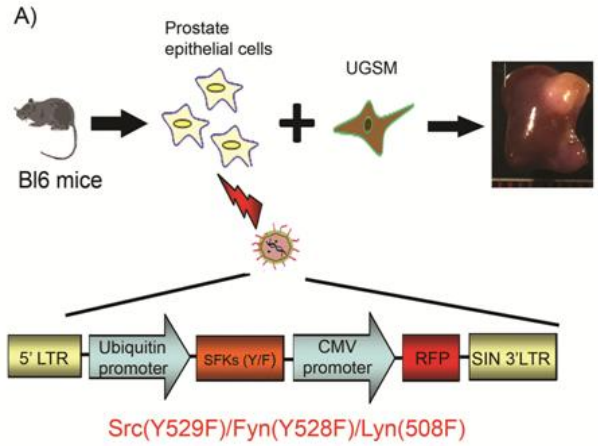
A)
Prostate epithelial cells
UGSM
Bl6 mice
5' LTR
Ubiquitin promoter
SFKs (Y/F)
CMV promoter
RFP
SIN 3'LTR
Src(Y529F)/Fyn(Y528F)/Lyn(508F)

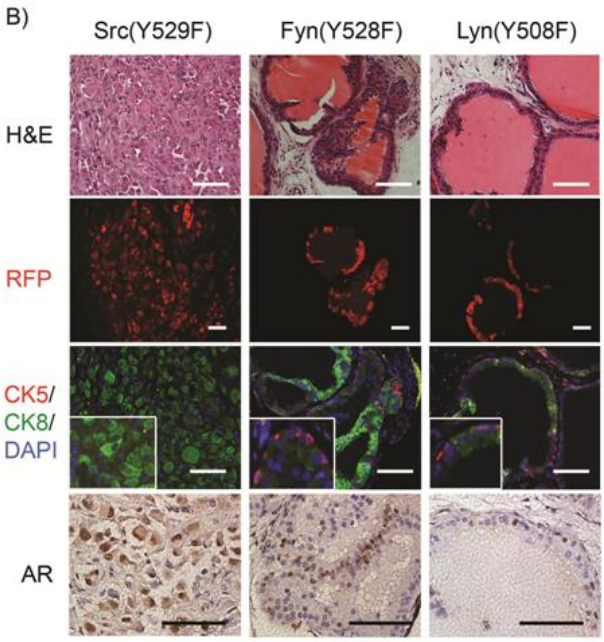
B)
Src(Y529F)
Fyn(Y528F)
Lyn(Y508F)
H&E
RFP
CK5/
CK8/
DAPI
AR

Figure 5

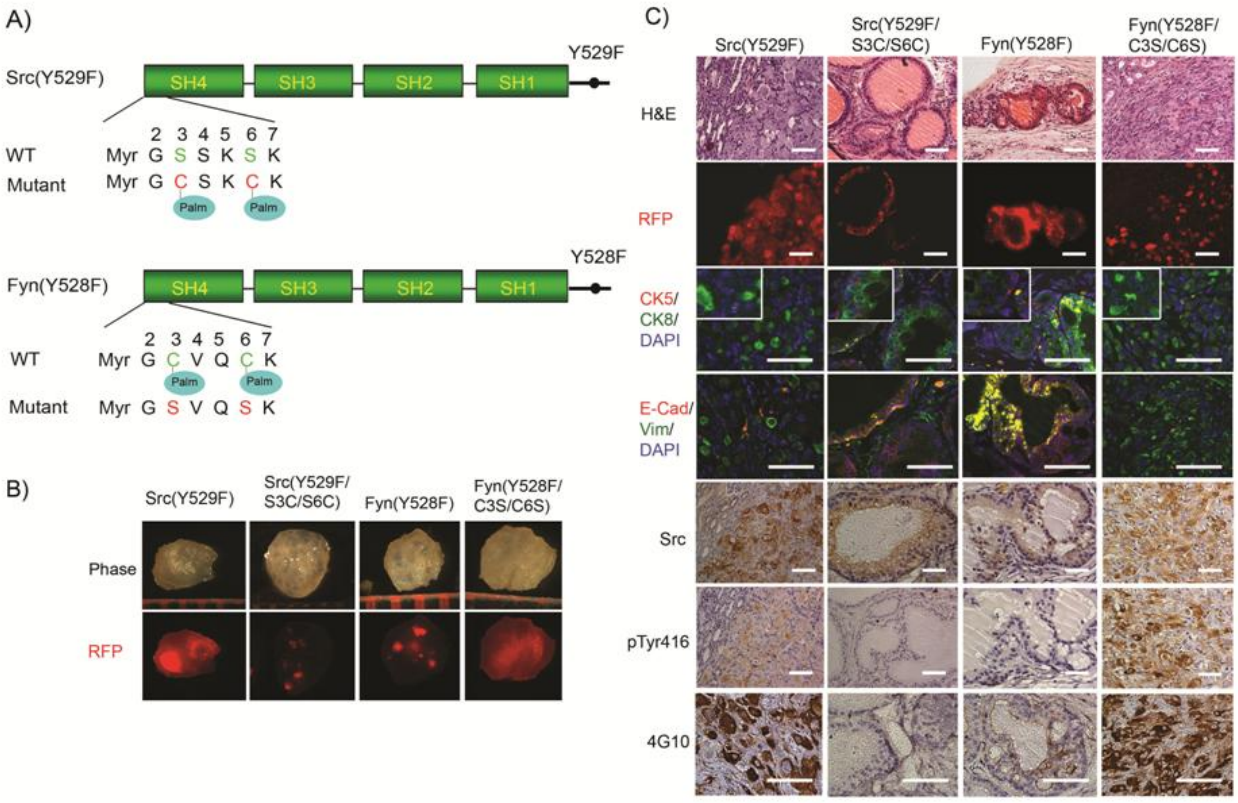
A)
Src(Y529F)
SH4
SH3
SH2
SH1
Y529F
2 3 4 5 6 7
WT Myr G S S K S K
Mutant Myr G C S K C K
Palm
Palm
Fyn(Y528F)
SH4
SH3
SH2
SH1
Y528F
2 3 4 5 6 7
WT Myr G C V Q C K
Palm
Palm
Mutant Myr G S V Q S K
B)
Src(Y529F)
Src(Y529F/ S3C/S6C)
Fyn(Y528F)
Fyn(Y528F/ C3S/C6S)
Phase
RFP
C)
Src(Y529F)
Src(Y529F/ S3C/S6C)
Fyn(Y528F)
Fyn(Y528F/ C3S/C6S)
H&E
RFP
CK5/ CK8/ DAPI
E-Cad/ Vim/ DAPI
Src
pTyr416
4G10

Supplemental Materials and Methods

Soft Agar Assay and western analysis of SFKs expression

SYF fibroblast or 293T cells were transduced with either control or lentivirus carrying wild type, constitutively active, or their palmitoylation mutants of Src, Fyn or Lyn. Transduced RFP^+ cells were sorted by FACS (FACSVantage, BD Biosciences). The soft agar assay was performed according to the manufacturer supplied protocol (Millipore, #ECM570). Briefly, 5000 cells from each condition were plated in 60 mm tissue culture dishes and incubated for 21 days. Colonies larger than 500 μm in diameter were counted and representative photos for each condition were taken.

For western analysis, sorted SYF cells or 293T cells from each condition were cultured in DMEM supplemented with 10% FBS. At ~80% confluence, cells were harvested and protein lysates were prepared using lysis buffer (20mM Tris pH7.4, 150mM NaCl, 1mM EDTA, 1% TritonX-100, 5% glycerol, 2% n-octyl-beta-D-glucoside) supplemented with phosphatase inhibitor cocktail 1 and 2 (P5726 and P2850, SIGMA). Expression of SFK members were assessed by western analysis with ERK1/2 as a loading control. Primary antibodies for Src kinase (1:1000; Cell Signaling), Fyn kinase (1:1000; Cell Signaling), Lyn(1:1000; Cell Signaling), phospho-Src family (Tyr416) (1:1000; Cell Signaling), Erk2 (1:5000; Santa Cruz Biotechnology) were used in western analysis.

Supplemental Figure Legends

Figure S1. Expression analysis of SFK members Src, Fyn and Lyn in primary cells, cell lines and transduced cells.

A) SFKs are expressed in normal murine prostate tissues. Src, Fyn, and Lyn kinase expression patterns in normal murine prostate tissue, human prostate cancer cell lines LNCap and PC3 and murine spleen (control) were determined by western analysis.

B) Transduction into 293T cells leads to robust expression of Src, Fyn and Lyn kinases. To confirm over-expression, 293T cells were transduced with lentivirus bearing Src, Fyn or Lyn kinase. Lysates were prepared 48 hours post-transduction and expression was detected by western analysis.

Figure S2. Prostate epithelial cells from inbred (BL6), mixed genetic background (BL6/129S7), and $Fyn^{+/-}$ (BL6/129S7) mice respond similarly to control and paracrine FGF10 UGSM.

Histological features show normal glandular structure in controls with development of multifocal adenocarcinoma in response to FGF10.

Figure S3. Loss of SFK members Src, Fyn, or Lyn in prostate epithelium does not alter AR expression in grafts regenerated with normal UGSM.

AR expression was determined by IHC analysis of regenerated tissues derived from primary prostate cells of WT, $Src^{-/-}Fyn^{+/-}$, $Fyn^{-/-}$, and $Lyn^{-/-}$ combined with GFP-UGSM.

Figure S4. Mutation of palmitoylation sites modulates transformation potential of Src and Fyn kinases *in vitro.*

A and C) SYF cells were transduced with Src, Src (Y529F) or palmitoylation mutants (A); Fyn, Fyn (Y528F) or palmitoylation mutants (C). Only colonies above 500 μm in diameter were counted. While the difference in colony number between Fyn (Y528F) and Fyn (Y528F/C3S/C6S) was not

significant, the percentage of large colonies (>1000 μm) in Fyn (Y528F/C3S/C6S) was significantly higher than Fyn (Y528F) (C, insert).

B and D) Representative images of colonies formed by SYF cells over-expressing Src and Fyn kinases or palmitoylation mutants. Colonies in Src (Y529F/S3C/S6C) or Src (S3C/S6C) conditions were smaller than respective Src(Y529F) or Src. Colony size was not significantly different between Fyn and Fyn (C3S/C6S).

E) Western analysis of Src kinase, phospho-Src, and Erk1/2 loading control in SYF cells over-expressing Src kinase or palmitoylation mutant derivatives.

Figure S5. Expression of phospho-FAK, phospho-ERK, phospho-AR, and Cbp in constitutively active Src and Fyn palmitoylation mutants. IHC staining of phospho-FAK, phospho-ERK, phospho-AR, and Cbp in regenerated tissues derived from primary prostate cells infected with Src(Y529F), Src(Y529F/S3C/S6C), Fyn(Y528F) and Fyn(Y528F/C3S/C6S). Scale bar: 100μm.

Figure S6. Loss of palmitoylation at C3 of constitutively active Lyn kinase, Lyn(Y508F/C3S), does not modulate tumorigenic potential.

A) The cysteine 3 of Lyn (Y508F) was mutated to serine, preventing palmitoylation of constitutively active Lyn (Y508F) kinase.

B) Regenerated prostate tissues were derived from $2x10^5$ prostate cells transduced with Lyn (Y508F) or Lyn (Y508F/C3S).

C) H&E staining (low magnification bar = 800 μm; high magnification bar = 100μm), RFP signal, and IHC analysis of Lyn expression in regenerated tissues derived from primary prostate cells transduced with Lyn(Y508F) and Lyn(Y508F/C3S). The results indicate that loss of palmitoylation mutation in Lyn (Y508F) does not alter the histology. Scale bar: 100μm.

Supplemental Fig. 1

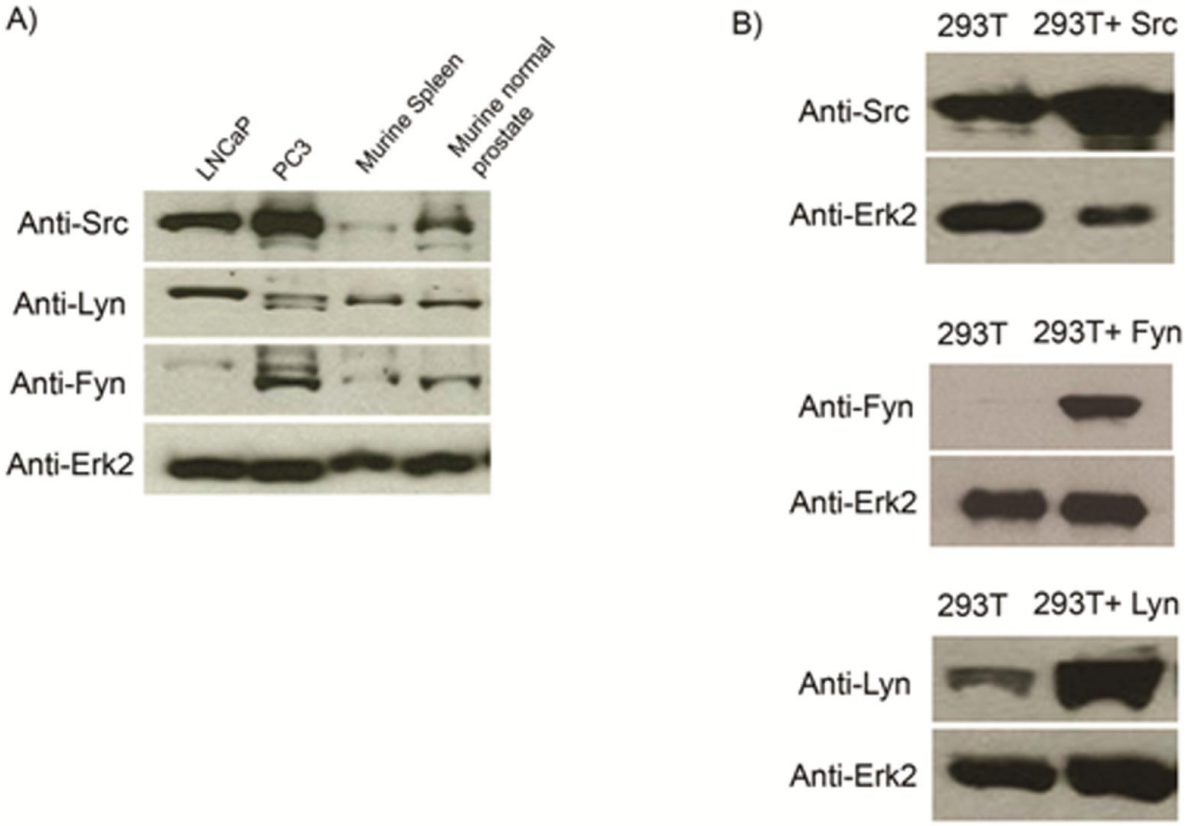

Supplemental Fig. 2

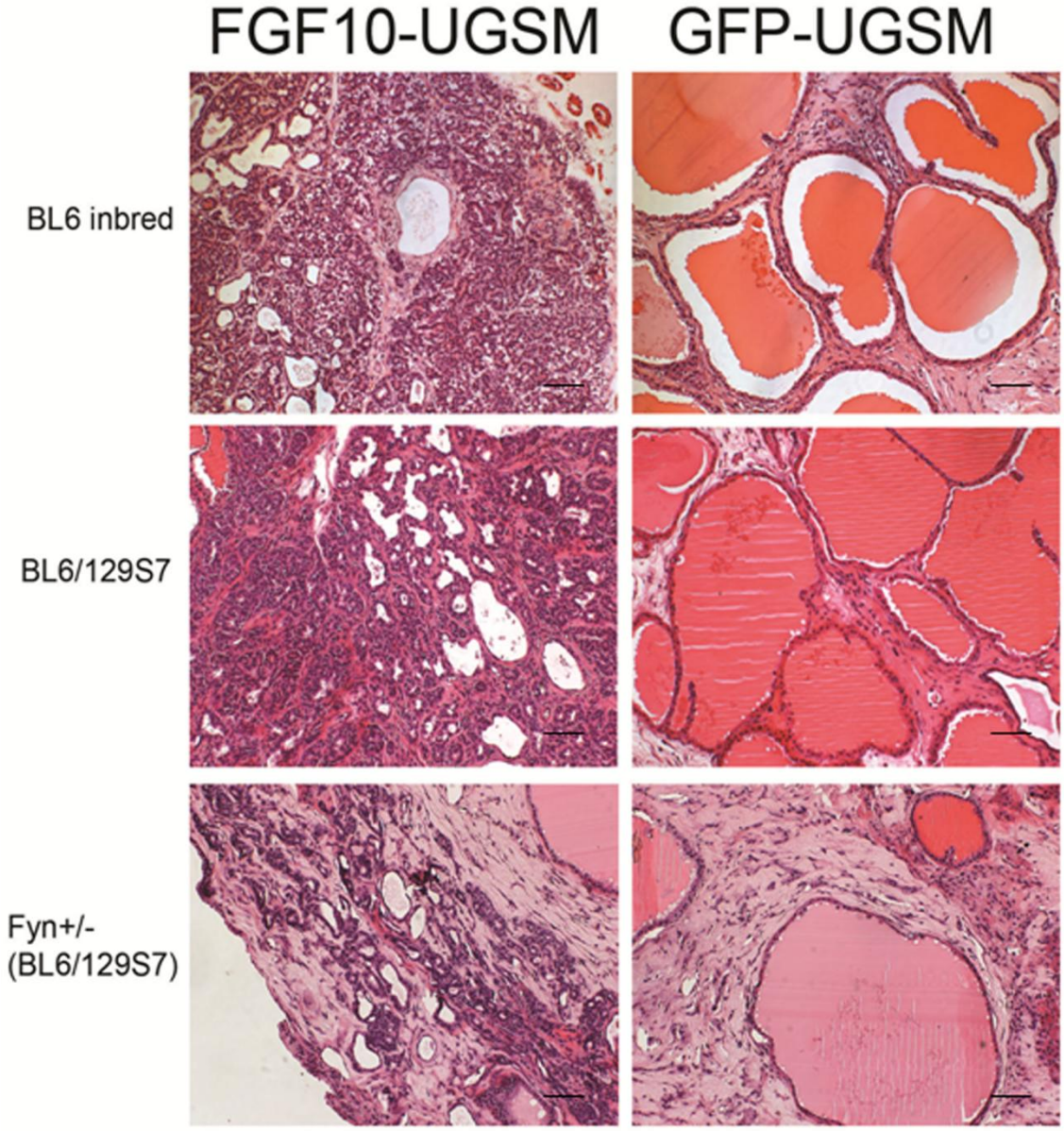

Supplemental Fig. 3

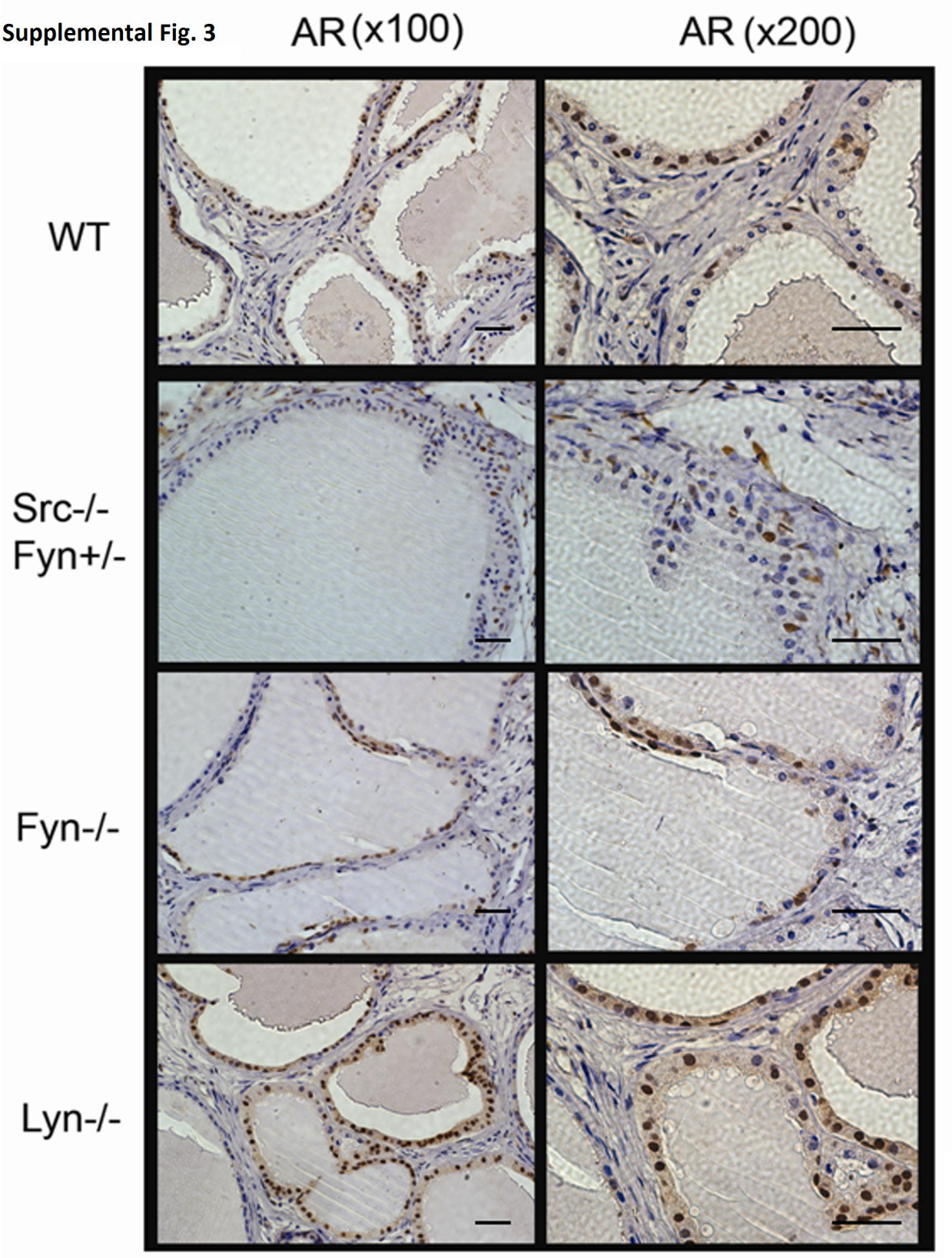

Figure S4

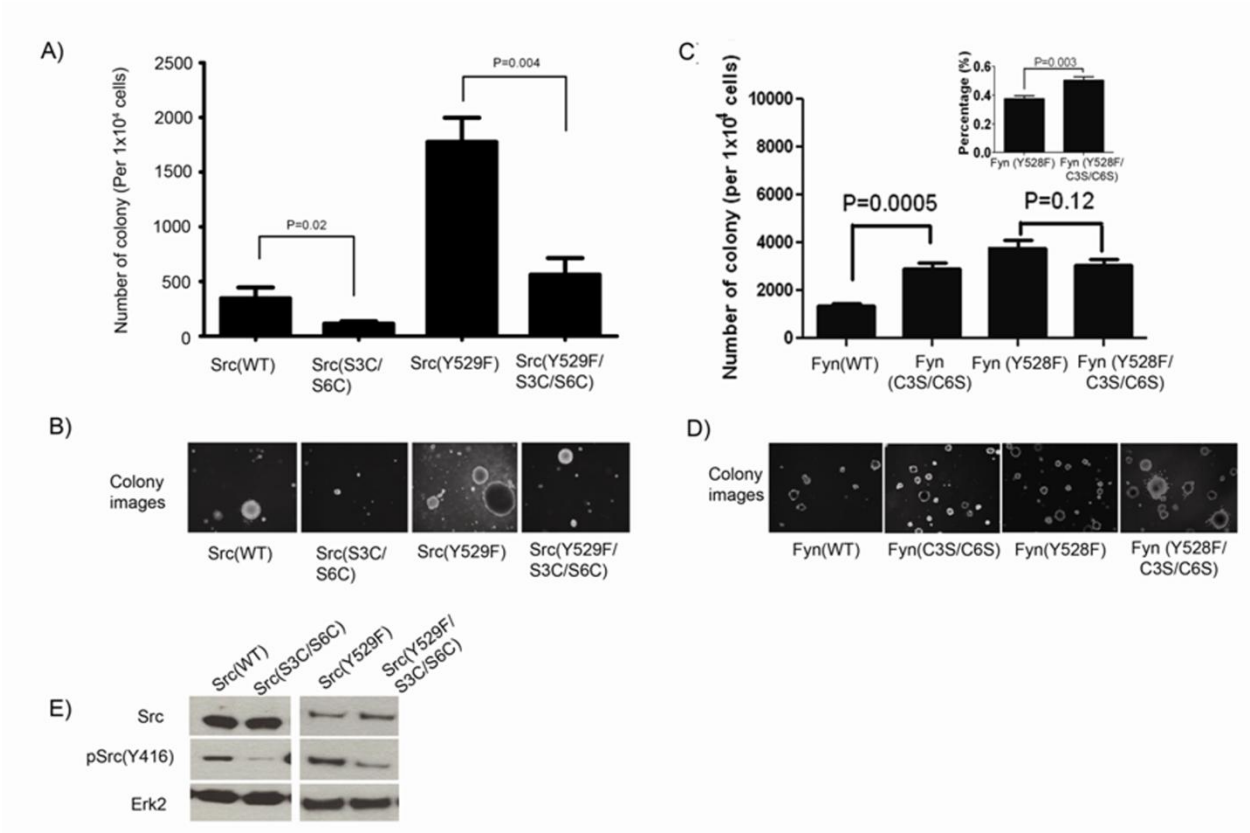
A)
Number of colony (Per 1x10⁴ cells)
2500
2000
1500
1000
500
0
P=0.02
P=0.004
Src(WT)
Src(S3C/ S6C)
Src(Y529F)
Src(Y529F/ S3C/S6C)
C)
Number of colony (per 1x10⁴ cells)
10000
8000
6000
4000
2000
0
P=0.0005
P=0.12
Percentage (%)
0.6
0.4
0.2
0.0
P=0.003
Fyn (Y528F)
Fyn (Y528F/ C3S/C6S)
Fyn(WT)
Fyn (C3S/C6S)
Fyn (Y528F)
Fyn (Y528F/ C3S/C6S)
B)
Colony images
Src(WT)
Src(S3C/ S6C)
Src(Y529F)
Src(Y529F/ S3C/S6C)
D)
Colony images
Fyn(WT)
Fyn(C3S/C6S)
Fyn(Y528F)
Fyn (Y528F/ C3S/C6S)
E)
Src(WT)
Src(S3C/S6C)
Src(Y529F)
Src(Y529F/ S3C/S6C)
Src
pSrc(Y416)
Erk2

Figure S5

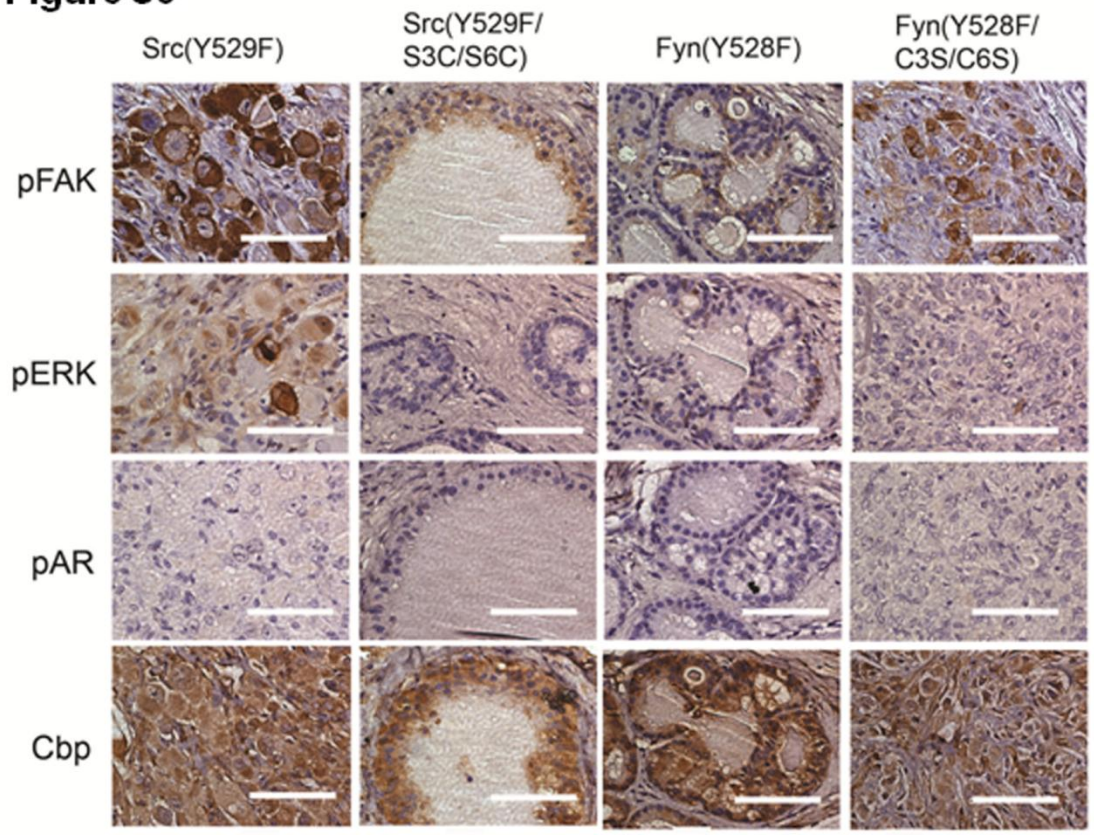

Figure S6

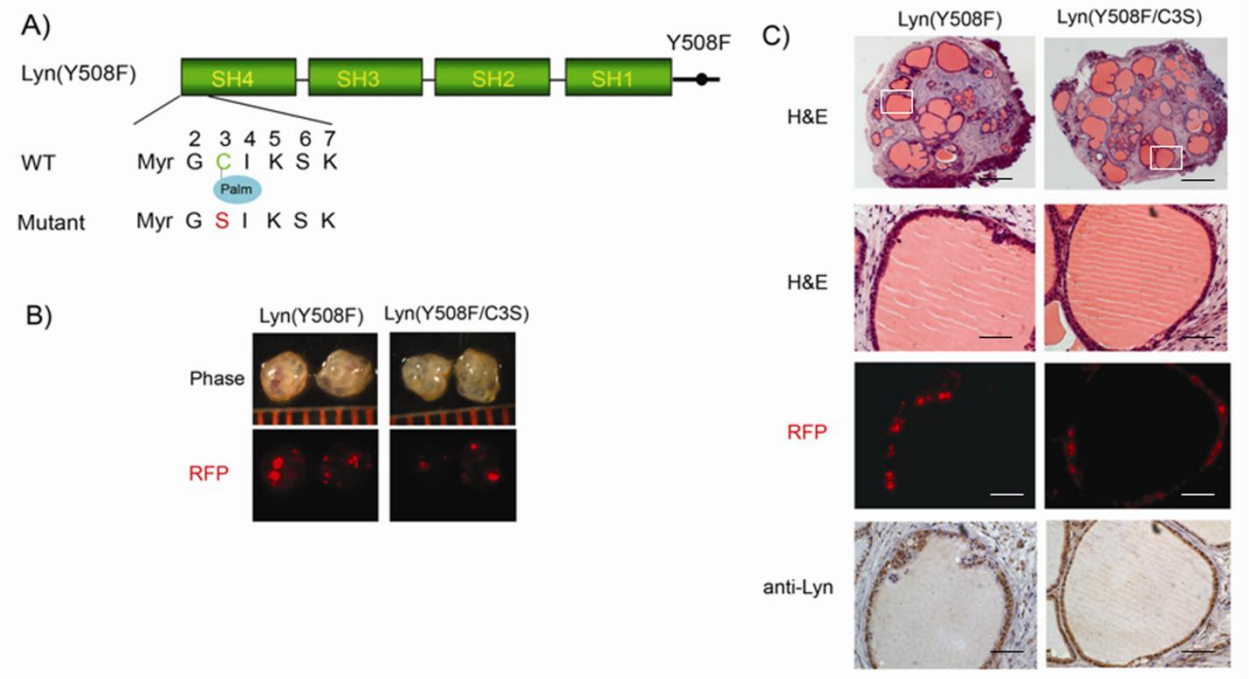

Supplemental Table 1

Organisms	Primer name	Primer sequence
Mouse	palm-Src-F	5'-GTCGACTCTAGAAGGACCATGggcTgcaacaagagc-3'
Mouse	palm-Fyn-F	5'-GTCGACTCTAGATTGgataatgggcagtgtgcaaagtaaggataaag-3'
Mouse	palm-lyn-F	5'- CTGCAGGTCGACTCTAGAATGGGAAGTataaaatcaaaagg-3'
Mouse	Src(F)-Gene	5'- CATTCTAGAAGGACCATGGGCAGCAAC-3'
Mouse	Src(R)-Gene	5'- CATGAATTCACAGTCCCTATAGGTTCTCC-3'
Mouse	Fyn(F)-Gene	5'- CATTCTAGATTGGATAATGGGCTGTGTGCA-3'
Mouse	Fyn(R)-Gene	5'- CATGAATTCGAAGCGCAGGCTCTCACAGG-3'
Human	Lyn(F)-Gene	5'-CATTCTAGAATGGGATGTATAAAATCAAAAGGG-3'
Mouse	Src(Y529F)-F	5'- CCACTGAGCCACAGTTCCAGCCCGGGGAGAAC-3'
Mouse	Src(Y529F)-R	5'- GTTCTCCCCGGGCTGGAACTGTGGCTCAGTGG-3'
Mouse	Fyn(Y528F)-R	5'-CATGAATTCTCACAGGTTTTCACCGGGCTGTTTCTGGGGCTC-3'
Mouse	Lyn(Y508F)-R	5'-CATGAATTCCTAAGGCTGCTGCTGGAATTGCC-3'

References

1. Martin GS (2001) The hunting of the Src. *Nat Rev Mol Cell Biol* 2(6):467-475.

2. Irby RB & Yeatman TJ (2000) Role of Src expression and activation in human cancer. *Oncogene* 19(49):5636-5642.

3. Aleshin A & Finn RS (2010) SRC: a century of science brought to the clinic. *Neoplasia* 12(8):599-607.

4. Orphanos GS, Ioannidis GN, & Ardavanis AG (2009) Cardiotoxicity induced by tyrosine kinase inhibitors. *Acta Oncol* 48(7):964-970.

5. Hartmann JT, Haap M, Kopp HG, & Lipp HP (2009) Tyrosine kinase inhibitors - a review on pharmacology, metabolism and side effects. *Curr Drug Metab* 10(5):470-481.

6. Soriano P, Montgomery C, Geske R, & Bradley A (1991) Targeted disruption of the c-src proto-oncogene leads to osteopetrosis in mice. *Cell* 64(4):693-702.

7. Stein PL, Lee HM, Rich S, & Soriano P (1992) pp59fyn mutant mice display differential signaling in thymocytes and peripheral T cells. *Cell* 70(5):741-750.

8. Chan VW, Meng F, Soriano P, DeFranco AL, & Lowell CA (1997) Characterization of the B lymphocyte populations in Lyn-deficient mice and the role of Lyn in signal initiation and down-regulation. *Immunity* 7(1):69-81.

9. Kralisz U & Cierniewski CS (1998) Association of pp60c-src with alpha IIb beta 3 in resting platelets. *Biochem Mol Biol Int* 45(4):735-743.

10. Briddon SJ & Watson SP (1999) Evidence for the involvement of p59fyn and p53/56lyn in collagen receptor signalling in human platelets. *Biochem J* 338 (Pt 1):203-209.

11. Ding Q, Stewart J, Jr., Olman MA, Klobe MR, & Gladson CL (2003) The pattern of enhancement of Src kinase activity on platelet-derived growth factor stimulation of glioblastoma cells is affected by the integrin engaged. *J Biol Chem* 278(41):39882-39891.

12. Kraus S, Gioeli D, Vomastek T, Gordon V, & Weber MJ (2006) Receptor for activated C kinase 1 (RACK1) and Src regulate the tyrosine phosphorylation and function of the androgen receptor. *Cancer Res* 66(22):11047-11054.

13. Cai H, Babic I, Wei X, Huang J, & Witte ON (2011) Invasive Prostate Carcinoma Driven by c-Src and Androgen Receptor Synergy. *Cancer Res* 71(3):862-872.

14. Memarzadeh S*, et al.* (2007) Enhanced paracrine FGF10 expression promotes formation of multifocal prostate adenocarcinoma and an increase in epithelial androgen receptor. *Cancer Cell* 12(6):572-585.

15. Xin L, Lawson DA, & Witte ON (2005) The Sca-1 cell surface marker enriches for a prostate-regenerating cell subpopulation that can initiate prostate tumorigenesis. *Proc Natl Acad Sci U S A* 102(19):6942-6947.

16. Bhowmick NA, Neilson EG, & Moses HL (2004) Stromal fibroblasts in cancer initiation and progression. *Nature* 432(7015):332-337.

17. Freeman KW*, et al.* (2003) Inducible prostate intraepithelial neoplasia with reversible hyperplasia in conditional FGFR1-expressing mice. *Cancer Res* 63(23):8256-8263.

18. Acevedo VD*, et al.* (2007) Inducible FGFR-1 activation leads to irreversible prostate adenocarcinoma and an epithelial-to-mesenchymal transition. *Cancer Cell* 12(6):559-571.

19. Sandilands E*, et al.* (2007) Src kinase modulates the activation, transport and signalling dynamics of fibroblast growth factor receptors. *EMBO Rep* 8(12):1162-1169.

20. Xin L, Ide H, Kim Y, Dubey P, & Witte ON (2003) In vivo regeneration of murine prostate from dissociated cell populations of postnatal epithelia and urogenital sinus mesenchyme. *Proc Natl Acad Sci U S A* 100 Suppl 1:11896-11903.

21. Miyazaki T*, et al.* (2004) Src kinase activity is essential for osteoclast function. *J Biol Chem* 279(17):17660-17666.

22. Tatarov O*, et al.* (2009) SRC family kinase activity is up-regulated in hormone-refractory prostate cancer. *Clin Cancer Res* 15(10):3540-3549.

23. Goldenberg-Furmanov M*, et al.* (2004) Lyn is a target gene for prostate cancer: sequence-based inhibition induces regression of human tumor xenografts. *Cancer Res* 64(3):1058-1066.

24. Posadas EM*, et al.* (2009) FYN is overexpressed in human prostate cancer. *BJU Int* 103(2):171-177.

25. Resh MD (1994) Myristylation and palmitylation of Src family members: the fats of the matter. *Cell* 76(3):411-413.

26. Oneyama C*, et al.* (2008) The lipid raft-anchored adaptor protein Cbp controls the oncogenic potential of c-Src. *Mol Cell* 30(4):426-436.

27. Resh MD (2006) Palmitoylation of ligands, receptors, and intracellular signaling molecules. *Sci STKE* 2006(359):re14.

28. Patwardhan P & Resh MD (2010) Myristoylation and membrane binding regulate c-Src stability and kinase activity. *Mol Cell Biol* 30(17):4094-4107.

29. Dalton RN, Chetty R, Stuart M, Iacona RB, & Swaisland A (2010) Effects of the Src inhibitor saracatinib (AZD0530) on renal function in healthy subjects. *Anticancer Res* 30(7):2935-2942.

30. Giehl M*, et al.* (2010) Detection of centrosome aberrations in disease-unrelated cells from patients with tumor treated with tyrosine kinase inhibitors. *Eur J Haematol* 85(2):139-148.

31. Oneyama C*, et al.* (2009) Transforming potential of Src family kinases is limited by the cholesterol-enriched membrane microdomain. *Mol Cell Biol* 29(24):6462-6472.

32. Thomas SM, Soriano P, & Imamoto A (1995) Specific and redundant roles of Src and Fyn in organizing the cytoskeleton. *Nature* 376(6537):267-271.

33. Lu KV*, et al.* (2009) Fyn and SRC are effectors of oncogenic epidermal growth factor receptor signaling in glioblastoma patients. *Cancer Res* 69(17):6889-6898.

34. Sato I*, et al.* (2009) Differential trafficking of Src, Lyn, Yes and Fyn is specified by the state of palmitoylation in the SH4 domain. *J Cell Sci* 122(Pt 7):965-975.

35. Chen Y, Sawyers CL, & Scher HI (2008) Targeting the androgen receptor pathway in prostate cancer. *Curr Opin Pharmacol* 8(4):440-448.

36. DaSilva J, Gioeli D, Weber MJ, & Parsons SJ (2009) The neuroendocrine-derived peptide parathyroid hormone-related protein promotes prostate cancer cell growth by stabilizing the androgen receptor. *Cancer Res* 69(18):7402-7411.

37. Guo S, Wahl MI, & Witte ON (2006) Mutational analysis of the SH2-kinase linker region of Bruton's tyrosine kinase defines alternative modes of regulation for cytoplasmic tyrosine kinase families. *Int Immunol* 18(1):79-87.

38. Brown MT & Cooper JA (1996) Regulation, substrates and functions of src. *Biochim Biophys Acta* 1287(2-3):121-149.

CHAPTER 4

Interleukin-6 and oncostatin-M synergize with the PI3K/AKT pathway to promote aggressive prostate malignancy in mouse and human tissues

Daniel A. Smith[1], Atsushi Kiba[5], Yang Zong[4] and Owen N. Witte[2, 3, 4]

[1]Molecular Biology Interdepartmental Program,

[2]Department of Microbiology, Immunology, and Molecular Genetics,

[3]Eli and Edythe Broad Center for Regenerative Medicine and Stem Cell Research,

[4]Howard Hughes Medical Institute, David Geffen School of Medicine, University of California, Los Angeles, CA 90025 and

[5]Pharmaceutical Research Division, Takeda Pharmaceutical Company Limited, Kanagawa, Japan.

Abstract

Chronic inflammation has been proposed as an etiological and progression factor in prostate cancer. In this study, we used a dissociated prostate tissue recombination system to interrogate the role of interleukin 6 (IL6) and the related cytokine oncostatin M (OSM) in the initiation and progression of prostate cancer. We identified that prostatic intraepithelial neoplasia (PIN) lesions induced by PTEN loss of function ($PTEN^{LOF}$) progress to invasive adenocarcinoma following paracrine expression of either cytokine. Increased expression of OSM was also able to drive progression of benign human epithelium when combined with constitutively activated AKT. Malignant progression in the mouse was associated with loss of basal cells in high-grade foci, disorganized E-cadherin expression and invasion into the surrounding mesenchyme. We observed increased activation of STAT3 in $PTEN^{LOF}$ grafts expressing IL6 or OSM and increased activation of ERK1/2 in grafts expressing OSM, supporting involvement of the JAK/STAT and MAPK pathways in mediating the observed synergy. Collectively, our work indicates that pro-inflammatory cytokines such as IL6 or OSM could activate pathways associated with prostate cancer progression and synergize with cell autonomous oncogenic events to promote aggressive malignancy.

Introduction

Prostate cancer is the most commonly diagnosed non-cutaneous cancer in Western men and the second leading cause of cancer-related mortality (1). Understanding factors involved in tumor initiation and progression are critical to developing effective preventative and therapeutic strategies. Chronic inflammation is observed in nearly all forms of cancer and may represent a contributing factor at initiation, progression and metastasis (2–5). Numerous factors have been proposed to contribute to prostatic inflammation, including diet, chronic infection, urine reflux, deregulated sex hormones and physical trauma (6). The pervasive quality of inflammation has also been proposed to

play a role driving in the multifocal nature of prostate cancer (6). Recent studies employing bacterial colonization of the prostate to elicit chronic inflammatory conditions have observed increased oxidative DNA damage (7) and loss of expression of the tumor suppressor Nkx 3.1 (8), leading to epithelial reactive hyperplasia (9) and PIN lesions (10). Increased expression of inflammatory cytokines, including members of the interleukin-6 (IL6) family and others, has been observed in these models and could represent a functional mechanism (9). Studies using immunohistochemical analysis of human prostate biopsies have shown increased expression of IL6 and the related oncostatin-M (OSM) ligands with prostate cancer progression. Additionally, co-expression of their respective receptor subunits in high Gleason grade lesions lead the authors to speculate on the potential for an autocrine signaling loop (11). We sought to interrogate the role of inflammation by monitoring transformation of prostate epithelial cells in a pro-inflammatory environment induced by ectopic expression of IL6 or the related OSM in the stroma of tissue recombination experiments. The interleukin-6 family of cytokines consists of several related ligands, including interleukin-6 (IL6), oncostatin-M (OSM), leukemia inhibitory factor (LIF) and others, that signal through a common GP130 signal transducer with receptor adaptors modulating ligand specificity (12). The members of this family are responsible for mediating a variety of cellular processes, including acute-phase protein response, liver development and regeneration, hematopoiesis, and inflammation (for review, see 18). Ligand engagement activates constitutively associated Janus kinases (JAK) which phosphorylate the cytoplasmic tails of the receptor complex (14). These phosphorylated residues act as docking sites for intracellular signaling modules such as STATs and Shp2/Shc, which mediate activation of the MAPK and AKT pathways (15).

IL6 has been proposed to be a major inflammatory mediator of prostate cancer initiation and progression. It is expressed in several prostate cancer cell lines and generally confers a growth

advantage (16,17). Ectopic expression of IL6 in LNCaP and LuCaP xenografts is sufficient for androgen-independent conversion in castrated male mice, while treatment with an IL6 inhibitory antibody can induce regression of PC3 xenografts (18–20). Several studies have identified increased serum levels of IL6 in prostate cancer patients with correlations to increasing clinical stage (21), advanced hormone refractory disease (22,23) and clinically observable metastasis (24). IL6 has also been shown to promote tumorigenic transformation of benign, SV40T-immortalized human prostate epithelial cells (25).

OSM was originally described for its inhibitory effect on melanoma cell lines and was later determined to be a part of the IL6 family based on homology and use of the GP130 signal transducer (26). While OSM has been implicated in various pathologies, its effect on prostate cancer growth remains unclear. Work in cell lines indicates increased growth in DU-145 and PC-3 cells through activation of the JAK/STAT signaling axis, while the increased growth of 22Rv1 cells treated with OSM is dependent on AKT and p38 MAPK pathways (27,28). Some evidence suggests that OSM activates AR signaling though an androgen-independent mechanism (29). These studies highlight not only the mitogenic capacity of IL6-type cytokines, but also the diversity of signaling mechanisms that are activated following ligand engagement.

While mounting correlative and *in vitro* evidence strongly suggests involvement of IL6 and OSM in prostate cancer, there have been no *in vivo* experiments performed using naïve prostate epithelium with defined oncogenic stress. We sought to interrogate the functional roles of IL6 and OSM in prostate cancer *in vivo* using a dissociated tissue recombination system developed in our laboratory (30). This system allows for interrogation of both cell autonomous and paracrine factors that affect prostate transformation through independent manipulation of both the prostate epithelium and the

surrounding mesenchyme. We identified that paracrine expression of either IL6 or OSM is sufficient to promote invasive progression from intermediate PIN lesions induced by $PTEN^{LOF}$ mouse tissues or activation of AKT in human tissues. Lesions exhibited heterogeneous transformation ranging from high-grade PIN to poorly differentiated adenocarcinoma. Increased expression of either IL6 or OSM in the context of PTEN loss resulted in increased activation of STAT3 over PTEN loss alone while OSM grafts exhibited a mild increase in ERK1/2 activation, indicating the potential for multiple signaling mechanisms. Our data supports that IL6 and OSM can synergize with oncogenic stimuli commonly associated with prostate cancer to promote aggressive prostate malignancy through activation of multiple pathways. That cytokines related to IL6 exhibit similar cancer progression behavior indicates that highly targeted therapies aimed solely at disrupting IL6 signaling could be less effective than those targeting signaling nodes common to the IL6 family.

Materials and Methods

Plasmid and Vector Construction

Third-generation FU-CRW and FU-CGW lentivirus vectors were used for constructing IL6, OSM, Cre and myrAKT expression vectors (30,31). Human IL6 and OSM cDNA constructs were purchased from Open Biosystems (#MHS1010-58061 and #MHS1011-75865, respectively), amplified by PCR and cloned into the TOPO TA system (Invitrogen, #450641). cDNA fidelity was confirmed by sequencing and then digested with EcoRI, gel purified and sub-cloned into the FU-CRW and FU-CGW vectors downstream of the ubiquitin promoter. Generation of Cre-CGW and myrAKT-CRW vectors have been described previously (30,32).

Mouse Strains and Regeneration Assay

Housing, maintenance, and all surgical and experimental procedures were undertaken in compliance with the regulations of the Division of Laboratory Animal Medicine of the University of California,

Los Angeles. Homozygous *Pten*$^{fl/fl}$, strain B6.129S4-*Pten*^{tm1Hwu}/J, were purchased from Jackson Laboratory and maintained in our facility. The process of lentivirus preparation, titering and infection, and regeneration of dissociated cells were performed as previously described under safety regulations for lentivirus use set by Environmental Health and Safety (EH&S) at University of California, Los Angeles. Briefly, prostate tissue from 6-12 week old male mice was minced, digested and dissociated according to published protocols (33). Dissociated cells (1-2 x 10^5) were infected with lentivirus at an MOI of 50, recombined with UGSM (1-2 x 10^5) and suspended in collagen. The collagen plug was then engrafted under the renal capsule and allowed to regenerate *in vivo* for 6-10 weeks. Following regeneration, hosts were sacrificed and grafts were recovered via surgical resection of the kidney and fixed in 10% buffered formalin overnight or flash frozen. UGSM were prepared from pregnant BL6 females on embryonic day 14 and cultured in UGSM media [DMEM, 5% FBS, 5% NuSerum (BD #355504), 1X selenium-transferrin-insulin (Gibco #51500-056), 2 mM l-glutamine].

Human prostate regenerations

For preparation of primary human cells, we used a protocol approved through the UCLA Office for the Protection of Research Subjects and all human tissue samples were de-identified to protect patient confidentiality. A total of 3 patient samples were used for this study and all specimens were processed as described previously (34). Briefly, surgical prostate specimens were removed and frozen slides were prepared and stained with H&E by TPCL technicians. Slides were examined by a trained pathologist and cancerous areas were marked, mapped to the fresh tissue and separated from the benign tissue. Basal epithelial cells were isolated by FACS from dissociated benign tissue stained with primary antibodies PE-conjugated CD49f (eBiosciences #12-0495-83) and APC-conjugated Trop2 (FAB650A, R&D Systems). Cells were stained in PrEGM supplemented with 2.5 μg/ml

Fungizone (Gibco) and 10 μm of the p160 ROCK inhibitor Y-27632 dihydrochloride (Tocris Bioscience #1254). Sorting was performed on a BD FACS Aria II (BD Biosciences).

Immunohistochemistry and Immunofluorescence

Fixed or frozen tissues were embedded in paraffin or OCT medium and 4 um sections were cut by UCLA Translational Pathology Core Laboratory (TPCL) with select sections stained with hematoxylin and eosin (H&E) for representative histology. Paraffin-embedded sections were heated to 65° C for 2 hours then de-waxed and rehydrated in a xylenes/ethanol/PBS series. Antigen retrieval was performed using citric acid at pH 6.0 unless otherwise noted. Santa Cruz, Covance, BD Transduction and Abcam antibodies were diluted in PBS, 0.1% Tween-20, 5% normal goat serum. Cell Signaling antibodies were diluted in SignalStain antibody diluent (Cell Signaling #8112). Immunohistochemistry primary antibodies used were AR (1:200; Santa Cruz Biotechnology sc-816), p63 (1:200; Santa Cruz Biotechnology sc-8431), PTEN (1:200; Cell Signalling #9559), AKT (1:250; Cell Signaling #2920), pAKT S473 (1:200; Cell Signaling #4060), STAT3 (1:600; Cell Signaling #9139), pSTAT3 Y705 (1:400; Cell Signaling #9145, antigen retrieval in 10 mM EDTA, pH 8.0), ERK1/2 (1:500; Cell Signaling #4696), pERK1/2 pT202/Y204 (1:400; Cell Signaling #4370). ImmPRESS HRP-conjugated secondary antibodies were used (RTU; Vector Labs #MP-7401 and #MP-7402) and visualized using DAB+ reagent (DAKO, K3468). Immunofluorescent primary antibodies used were CK5 (1:1000; Covance PRB-160P), CK8 (1:1000; Covance MMS-162P), e-Cadherin (1:250; BD Transduction Labs #610181), collagen IV (1:500; Abcam ab-19808) and visualized by Alexa-594 or Alexa-488 conjugated secondary antibodies (1:1000; Invitrogen). Images were acquired using Axio Imager A1 (Zeiss) with a Retiga EXi Fast 1394 camera (Q Imaging) using Image-Pro Premier software (Media Cybernetics, Version 9.0.2). Fluorescent source was X-Cite 120 (EXFO). Confocal microscopy was performed on a Zeiss LSM 510 Meta.

Cell Lines, Cytokines and Western Analysis

PEB cells were a kind gift from Dr. Lynnette Wilson maintained in PrEGM (Lonza, # CC-4177 and CC-3165) supplemented with 10% FBS (35). CaP8 cells were and kind gift from Dr. Hong Wu maintained in UGSM media (36). Human recombinant IL6 and OSM were purchased from Cell Signaling (#8904SF and #5367SF, respectively) and were reconstituted in 1X PBS supplemented with 1% BSA. For western analysis, cells were serum starved in DMEM supplemented with 0.2% FBS and 2 mM L-glutamine for 6-18 hours and treated with cytokines for indicated times. Cells were then washed in ice-cold 1X PBS, lysed in 2% SDS Lysis buffer [62.5 mM Tris, 2% SDS, pH 6.8, protease inhibitor cocktail (Roche #11697498001), and phosphatase inhibitor 2 and 3 (Sigma #P5726 and #P0044)], sonicated and centrifuged at 350K RCF (avg) for 30 minutes to pellet genomic DNA. Clarified lysates were quantified using by BCA assay (Pierce #23227) and supplemented with 5X Sample Loading Buffer (Fermentas R0891) and boiled at 95° C for 5 minutes. Extracts (10–50 μg) were subjected to 4-20% SDS-PAGE, followed by blotting to nitrocellulose with the indicated antibodies. Primary antibodies were same as IHC antibodies at the following concentrations: AKT (1:2000), pAKT S473 (1:2000), STAT3 (1:1000), pSTAT3 Y705 (1:2000), ERK1/2 (1:2000), pERK1/2 pT202/Y204 (1:2000). Antibodies for western analysis only were interleukin 6 (1:500; Santa Cruz sc-7920) and oncostatin-M (1:2000; R&D Systems #AF-295-NA) Appropriate HRP-conjugated secondary antibodies (Bio-Rad #170-6515, #170-6516 and #172-1034) were used at 1:10K-20K and visualized using Immobilon kit (Millipore WBKLS0500). For bio-activity assay in Fig. 1B, western analyses were imaged using Licor Odyssey CLx with Image Studio software (Version 3.1) using the "Auto" exposure parameters at 84 μm resolution the under "High Quality" setting. Secondary antibodies used were goat anti-mouse IRDye 680RD and goat anti-rabbit IRDye 800CW (Licor # 926-68170 and #827-08365, respectively) and diluted to 1:15K.

Results

Interleukin 6 and Oncostatin M expression promote progression to invasive prostate cancer in mouse and human tissues

To assess the potential role of IL6 and OSM in prostate cancer in transformation of both mouse and human prostate epithelium, we utilized the dissociated prostate regeneration system developed in our laboratory (30,34). For interrogation of mouse tissues, dissociated prostate cells from adult male homozygous *Pten*$^{fl/fl}$ conditional knockout (37) mice were transduced with lentivirus constructs with either green fluorescent protein (GFP) alone or Cre recombinase with a GFP marker and combined with urogenital sinus mesenchyme (UGSM) transduced with control, IL6, or OSM lentivirus, each with a linked red fluorescent protein (RFP) marker (Fig. 1A). Western analysis was used to confirm increased expression and activity of secreted IL6 and OSM in lysates and conditioned media of transduced UGSM (Fig. 1B).

Control grafts exhibited regeneration of normal prostate cellular architecture with a bi-layered epithelium and abundant luminal secretions (Fig. 1C). PTEN-intact grafts expressing either IL6 or OSM exhibited reduced epithelial regeneration while IL6-expressing grafts exhibited mild, focal hyperplasia that was not observed in OSM grafts. PTEN^{LOF} epithelium combined with control UGSM exhibited formation of PIN lesions with characteristic neoplastic growth into the luminal interior and an intact epithelial-mesenchymal boundary, similar to previously published data (38). PTEN^{LOF} combined with UGSM expressing either IL6 or OSM exhibited a heterogeneous range of transformation states. IL6-expressing grafts largely exhibited high-grade PIN lesions with a few lesions exhibiting localized invasive growth. In contrast, OSM-expressing grafts often presented as highly invasive, poorly differentiated adenocarcinoma with anaplastic features, indicating that OSM could promote a more aggressive disease. While PTEN^{LOF} grafts with OSM-expressing UGSM were

slightly larger than $PTEN^{LOF}$ alone, these results were not statistically significant (Supplementary Fig. S1A and B). Grafts displayed several immunohistochemical features of human prostate cancer (Fig. 1D and Supplementary Fig. S1C). Androgen receptor (AR) expression was predominantly nuclear in all lesions, indicating intact androgen response in all regenerated and transformed tissues. P63-expressing basal cells were restricted to the basement membrane in normal regenerations, scattered in PIN lesions and absent in poorly-differentiated adenocarcinoma foci identified in grafts expressing OSM.

For human experiments, expression of constitutively active AKT was used as a surrogate for loss of PTEN that is commonly observed in human disease (39). Benign human epithelium was isolated from radical prostatectomy samples and transduced with lentivirus constructs with either RFP or AKT with a RFP marker. Transduced cells were then combined with UGSM previously transduced with GFP, IL6- or OSM-GFP lentivirus, suspended in matrigel and injected subcutaneously into immune deficient hosts (Fig. 2A). Control grafts exhibited normal epithelial regeneration with nuclear AR expression in luminal epithelium and P63 expression in basal cells (Fig. 2B, C). Expression of activated AKT resulted in PIN lesions similar to those observed in mouse PTEN knockout regenerations (Fig. 2B). Over-expression of AKT was confirmed by IHC analysis for total protein (Supplementary Fig. S2B) and phospho-serine 473 AKT levels (Fig. 2C). Paracrine expression of either IL6 or OSM alone dramatically inhibited epithelial regeneration with only a few small nests of epithelial cells primarily composed of P63-expressing basal cells (Supplementary Fig. S2A). Similarly, paracrine expression of IL6 in grafts with AKT-infected epithelium also exhibited significant inhibition and no epithelial regeneration or transformation was observed (Fig. 2B and C). Grafts expressing OSM in combination with AKT exhibited small nests of dysplastic epithelial cells that express AR, though they retained P63-expressing cells, indicating the lesions had not progressed

to clinical adenocarcinoma (Fig. 2B and C). The less aggressive phenotype observed in the human system is consistent with previous studies from our laboratory that indicate that human cells appear to be more resistant to transformation and require additional oncogenic stimuli to match phenotypes observed in mouse systems (34). Therefore, we chose to focus on the mouse system for further interrogation of the synergy between activation of the PTEN/PI3K/AKT pathway and the IL6 family of cytokines.

Exogeneous expression of IL6 and OSM lead to increased epithelial invasion into the surrounding mesenchyme

Cytokeratin (CK) expression can be used to qualitatively assess cancer progression as invasive carcinoma lesions tend to lose CK5-expressing basal cells while advanced, poorly differentiated lesions can also down-regulate luminal CK8 expression (40). We used immunofluorescent microscopy to interrogate the CK status in mouse tissues in the context of PTEN loss alone or with either IL6 or OSM expression. Control grafts exhibited normal CK5 and CK8 expression in the basal and luminal compartments, respectively (Fig. 3). Grafts expressing either IL6 or OSM alone exhibit normal CK5 and CK8 expression patterns (Supplementary Fig. S3A) PIN lesions present in $PTEN^{LOF}$ grafts exhibited increased CK8-expressing luminal cells with CK5-expressing basal cells detached from the basement membrane (Fig. 3). Tumor foci from $PTEN^{LOF}$ grafts with either IL6 of OSM largely retained both CK8- and CK5-expressing cells despite their invasive morphology. However, a few poorly-differentiated lesions observed in $PTEN^{LOF}$ with OSM exhibited dramatic loss of CK5 expressing basal cells as well as frequent loss of CK8 expression, consistent with observations in clinical specimens (Supplementary Fig. S3B).

We then used immunofluorescent confocal microscopy to qualitatively assess the extent of epithelial invasion into the surrounding mesenchyme, using E-cadherin to identify epithelial cells with respect to the basement membrane component collagen IV. E-cadherin expression was largely localized along the cell membrane in normal and PIN lesions with disorganized staining in invasive lesions present in $PTEN^{LOF}$ grafts with IL6 or OSM (Fig. 4). The basement membrane remained intact in normal and PIN lesions from control and $PTEN^{LOF}$ alone, indicating that PTEN loss alone does not promote invasive behavior in our model system. PTEN-intact grafts expressing either IL6 or OSM alone did not exhibit any observable invasive behavior as indicated by the intact basement membrane (Supplementary Fig. S4). Locally invasive lesions observed in $PTEN^{LOF}$ grafts with IL6 exhibited partial breakdown of the basement membrane and resulted in increased invasion of E-cadherin positive epithelial cells into the surrounding stroma (Fig. 4). $PTEN^{LOF}$ grafts expressing OSM often exhibited total loss of the basement membrane boundary with the epithelial cells intercalating into the surrounding mesenchyme.

Invasive tumor foci identified in grafts expressing IL6 or OSM with loss of PTEN exhibited increased activation of JAK/ STAT pathway

Ligand engagement of IL6-family members activates constitutively bound JAKs, resulting in activation of the STAT, MAPK, and AKT pathways. To interrogate whether IL6 and OSM exhibit differential activation of downstream pathways, we treated benign PEB and tumorigenic CaP8 cell lines with human recombinant IL6 and OSM and assessed activation of STAT3, AKT and ERK1/2 by western analysis for protein phosphorylation (Fig. 5A). Treatment with carrier resulted in transient activation of ERK1/2 in both cell lines with a slight increase in AKT and STAT3 activation. Treatment with IL6 or OSM resulted in a significant increase in STAT3 and AKT activation in both PEB and CaP8 cell lines compared to controls, with OSM exhibiting a greater

increase over IL6 for both signaling pathways. Neither IL6 nor OSM exhibited a dramatic increase in ERK1/2 activation over carrier treated cells.

We then used IHC analysis to interrogate activation of pathways downstream of IL6 and OSM from *in vivo* transformations (Fig. 5B). Control regenerations exhibited little-to-no activation of AKT, ERK1/2 or STAT3. Increased levels of AKT activation were observed in all $PTEN^{LOF}$ lesions and were similar across $PTEN^{LOF}$ alone and with IL6 or OSM. Loss of PTEN resulted in increased levels of ERK1/2 activation over control grafts with similar levels observed in grafts from $PTEN^{LOF}$ with IL6. $PTEN^{LOF}$ grafts with OSM exhibited mild though consistently increased levels of ERK1/2 activation. Loss of PTEN resulted in increased levels of STAT3 compared to control grafts with further increased levels observed in grafts from both $PTEN^{LOF}$ with IL6 or OSM. IHC analysis for total proteins confirmed basal expression levels in control grafts with all $PTEN^{LOF}$ grafts exhibiting in increased expression of total AKT, ERK1/2 and STAT3 protein levels (Supplementary Fig. S5). These results indicate that tumor progression via IL6 and OSM is associated with increased activation of the STAT pathway, though OSM synergy could be also be mediated in part by other pathways including MAPK.

Discussion

Factors that promote progression from benign to aggressive prostate cancer are still poorly understood. Correlative and *in vitro* data strongly indicate that chronic inflammation could act as a potential etiological and progression factor, highlighting the need for further validation using *in vivo* models. Our study identified that both IL6 and OSM exhibited synergy with loss of PTEN and display heterogeneous transformation phenotypes ranging from high grade PIN lesions with micro-invasion to poorly differentiated adenocarcinoma with anaplastic features. These tumors share

immunohistochemical features of the human disease such as sustained androgen receptor expression and loss of p63 expressing basal cells in regions of high-grade adenocarcinoma. We speculate that this complexity is a result of variations in the local concentration of IL6 or OSM and could serve as a model for the heterogeneity commonly observed in human prostate cancer.

While our work focused on the interaction of IL6 and OSM in the context of PTEN loss, other studies indicate that this synergy could extend to other oncogenic insults. Exogenous expression of IL6 has been shown to transform a non-tumorigenic prostate epithelial cell line immortalized with SV40 Large T-antigen, indicating potential functional synergy with inhibition of the TP53 and RB pathways (25,41). Work by Kan and colleagues identified that while OSM suppressed the growth of normal human breast epithelium, co-expression of cMYC abrogated growth arrest and resulted in transformation (42). Our results support this finding as neither cytokine was sufficient to transform mouse or human prostate epithelium on its own in our system. Oncogenic response to IL6 and related cytokines therefore seems to be dependent on the presence co-incident mutations within the prostate.

Inflammatory cytokines such as IL6 and OSM could promote activation of the several potentially oncogenic pathways in the absence of mutation.

Sequencing studies indicate that prostate cancer does not exhibit dramatic mutation rates compared to many other cancers (43). Studies from our laboratory and others have shown that most single oncogenes are not sufficient to induce invasive prostate cancer, indicating that it is necessary to activate multiple signaling pathways (30,34,44). The pathways activated by a single cytokine are often diverse, indicating that the potential for prostate cancer progression would be dramatically increased in this environment. Both IL6 and OSM have been shown to activate STAT3, AKT, and MAPK in

several cell types, as well as Src-family kinase members in more select contexts (45). Each of these pathways has individually been implicated in various cancers and several have been shown to exhibit synergy when co-activated. Chronic inflammation could expose cells to a diverse array of cytokines, including those of the IL6 family, that could activate oncogenic pathways and serve as a surrogate for direct mutation.

In our model system, loss of PTEN with increased expression of OSM exhibited a moderate increase in ERK1/2 activation. Several studies have observed increased activation of the MAPK pathway in advanced prostate cancers and a recent report identified a strong oncogenic synergy between loss of PTEN and activation of KRAS (46,47). However, other studies indicate that upstream MAPK signaling proteins such as RAS or RAF are rarely mutated prostate cancer (48). It is possible that increased exposure to cytokines could result in increased activation of the MAPK pathway and explain in part the disparity between ERK activation and the paucity of mutations in this pathway. $PTEN^{LOF}$ grafts expressing either IL6 or OSM also exhibited strong activation of the JAK/STAT3 pathway, which is consistent which clinical prostate cancer specimens and has been shown to mediate several pro-tumorigenic effects (49). Whether a single pathway is dominant over another is yet to be shown and could have implications for treatment strategies.

Alternative IL6 family members could act as surrogates for IL6 in transformation states, and has therapeutic implications.

Current therapeutic research strategies are increasingly using highly targeted drugs such as antibody-based therapeutics designed to inhibit the IL6 ligand or the IL6Ra subunit. The humanized antibody CNTO 328 inhibits the conversion to androgen independent disease and modulates activation of STAT3 and ERK1/2 in prostate cancer xenografts (20,50). However, CNTO 328 has shown poor

performance in subsequent Phase II trials and seems to lack clinical efficacy. Our studies indicate that other members of the IL6 family, and likely other cytokines in general, can also exhibit pro-tumorigenic functions that can even exceed those of IL6. Highly targeted therapies directed at single ligands such as IL6 could exhibit reduced efficacy due to co-expression of family members with redundant activity. Therapies targeting signaling nodes such as the JAK family could therefore exhibit greater efficacy through inhibition of both related family members and shared downstream pathways such as STAT3 and ERK1/2. Therapeutic strategies such as this would benefit greatly from an increased understanding of how cytokine profiles could be used as diagnostic biomarkers.

Author Contributions

Conception and design: D.A. Smith, A. Kiba, Y. Zong, O.N. Witte

Development of methodology: D.A. Smith, A. Kiba, Y. Zong, O.N. Witte

Acquisition of data: D.A. Smith, Y. Zong

Analysis and interpretation of data: D.A. Smith, A. Kiba, Y. Zong, O.N. Witte

Writing, review and/or revision of the manuscript: D.A. Smith, A. Kiba, Y. Zong, O.N. Witte

Study supervision: O.N. Witte

Acknowledgements

We would like to thank all of the members of the Witte laboratory for their helpful comments and insightful discussion and the technicians of the UCLA Translational Pathology Core Laboratory for their assistance in tissue processing and H&E staining. We would also like to especially thank our FACS specialist Dr. Donghui Cheng and Dr. Jioati Huang of the UCLA Pathology department for always sharing his pathology expertise. DAS is supported by UCLA Tumor Biology Program, US Department of Health and Human Services, Ruth L. Kirschstein Institutional National Research

Service Award no. T32 CA009056 and is a Collegium of University Teaching Fellow with the University of California, Los Angeles. AK was a visiting Fellow on sabbatical and is a scientist with Takeda Pharmaceutical Company Limited, Kanagawa, Japan. ONW is supported by a Prostate Cancer Foundation Challenge Award (PI: Owen Witte).YZ is an Associate of and ONW is an Investigator for the Howard Hughes Medical Institute.

Figure Legends

Figure 1: Paracrine expression of IL6 or OSM synergizes with epithelial loss of PTEN to promote invasive adenocarcinoma.

A) Diagram of regeneration and transformation process with lentiviral vector diagrams.

B1-3) Western analysis of UGSM cells infected with control, IL6 and OSM vectors showing heightened expression of IL6 and OSM in their respective cell lines, with a mild increase in IL6 expression in OSM-infected UGSM. Loading control is ERK1/2.

B4-5) Secretion and activity of the IL6 and OSM cytokines was confirmed by treating serum-starved 3T3 cells with conditioned media from infected UGSM. Increased phosphorylation of STAT3 in cells treated with IL6 and OSM conditioned media indicates functional activity. Imaged using Licor Odyssey CLx with Image Studio software.

C) Representative histological sections of prostate regenerations and transformation by $PTEN^{LOF}$ combined with IL6 or OSM following 6-8 weeks *in vivo*. Control grafts exhibit normal prostate epithelial architecture with $PTEN^{LOF}$ grafts exhibiting PIN lesions. Tumor foci from $PTEN^{LOF}$ with IL6 or OSM exhibit invasion into the surrounding mesenchyme. Scale Bars: 10X, 200 um; 40X, 100 um.

D) IHC analysis of AR and p63 in prostate regenerations. All prostate epithelial regenerations and tumor foci retained high expression of nuclear AR. Normal regenerations exhibited P63-expressing

basal cells along the basement membrane and were detached from the membrane in PIN lesions present in $PTEN^{LOF}$ grafts and $PTEN^{LOF}$ grafts with IL6. High grade lesions present in $PTEN^{LOF}$ with OSM exhibited loss of P63-expressing basal cells. Scale Bars: 20X, 100 μm; 63X, 50 μm

Figure 2: Cell autonomous expression of AKT with increased paracrine expression of OSM results in tumor progression of benign human prostate epithelium.

A) Diagram of human prostate regeneration with lentiviral constructs.

B) Representative histology of human prostate epithelial regenerations following 8-10 weeks *in vivo*. Benign regenerations show normal glandular epithelium while those transduced with AKT show PIN lesions. No regeneration or transformation was observed in grafts expressing activated AKT with IL6. Grafts with activated AKT and OSM exhibit dramatic morphological progression. Scale Bars: 20X, 100 μm.

C) IHC analysis of AR and p63 from human prostate regenerations. All grafts and tumor foci retain nuclear expression of AR. Normal regenerations exhibited P63-expressing basal cells along the basement membrane while PIN lesions induced by AKT alone exhibited P63-expressing basal cells detached from the basement membrane similar to murine PIN lesions. Tumor foci from AKT with OSM retain P63 expressing basal cells despite invasive morphological characteristics. Scale Bars: 20X, 100 μm; 63X 50 μm.

Figure 3: Increased expression of IL6 or OSM with loss of PTEN results in invasive lesions that retain expression of normal cytokeratin profiles.

Immunofluorescent microscopy of prostate regenerations and transformations showing basal CK5 (red) and luminal CK8 (green). Wild-type regenerations exhibit normal basal and luminal localization while high-grade PIN lesions in $PTEN^{LOF}$ grafts show high levels of CK8-expressing luminal cells

with CK5-expressing basal cells detached from the basement membrane. Invasive lesions from $PTEN^{LOF}$ with IL6 or OSM largely retain expression of anticipated cyokeratins despite the highly invasive phenotype. Scale Bars: 20X, 100 μm; 63X, 50 μm.

Figure 4: Expression of IL6 or OSM in the context of PTEN loss drive invasion of malignant epithelium into the surrounding mesenchyme.

Confocal immunofluorescent imaging of e-cadherin and collagen IV from wild-type, $PTEN^{LOF}$ and $PTEN^{LOF}$ with IL6 or OSM grafts. Wild-type and $PTEN^{LOF}$ grafts exhibited clearly delineated boundary between e-cadherin expressing epithelial cells and the collagen IV of the basement membrane and surrounding mesenchyme. $PTEN^{LOF}$ grafts with IL6 exhibited partial invasion through the basement membrane with OSM expressing grafts exhibiting full epithelial invasion into the surrounding mesenchyme. Scale Bars: 40X, 50 μm.

Figure 5: Increased expression of OSM in $PTEN^{LOF}$ grafts results in increased phosphorylation of STAT3 and ERK1/2 downstream of IL6 and OSM.

A) Western analysis of PEB and CaP8 cells treated with carrier or 10 ng/uL of IL6 or OSM in DMEM with 0.2% FBS for indicated times. Treatment of either IL6 or OSM exhibited activation of both AKT and STAT3 pathways with OSM consistently exhibiting increased activation over IL6. Activation of ERK1/2 above background was not consistently observed.

B) IHC analysis of AKT, ERK1/2 and STAT3 from normal, $PTEN^{LOF}$, and $PTEN^{LOF}$ with IL6 or OSM. All grafts with $PTEN^{LOF}$ exhibited increased activation of AKT, ERK1/2 and STAT3 above basal levels in normal regenerations. $PTEN^{LOF}$ grafts with IL6 exhibited increased levels of STAT3 phosphorylation over $PTEN^{LOF}$ alone with no discernible increase in ERK1/2 activation. $PTEN^{LOF}$

with OSM exhibited consistently higher levels of STAT3 phosphorylation with a mild increase in ERK1/2 phosphorylation. Scale Bars: 20X 100 μm; 63X 50 μm.

Figure 1

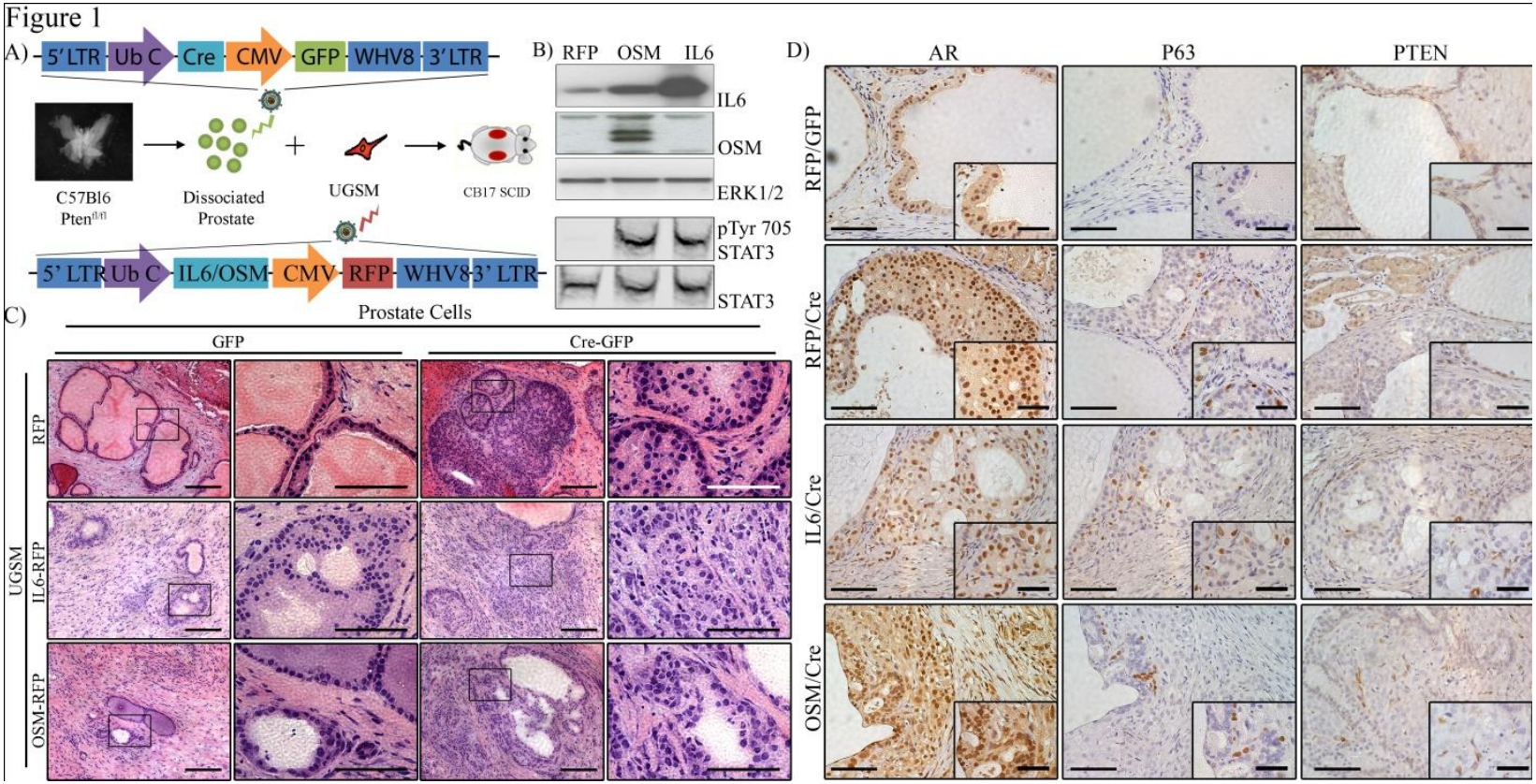
A)
5'LTR
Ub C
Cre
CMV
GFP
WHV8
3'LTR
C57Bl6
Pten(f/f)
Dissociated
Prostate
UGSM
CB17 SCID
5' LTR
Ub C
IL6/OSM
CMV
RFP
WHV8
3' LTR
B)
RFP
OSM
IL6
IL6
OSM
ERK1/2
pTyr 705
STAT3
STAT3
C)
Prostate Cells
GFP
Cre-GFP
UGSM
RFP
IL6-RFP
OSM-RFP
D)
AR
P63
PTEN
RFP/GFP
RFP/Cre
IL6/Cre
OSM/Cre

Figure 2

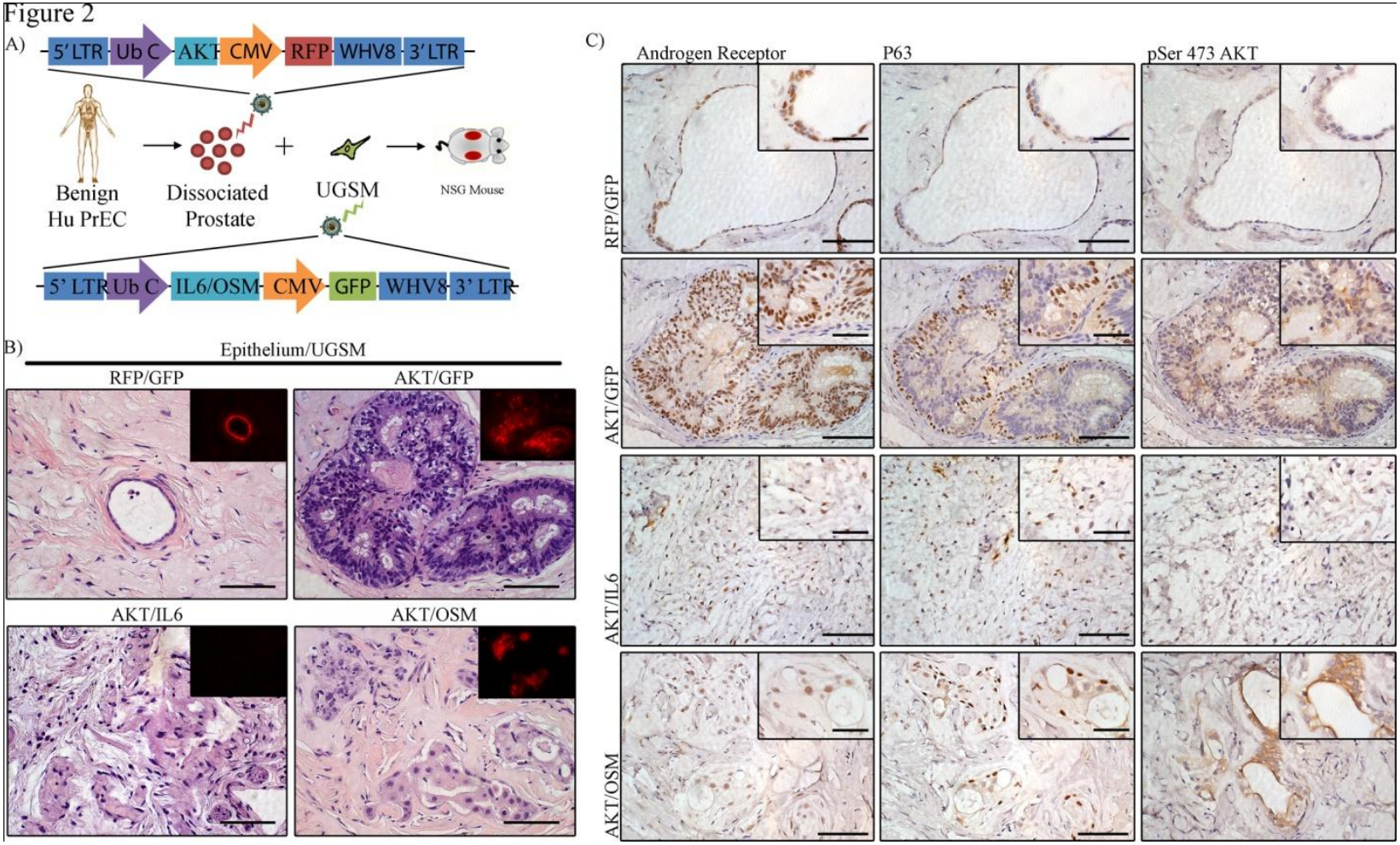
A)
5' LTR
Ub C
AKT
CMV
RFP
WHV8
3' LTR
Benign
Hu PrEC
Dissociated
Prostate
UGSM
NSG Mouse
5' LTR
Ub C
IL6/OSM
CMV
GFP
WHV8
3' LTR
B)
Epithelium/UGSM
RFP/GFP
AKT/GFP
AKT/IL6
AKT/OSM
C)
Androgen Receptor
P63
pSer 473 AKT
RFP/GFP
AKT/GFP
AKT/IL6
AKT/OSM

Figure 3

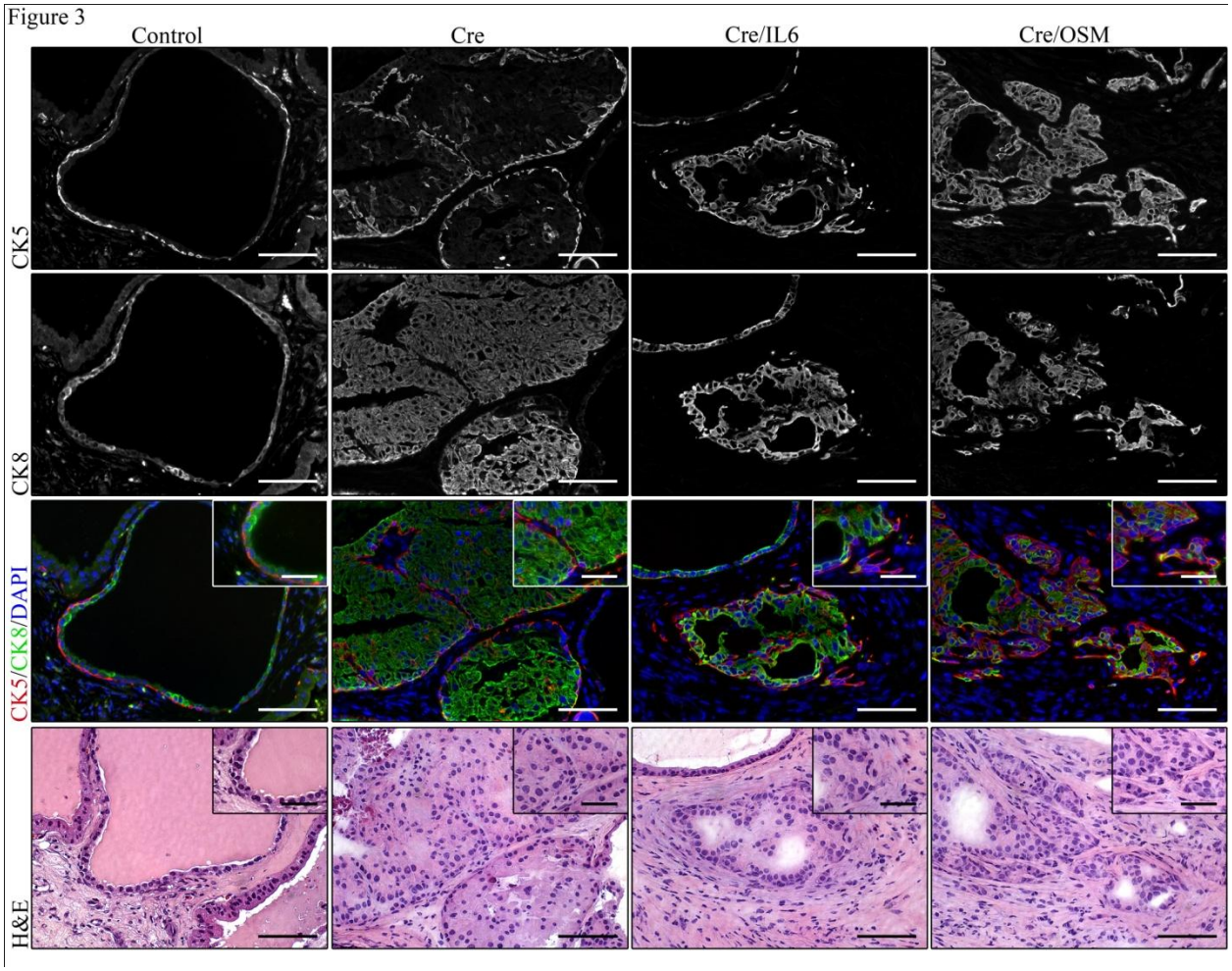

Figure 4

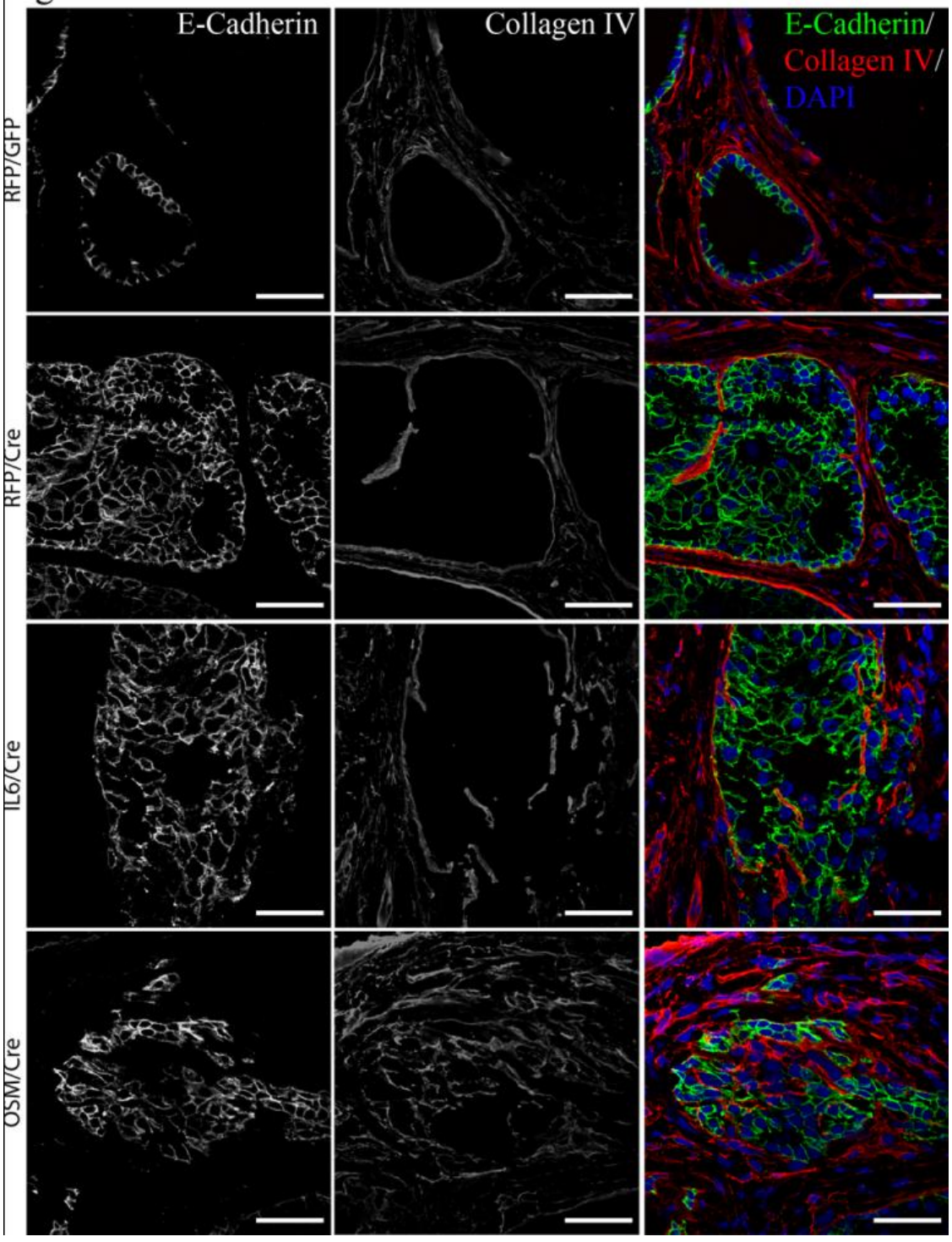
E-Cadherin
Collagen IV
E-Cadherin/
Collagen IV/
DAPI
RFP/GFP
RFP/Cre
IL6/Cre
OSM/Cre

Figure 5

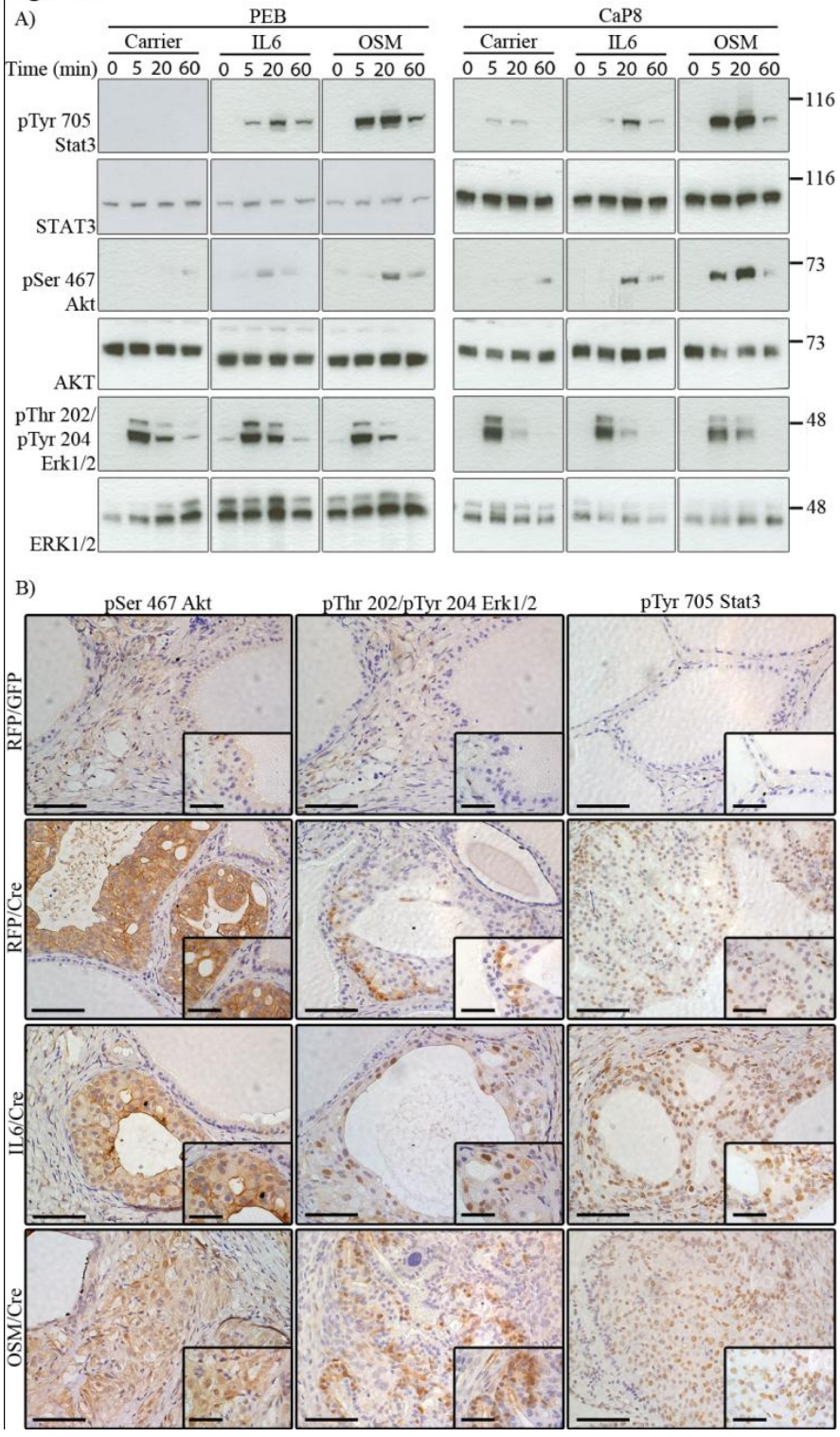
A)
PEB
CaP8
Carrier
IL6
OSM
Carrier
IL6
OSM
Time (min) 0 5 20 60 0 5 20 60 0 5 20 60 0 5 20 60 0 5 20 60
pTyr 705 Stat3
116
STAT3
116
pSer 467 Akt
73
AKT
73
pThr 202/ pTyr 204 Erk1/2
48
ERK1/2
48
B)
pSer 467 Akt
pThr 202/pTyr 204 Erk1/2
pTyr 705 Stat3
RFP/GFP
RFP/Cre
IL6/Cre
OSM/Cre

Supplemental Figure Legends

Supplementary Figure 1: Expression of IL6 or OSM with loss of PTEN does not dramatically increase graft size or weight.

A) *Ex vivo* trans-illuminated and fluorescent imaging of grafts following surgical resection showing no significant changes in graft size. Grafts expressing either IL6 or OSM were more opaque in appearance compared to grafts with control UGSM. Scale bar: 2 mm.

B) Wet weights of grafts show no significant differences in weight between each condition, though there is a general trend for larger grafts following loss of PTEN in all grafts with a further increase in $PTEN^{LOF}$ with OSM. Error bars are mean with 95% confidence interval.

C) PTEN-intact grafts expressing IL6 or OSM alone retain nuclear AR expression and P63-expressing basal cells similar to normal regenerations. Scale Bars: 20X, 100 μm; 63X 50 μm.

Supplementary Figure 2: Human regenerations with IL6 and OSM alone exhibit dramatic inhibition of epithelial regeneration.

A) Regeneration of prostatic epithelium from human cells with IL6 or OSM expression was significantly inhibited and resulted in primarily small nests of epithelial cells. The cells largely stained positive for both AR and P63, possibly representing some form of intermediate cell. Consistent with control infection, cells expressed low levels of activated AKT. Scale Bars: 20X, 100 μm; 63X 50 μm.

B) Total protein expression of AKT shows basal levels in control, IL6 and OSM alone grafts with increased expression observed in transformed epithelial structures present in AKT and AKT with OSM grafts. Scale Bars: 20X, 100 μm; 63X 50 μm.

Supplementary Figure 3: Increased expression of IL6 or OSM alone does not alter normal cytokeratin status of prostate epithelial regenerations.

A) Grafts expressing IL6 or OSM exhibited normal expression patterns of basal CK5 and luminal CK8. The mild hyperplasia observed in grafts with IL6 alone seems to be limited to an expansion of the luminal CK8 expressing cells with normal CK5 patterning alone the basement membrane. Scale Bars: 20X, 100 μm; 63X, 50 μm.

B) High-grade lesions observed in $PTEN^{LOF}$ with OSM graft exhibits complete loss of basal CK5-expressing cells with decreased expression of luminal CK8, consistent with clinical observations of poorly differentiated prostate cancer. Scale Bars: 20X, 100 μm; 63X, 50 μm.

Supplementary Figure 4: Increased expression of either IL6 or OSM alone does not promote epithelial invasion.

Confocal immunofluorescent microscopy of E-cadherin and basement membrane component collagen IV from grafts expressing IL6 or OSM alone. PTEN-intact regenerations expressing either IL6 or OSM alone exhibited normal E-cadherin expression along the cell membrane and an intact basement membrane indicated by collagen IV staining, indicating that neither IL6 nor OSM are sufficient for invasive epithelial growth.

Supplementary Figure 5: Loss of PTEN results in increased expression of AKT, ERK1/2 and STAT3 in transformed epithelial tissues.

IHC analysis of total protein expression of AKT, ERK1/2 and STAT3 in control, $PTEN^{LOF}$ alone and $PTEN^{LOF}$ with either IL6 or OSM. Control grafts show low levels of AKT, ERK1/2 and STAT3 while grafts with loss of PTEN exhibit dramatically increased total protein levels for indicated proteins. Scale Bars: 20X 100 μm; 63X 50 μm.

Supplemental Figure 1

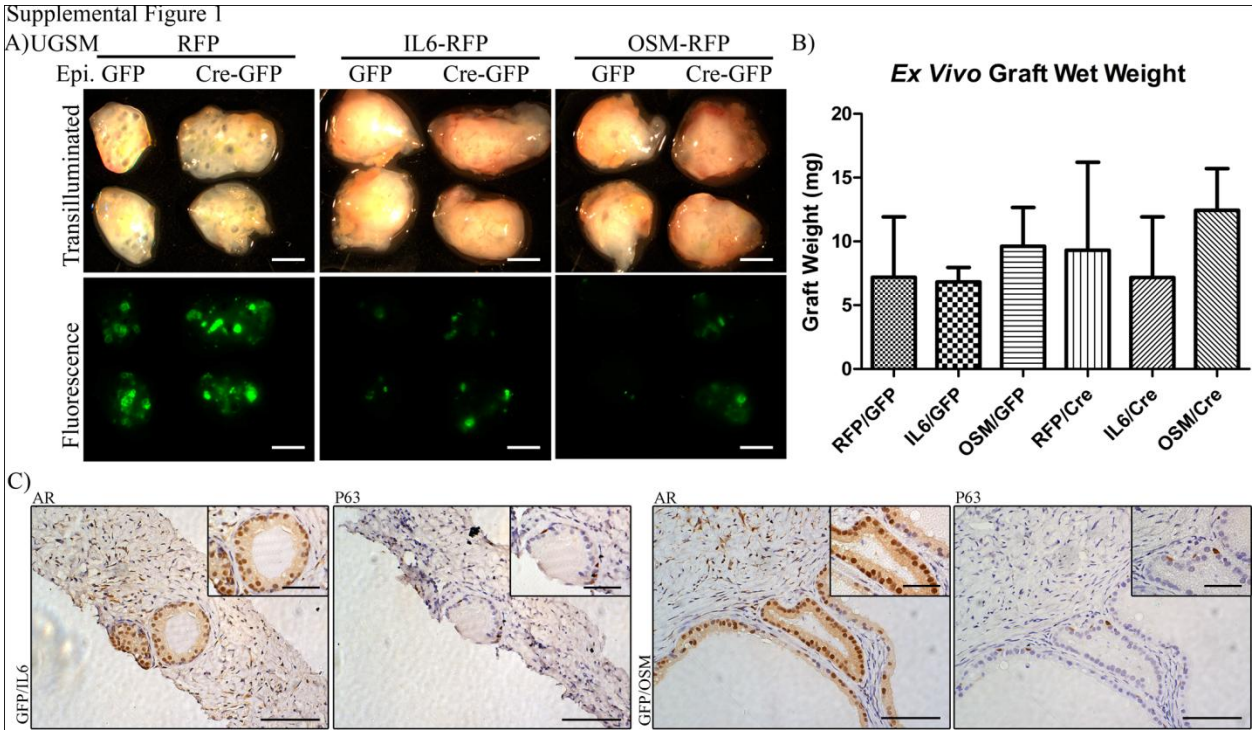

Supplemental Figure 2

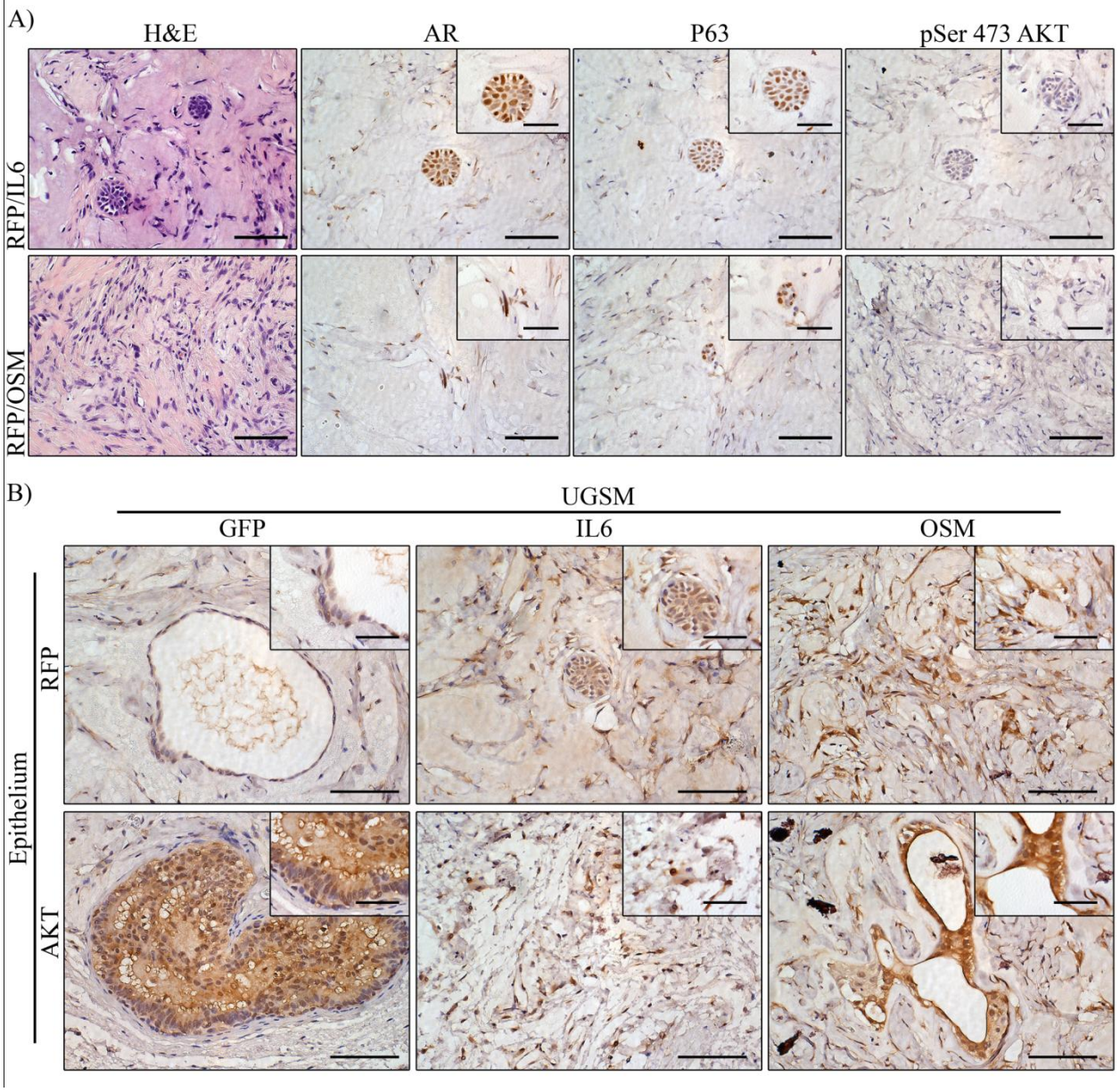

Supplemental Figure 3

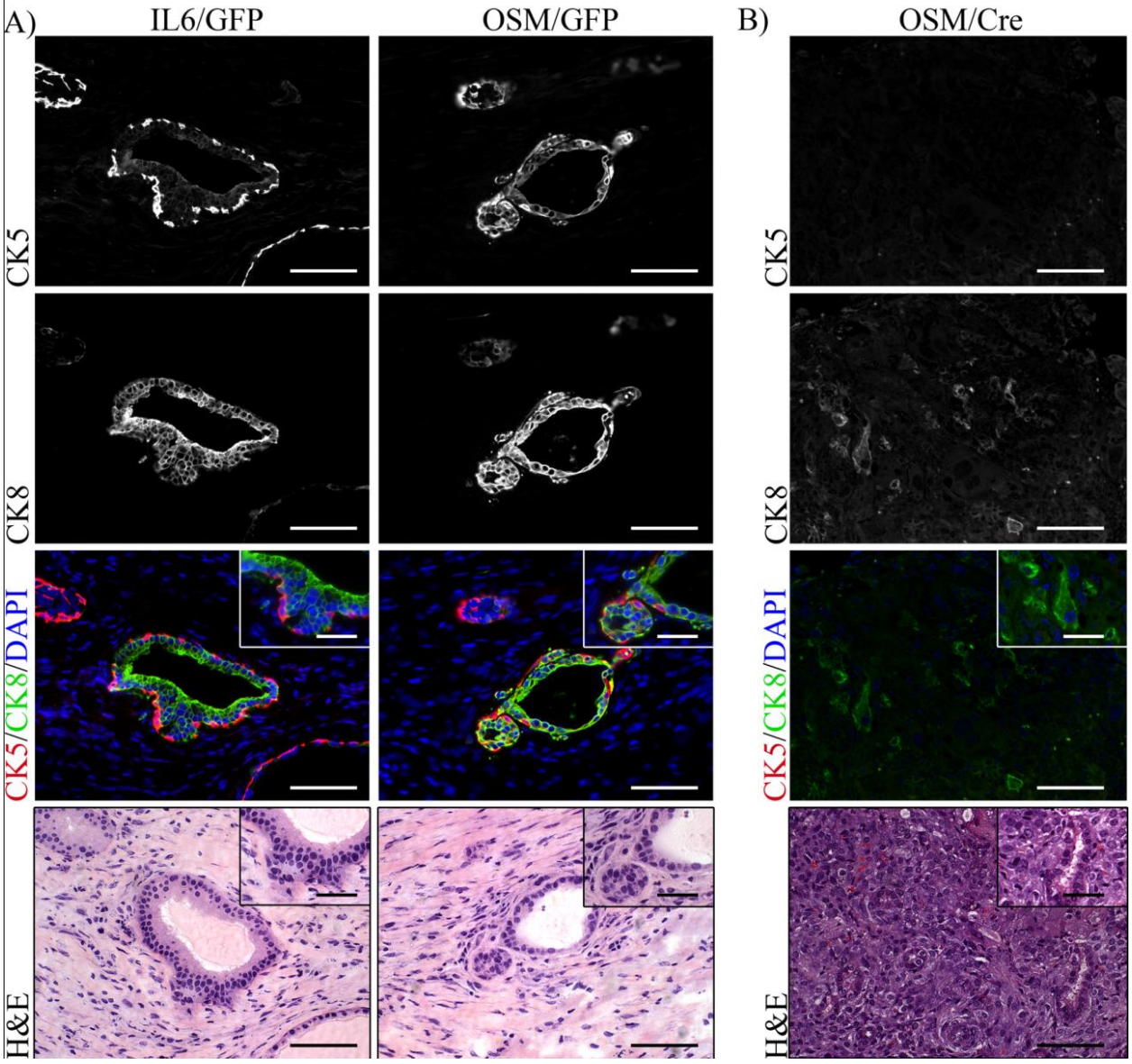

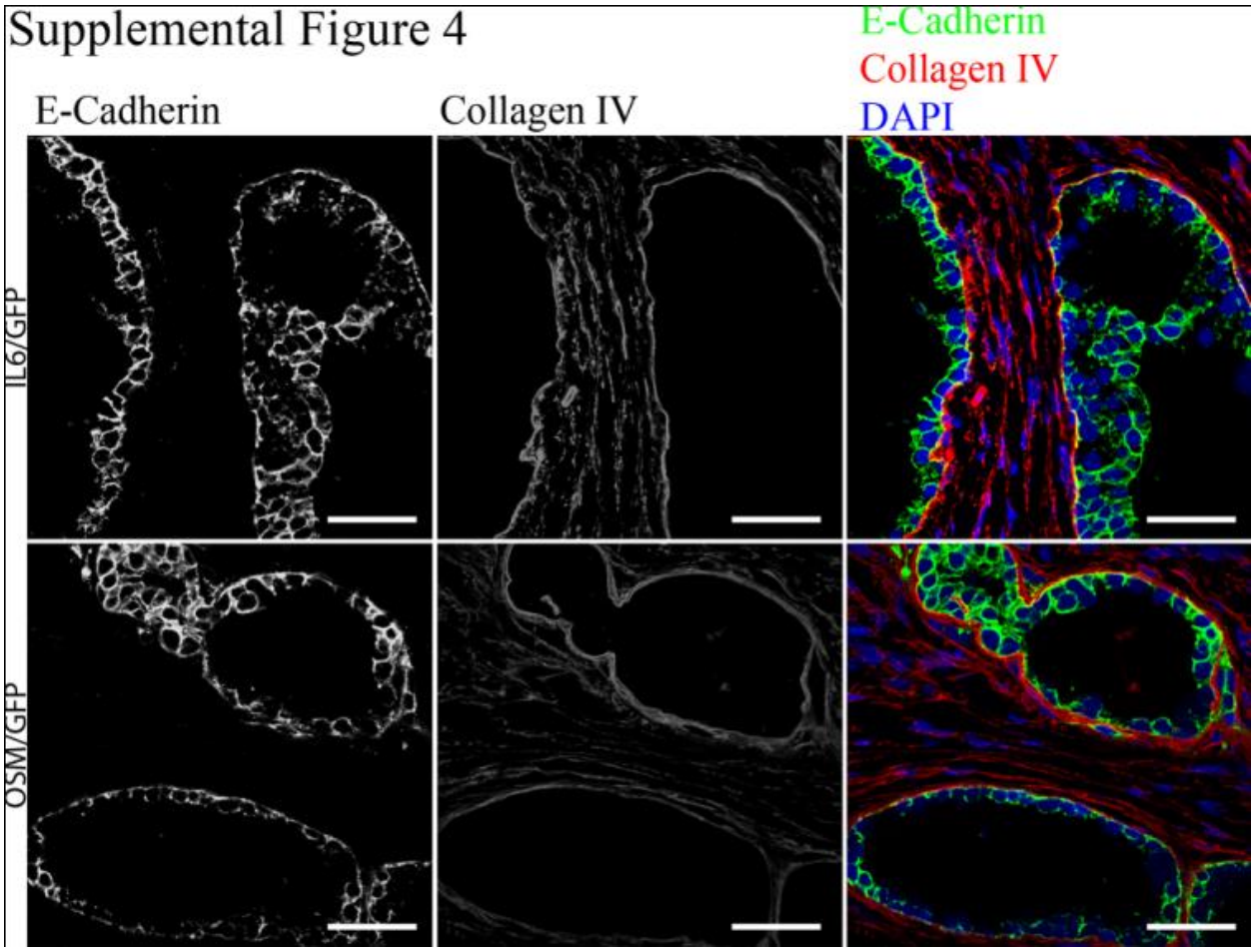
Supplemental Figure 4
E-Cadherin
Collagen IV
DAPI
E-Cadherin
Collagen IV
IL6/GFP
OSM/GFP

Supplemental Figure 5

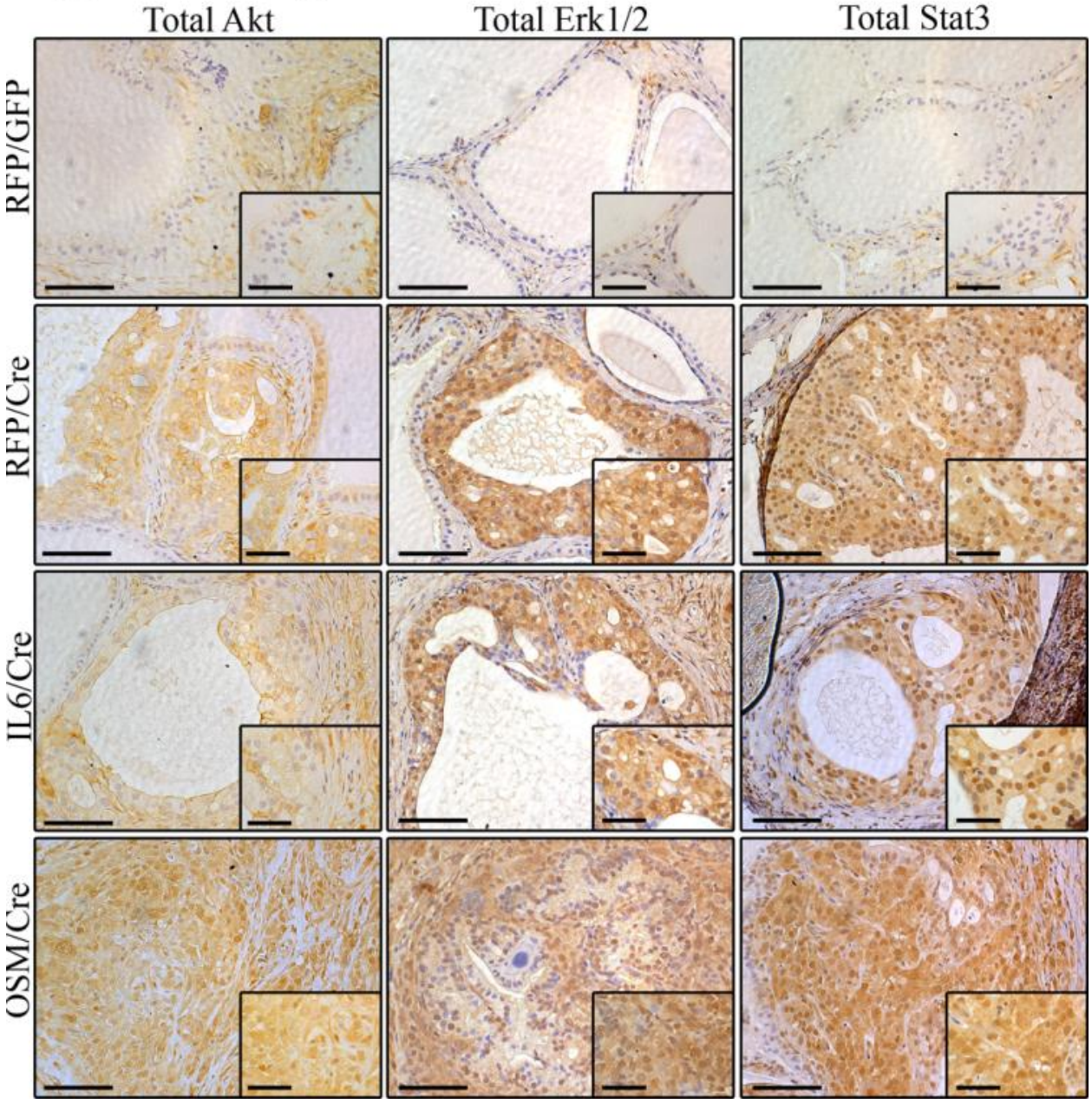

References

1. Siegel R, Naishadham D, Jemal A. Cancer statistics, 2013. CA: A Cancer Journal for Clinicians. 2013;63:11–30.

2. Hanahan D, Weinberg RA. Hallmarks of Cancer: The Next Generation. Cell. 2011;144:646–74.

3. Hussain SP, Hofseth LJ, Harris CC. Radical causes of cancer. Nature Reviews Cancer. 2003;3:276–85.

4. Visser KE de, Eichten A, Coussens LM. Paradoxical roles of the immune system during cancer development. Nature Reviews Cancer. 2006;6:24–37.

5. Qian B-Z, Pollard JW. Macrophage Diversity Enhances Tumor Progression and Metastasis. Cell. 2010;141:39–51.

6. De Marzo AM, Platz EA, Sutcliffe S, Xu J, Grönberg H, Drake CG, et al. Inflammation in prostate carcinogenesis. Nat. Rev. Cancer. 2007;7:256–69.

7. Elkahwaji JE, Zhong W, Hopkins WJ, Bushman W. Chronic bacterial infection and inflammation incite reactive hyperplasia in a mouse model of chronic prostatitis. The Prostate. 2007;67:14–21.

8. Khalili M, Mutton LN, Gurel B, Hicks JL, De Marzo AM, Bieberich CJ. Loss of Nkx3.1 expression in bacterial prostatitis: a potential link between inflammation and neoplasia. Am. J. Pathol. 2010;176:2259–68.

9. Boehm BJ, Colopy SA, Jerde TJ, Loftus CJ, Bushman W. Acute bacterial inflammation of the mouse prostate. The Prostate. 2012;72:307–17.

10. Elkahwaji JE, Hauke RJ, Brawner CM. Chronic bacterial inflammation induces prostatic intraepithelial neoplasia in mouse prostate. British Journal of Cancer. 2009;101:1740–8.

11. Royuela M, Ricote M, Parsons MS, García-Tuñón I, Paniagua R, De Miguel MP. Immunohistochemical analysis of the IL-6 family of cytokines and their receptors in benign, hyperplasic, and malignant human prostate. The Journal of Pathology. 2004;202:41–9.

12. Taga T, Kishimoto T. gp130 and the interleukin-6 family of cytokines. Annual Review of Immunology. 1997;15:797–819.

13. Heinrich PC, Behrmann I, Haan S, Hermanns HM, Müller-Newen G, Schaper F. Principles of interleukin (IL)-6-type cytokine signalling and its regulation. Biochem J. 2003;374:1–20.

14. Stahl N, Boulton T, Farruggella T, Ip N, Davis S, Witthuhn B, et al. Association and activation of Jak-Tyk kinases by CNTF-LIF-OSM-IL-6 beta receptor components. Science. 1994;263:92 –95.

15. Heinrich PC, Behrmann I, Muller-Newen G, Schaper F, Graeve L. Interleukin-6-type cytokine signalling through the gp130/Jak/STAT pathway. Biochem J. 1998;334:297–314.

16. Chung TDK, Yu JJ, Spiotto MT, Bartkowski M, Simons JW. Characterization of the role of IL-6 in the progression of prostate cancer. The Prostate. 1999;38:199–207.

17. Lou W, Ni Z, Dyer K, Tweardy DJ, Gao AC. Interleukin-6 induces prostate cancer cell growth accompanied by activation of Stat3 signaling pathway. The Prostate. 2000;42:239–42.

18. Lee SO, Lou W, Hou M, de Miguel F, Gerber L, Gao AC. Interleukin-6 Promotes Androgen-independent Growth in LNCaP Human Prostate Cancer Cells. Clinical Cancer Research. 2003;9:370–6.

19. Smith PC, Keller ET. Anti-interleukin-6 monoclonal antibody induces regression of human prostate cancer xenografts in nude mice. The Prostate. 2001;48:47–53.

20. Wallner L, Dai J, Escara-Wilke J, Zhang J, Yao Z, Lu Y, et al. Inhibition of Interleukin-6 with CNTO328, an Anti-Interleukin-6 Monoclonal Antibody, Inhibits Conversion of Androgen-Dependent Prostate Cancer to an Androgen-Independent Phenotype in Orchiectomized Mice. Cancer Research. 2006;66:3087–95.

21. Nakashima J, Tachibana M, Horiguchi Y, Oya M, Ohigashi T, Asakura H, et al. Serum Interleukin 6 as a Prognostic Factor in Patients with Prostate Cancer. Clinical Cancer Research. 2000;6:2702–6.

22. Twillie DA, Eisenberger MA, Carducci MA, Hseih W-S, Kim WY, Simons JW. Interleukin-6: A candidate mediator of human prostate cancer morbidity. Urology. 1995;45:542–9.

23. Drachenberg DE, Elgamal AA, Rowbotham R, Peterson M, Murphy GP. Circulating levels of interleukin-6 in patients with hormone refractory prostate cancer. The Prostate. 1999;41:127–33.

24. Adler HL, McCurdy MA, Kattan MW, Timme TL, Scardino PT, Thompson TC. Elevated levels of circulating interleukin-6 and transforming growth factor-beta1 in patients with metastatic prostatic carcinoma. J. Urol. 1999;161:182–7.

25. Rojas A, Liu G, Coleman I, Nelson PS, Zhang M, Dash R, et al. IL-6 promotes prostate tumorigenesis and progression through autocrine cross-activation of IGF-IR. Oncogene. 2011;30:2345–55.

26. Rose TM, Bruce AG. Oncostatin M is a member of a cytokine family that includes leukemia-inhibitory factor, granulocyte colony-stimulating factor, and interleukin 6. PNAS. 1991;88:8641–5.

27. Culig Z, Steiner H, Bartsch G, Hobisch A. Interleukin-6 regulation of prostate cancer cell growth. J. Cell. Biochem. 2005;95:497–505.

28. Godoy-Tundidor S, Cavarretta ITR, Fuchs D, Fiechtl M, Steiner H, Friedbichler K, et al. Interleukin-6 and oncostatin M stimulation of proliferation of prostate cancer 22Rv1 cells through the signaling pathways of p38 mitogen-activated protein kinase and phosphatidylinositol 3-kinase. The Prostate. 2005;64:209–16.

29. Godoy-Tundidor S, Hobisch A, Pfeil K, Bartsch G, Culig Z. Acquisition of Agonistic Properties of Nonsteroidal Antiandrogens after Treatment with Oncostatin M in Prostate Cancer Cells. Clinical Cancer Research. 2002;8:2356 –2361.

30. Xin L, Teitell MA, Lawson DA, Kwon A, Mellinghoff IK, Witte ON. Progression of prostate cancer by synergy of AKT with genotropic and nongenotropic actions of the androgen receptor. PNAS. 2006;103:7789–94.

31. Lois C, Hong EJ, Pease S, Brown EJ, Baltimore D. Germline transmission and tissue-specific expression of transgenes delivered by lentiviral vectors. Science. 2002;295:868–72.

32. Lukacs RU, Memarzadeh S, Wu H, Witte ON. Bmi-1 Is a Crucial Regulator of Prostate Stem Cell Self-Renewal and Malignant Transformation. Cell Stem Cell. 2010;7:682–93.

33. Lukacs RU, Goldstein AS, Lawson DA, Cheng D, Witte ON. Isolation, cultivation and characterization of adult murine prostate stem cells. Nat. Protocols. 2010;5:702–13.

34. Goldstein AS, Huang J, Guo C, Garraway IP, Witte ON. Identification of a cell of origin for human prostate cancer. Science. 2010;329:568–71.

35. Salm SN, Koikawa Y, Ogilvie V, Tsujimura A, Coetzee S, Moscatelli D, et al. Generation of active TGF-β by prostatic cell cocultures using novel basal and luminal prostatic epithelial cell lines. Journal of Cellular Physiology. 2000;184:70–9.

36. Jiao J, Wang S, Qiao R, Vivanco I, Watson PA, Sawyers CL, et al. Murine Cell Lines Derived from Pten Null Prostate Cancer Show the Critical Role of PTEN in Hormone Refractory Prostate Cancer Development. Cancer Res. 2007;67:6083–91.

37. Wang S, Gao J, Lei Q, Rozengurt N, Pritchard C, Jiao J, et al. Prostate-specific deletion of the murine Pten tumor suppressor gene leads to metastatic prostate cancer. Cancer Cell. 2003;4:209–21.

38. Mulholland DJ, Xin L, Morim A, Lawson D, Witte O, Wu H. Lin−Sca-1+CD49fhigh Stem/Progenitors Are Tumor-Initiating Cells in the Pten-Null Prostate Cancer Model. Cancer Research. 2009;69:8555 –8562.

39. Cairns P, Okami K, Halachmi S, Halachmi N, Esteller M, Herman JG, et al. Frequent Inactivation of PTEN/MMAC1 in Primary Prostate Cancer. Cancer Research. 1997;57:4997 –5000.

40. Alberti I, Barboro P, Barbesino M, Sanna P, Pisciotta L, Parodi S, et al. Changes in the expression of cytokeratins and nuclear matrix proteins are correlated with the level of differentiation in human prostate cancer. Journal of Cellular Biochemistry. 2000;79:471–85.

41. Ahuja D, Saenz-Robles MT, Pipas JM. SV40 large T antigen targets multiple cellular pathways to elicit cellular transformation. Oncogene. 24:7729–45.

42. Kan CE, Cipriano R, Jackson MW. c-MYC Functions as a Molecular Switch to Alter the Response of Human Mammary Epithelial Cells to Oncostatin M. Cancer Research. 2011;

43. Barbieri CE, Demichelis F, Rubin MA. Molecular genetics of prostate cancer: emerging appreciation of genetic complexity. Histopathology. 2012;60:187–98.

44. Chen Z, Trotman LC, Shaffer D, Lin H-K, Dotan ZA, Niki M, et al. Crucial role of p53-dependent cellular senescence in suppression of Pten-deficient tumorigenesis. Nature. 2005;436:725–30.

45. Sommer U, Schmid C, Sobota RM, Lehmann U, Stevenson NJ, Johnston JA, et al. Mechanisms of SOCS3 phosphorylation upon interleukin-6 stimulation. Contributions of Src- and receptor-tyrosine kinases. J. Biol. Chem. 2005;280:31478–88.

46. Gioeli D, Mandell JW, Petroni GR, Frierson HF Jr, Weber MJ. Activation of mitogen-activated protein kinase associated with prostate cancer progression. Cancer Res. 1999;59:279–84.

47. Mulholland DJ, Kobayashi N, Ruscetti M, Zhi A, Tran LM, Huang J, et al. Pten loss and RAS/MAPK activation cooperate to promote EMT and metastasis initiated from prostate cancer stem/progenitor cells. Cancer Research. 2012;

48. Gumerlock PH, Poonamallee UR, Meyers FJ, deVere White RW. Activated ras Alleles in Human Carcinoma of the Prostate Are Rare. Cancer Res. 1991;51:1632–7.

49. Barton BE, Karras JG, Murphy TF, Barton A, Huang HF-S. Signal transducer and activator of transcription 3 (STAT3) activation in prostate cancer: Direct STAT3 inhibition induces apoptosis in prostate cancer lines. Mol Cancer Ther. 2004;3:11–20.

50. Steiner H, Cavarretta IT, Moser PL, Berger AP, Bektic J, Dietrich H, et al. Regulation of growth of prostate cancer cells selected in the presence of interleukin-6 by the anti-interleukin-6 antibody CNTO 328. The Prostate. 2006;66:1744–52.

CHAPTER 5

Conclusions and Future Directions

The preceding chapters have presented the research performed in an effort to more fully characterize the molecular networks that drive tumorigenesis in the prostate. The dissociated prostate tissue regeneration system has allowed our laboratory to rapidly interrogate the functional consequences of genetic aberrations identified in primary human prostate cancer specimens (1–3). Further, the adaptability of this system allows for interrogation of primary human prostate samples and interrogation of defined oncogenes without unknown selection bias from *in vitro* culture (4). The findings presented here have shown that we can use this system to interrogate signaling networks activated by defined oncogenes and how modulating expression levels of non-mutated genes can promote prostate tumorigenesis (5, 6).

Interrogating the phosphoproteome of human primary samples

The highly reproducible nature of the dissociated prostate tissue system provided the means to induce tumorigenesis using defined sets of oncogenes and to functionally interrogate the signaling networks downstream of those oncogenes. This has lead to a more robust understanding of the mechanisms through which known oncogenes promote tumorigenesis as well as signaling nodes common across different oncogenic stimuli. Mass spectrometry provides a sensitive platform for the interrogation of proteomic samples, though current enrichment techniques require relatively large tumor samples for lysate preparation (6). Increasing the recovery of phosphorylated residues from tumor lysate preparations will facilitate the use of mass spectrometry techniques combined with phospho-peptide enrichment in determining activation signatures in primary human tumor samples

(7). Current work in our laboratory aims to utilize these enrichment techniques to interrogate signaling networks in human regenerations and transformations, as well as comparing tumors from different metastatic sites. Development of these techniques could provide the means to prospectively identify activated pathways that are specific to individual patients, allowing personalized therapeutic approaches in the clinic.

Further delineation of the inflammatory microenvironment in prostate cancer

The work presented in the above chapters concerning the role of inflammation in the prostate provides several meaningful results. To our knowledge, it is the first investigation to utilize benign epithelium to interrogate the functional consequences of heightened inflammatory signaling in the prostate. These results showed that in our model system, increased exposure to neither IL6 or OSM was sufficient for transformation, though potent synergy was observed upon loss of PTEN. This indicates that inflammation might not represent a potent *de novo* oncogenic stimulus but is instead reliant upon synergy with underlying oncogenic mutations. This is consistent with studies indicating similarly heightened expression of both IL6 and OSM in both benign conditions, such as benign prostatic hyperplasia and prostatic intraepithelial neoplasia, and malignant adenocarcinoma (8). Increased expression of inflammatory cytokines could be a result from tissue damage caused by lesions in their nascent stages. This increase in cytokine production could have little effect in the context of benign lesions while synergizing with more potent oncogenes such as loss of PTEN, promoting malignant conversion. Future work will include interrogating how cytokines such as IL6 and OSM interact with other oncogenes common to prostate cancer such as ETS-family re-arrangements and increased expression of the C-MYC oncogene (9, 10).

Further, tumor inflammation is a complex process that involves numerous signaling molecules that act in both cell autonomous and paracrine fashion. Studies utilizing bacterial colonization of the prostate have identified hyperplasia and PIN lesions in chronic inflammatory conditions (11). Identification of the predominant cytokines included IL6, though IL-1a and IL-1b, IL-8, and TNF-a, among others, were also significantly up-regulated (12). The contributions of these cytokines to the inflammatory environment and their role in promoting prostate tumorigenesis are still unclear and warrant further investigation. The balance of inflammatory cytokines could also be involved in determining outgrowth of prostate cancer subtypes. Studies by Huang and colleagues identified that increased expression of IL-8 was specifically localized to neuroendocrine cells in prostate cancer specimens and was up-regulated in castration resistant cancer with neuroendocrine-like phenotypes (13). Of the two IL-8 receptors, CXCR1 and CXCR2, malignant epithelial cells only expressed CXCR1 while neuroendocrine cells expressed CXCR2. This indicates the potential for functional differences between paracrine and autocrine response to IL-8. Importantly, understanding these nuances in signaling between malignant epithelium and the surrounding inflammatory signaling milieu could have profound effects on current immunotherapy techniques (14). As these techniques develop, it will be crucial to understand how inflammatory conditions affect the tumor microenvironment if we are to effectively utilize our endogenous immune system as a cancer therapeutic.

References

1. Xin L, Ide H, Kim Y, Dubey P, Witte ON (2003) In vivo regeneration of murine prostate from dissociated cell populations of postnatal epithelia and urogenital sinus mesenchyme. *Proc Natl Acad Sci* 100:11896–11903.

2. Xin L et al. (2006) Progression of prostate cancer by synergy of AKT with genotropic and nongenotropic actions of the androgen receptor. *Proc Natl Acad Sci* 103:7789–7794.

3. Zong Y et al. (2009) ETS family transcription factors collaborate with alternative signaling pathways to induce carcinoma from adult murine prostate cells. *Proc Natl Acad Sci* 106:12465–12470.

4. Goldstein AS, Huang J, Guo C, Garraway IP, Witte ON (2010) Identification of a cell of origin for human prostate cancer. *Science* 329:568–571.

5. Cai H et al. (2011) Differential transformation capacity of Src family kinases during the initiation of prostate cancer. *Proc Natl Acad Sci* 108:6579 –6584.

6. Drake JM et al. (2012) Oncogene-specific activation of tyrosine kinase networks during prostate cancer progression. *Proc Natl Acad Sci* 109:1643–1648.

7. Kettenbach AN, Gerber SA (2011) Rapid and Reproducible Single-Stage Phosphopeptide Enrichment of Complex Peptide Mixtures: Application to General and Phosphotyrosine-Specific Phosphoproteomics Experiments. *Anal Chem* 83:7635–7644.

8. Royuela M et al. (2004) Immunohistochemical analysis of the IL- 6 family of cytokines and their receptors in benign, hyperplasic, and malignant human prostate. *J Pathol* 202:41–49.

9. Tomlins SA et al. (2005) Recurrent Fusion of TMPRSS2 and ETS Transcription Factor Genes in Prostate Cancer. *Science* 310:644–648.

10. Williams K et al. (2005) Unopposed c-MYC expression in benign prostatic epithelium causes a cancer phenotype. *The Prostate* 63:369–384.

11. Elkahwaji JE, Zhong W, Hopkins WJ, Bushman W (2007) Chronic bacterial infection and inflammation incite reactive hyperplasia in a mouse model of chronic prostatitis. *The Prostate* 67:14–21.

12. Boehm BJ, Colopy SA, Jerde TJ, Loftus CJ, Bushman W (2012) Acute bacterial inflammation of the mouse prostate. *The Prostate* 72:307–317.

13. Huang J et al. (2005) Differential Expression of Interleukin-8 and Its Receptors in the Neuroendocrine and Non-Neuroendocrine Compartments of Prostate Cancer. *Am J Pathol* 166:1807–1815.

14. Begley J, Ribas A (2008) Targeted Therapies to Improve Tumor Immunotherapy. *Clin Cancer Res* 14:4385–4391.